5-2015

CHARACTERIZATION OF THE ROLES OF CARMA3 AND BCL10 IN VIRUS-TRIGGERED RIG-I/MAVS SIGNALING PATHWAY

Zhicheng Zhou Mr

TITLE OF DISSERTATION

CHARACTERIZATION OF THE ROLES OF CARMA3 AND BCL10 IN VIRUS-TRIGGERED RIG-I/MAVS SIGNALING PATHWAY

A

DISSERTATION

Presented to the Faculty of

The University of Texas

Health Science Center at Houston

and

The University of Texas

MD Anderson Cancer Center

Graduate School of Biomedical Sciences

in Partial Fulfillment

of the Requirements

for the Degree of

DOCTOR OF PHILOSOPHY

by

Zhicheng Zhou M.S.

Houston Texas

May, 2015

ACKNOWLEDGEMENTS

I would like to thank to my advisor, Dr. Xin Lin, for his six-year support. Without his support, I think that I cannot finish my Ph.D study. He patiently gave me the necessary advice, the good projects and encouragement to help me finish the dissertation and through the PH.D Program.

I also want to say thanks to the members of my advisor and exam committees, including Dr. Wei Zhang, Dr. Shao-Cong Sun, Dr. Hui-Kuan Lin, Dr. Bryant Darnay, Dr. Mong-hong Lee, Dr. Paul Chiao for their help and good suggestions. Their advice helps me a lot in finishing the dissertation. I appreciated it very much.

TABLE OF CONTENTS

LIST OF FIGURES

Characterization of The Roles of CARMA3 and BCL10 in Virus-Triggered RIG-I/MAVS Signaling Pathway

Zhicheng Zhou, M.S.

Advisory Professor: Xin Lin, Ph.D.

ABSTRACT

After RNA virus infection, the innate immunity utilizes RIG-I family of receptors in the cytoplasm to initiate the production of type-I IFNs and proinflammatory cytokines by mitochondrial protein MAVS, which forms a prion-like structure to recruit TBK1and IKK complex to activate IRF3 and NF-κB, respectively. Herein, we revealed the important roles of CARMA3 and BCL10 in RIG-I/MAVS signaling pathway for the first time. CARMA3 or BCL10 deficient cells exhibited partially defective NF-κB activation but hyperactivation of TBK1-IRF3 signaling pathway upon ssRNA virus infection. It led to less production of IL6 but more production of type I IFNs and resulted in CARMA3-deficient mice more resistant to virus infection, including VSV and H1N1 influenza virus. Mechanistic studies showed that CARMA3 and BCL10 physically interacted with MAVS and directly regulated MAVS aggregation. Overexpression of CARMA3 and BCL10 inhibited MAVS aggregation. Consistently, MAVS aggregation more easily occurred in CARMA3 deficient cells after VSV infection. VSV induced the cleavage of CARMA3 and led to more MAVS aggregation. These novel findings not only identified the important role of CARMA3 and BCL10 during influenza virus infection, which may provide the new target for future therapeutic interference but also revealed molecular mechanism by which CARMA3 and BCL10 orchestrated the NF-κB and IRF3 activation to balance the production of type I IFNs and proinflammatory cytokines.

CHAPTER 1: INTRODUCTION

The essential event of immunology system is to recognize the microbial pathology and to initiate the appropriate immune responses to fight against invasion pathology. In this process, pattern recognition receptors (PRRs) recognize small molecular motifs conserved within a class of microbes, also known as pathogen-associated molecular patterns(PAMPs) and activate a serious of signaling pathways to initiate innate immunity(Janeway 2013). The well-characterized mammal PRRs include membrane-associated Toll-like receptors(TLRs), c-type lectin receptors(CLRs), cytosolic receptors such as NOD-like receptors(NLRs), RIG-I like receptors(RIRs) and AIM_2-like receptors (ALRs)(Kawai and Akira 2011). Since our research mainly focused on two RNA virus, influenza A virus and vesicular stomatitis Indiana virus (VSV), the following chapter mainly describes the receptors and their downstream signaling pathways that are involved in RNA virus detection and clearance.

1.1 Toll-like receptors

TLRs are the first PRRs to be characterized. They comprise a large family of membrane-bound receptors, which are named from their similarity to the toll protein of drosophila identified in 1985 (Hansson and Edfeldt 2005). The vertebrate TLR family consists of 13 members, including TLR1, TLR2, TLR3, TLR4, TLR6, TLR7, TLR8, TLR9, TLR10, TLR11, TLR12 and TLR13, which are characterized by extracellular domain containing

leucine-rich repeats (LRRs), a transmembrane region and a cytoplasmic Toll/IL-1 receptor (TIR) domain(Lester and Li 2014). Each receptor senses the PAMPs derived from diverse microbes, including bacterial cell wall components such as lipoproteins(for TLR1, TLR2, and TLR6), lipopolysaccharide(LPS)(for TLR4), as well as bacterial flagellin(for TLR5), bacterial DNA(for TLR9),virus-derived double stranded(dsRNA)(for TLR3) and single-stranded(ssRNA)(forTLR7 and TLR8)(Table 1)(Akira, Uematsu et al. 2006).

Upon ligand recognition, TLRs recruit a serious of adaptor proteins to activate downstream signaling pathways. Based on different adapters, these signaling pathways can be divided into two types, myeloid differentiation primary response gene (88) (MyD88)- and the TIR-domain containing adaptor inducing IFN-β (TRIF)-dependent pathways. TLR3 and TLR4 recruit TRIF, while other TLRs with the exception of TLR3 utilize MyD88. Through these adapters, TLRs trigger the activation of nuclear factor kappa-light-chain-enhancer of activated B cells(NF-κB)/ the activator protein 1 (AP-1) and distinct IFN regulatory factor -3 and -7(IRF3/7) pathways to orchestrate innate and adaptive immune responses against the invasion of diverse pathogens(Kawai and Akira 2011).

TLRs play an important role in antivirus immune response. Viruses depend on the host cells to complete their replication cycle. During the virus life cycle, the virus-derived PAMPs are recognized by TLRs. The role of TLRs is to trigger the production of IFN (IFN) and/or proinflammatory cytokines. It has been shown that TLR3, TLR7/TLR8/TLR9, TLR4 and TLR2 have an important impact on antivirus innate immunity(Fig.1)(Lester and Li 2014).

TLR3 is located in endosome and is the first well-studied nucleotide-sensing TLR (Alexopoulou, Holt et al. 2001). TLR3 recognizes virus-derived dsRNA, a molecular

signature of many RNA viruses. Polyriboinosinic:polyribocytidylic acid (poly(I:C)),a synthetic dsRNA analog, also triggers the activation of TLR3-dependent signaling pathways. The *in vitro* binding assay revealed that TLR3 ectodomain was capable of interacting with the dsRNA with the length of 40–50 bps long, while the TLR3 signaling was activated by ligand with the length of 90bps or longer(Leonard, Ghirlando et al. 2008). As a PAMP, dsRNA itself constitutes virus genome or is generated as a replicative intermediate during virus life cycle. Therefore, TLR3 recognizes multiple types of viruses, including dsRNA virus, ssRNA virus and DNA virus. Upon viral dsRNA recognition, TLR3 undergoes tyrosine phosphorylation on Tyr858 and Tyr759 in its cytoplasmic domain (Lee, Xu et al. 2012, Yamashita, Chattopadhyay et al. 2012). Upon activation, the receptors recruit the TRIF- TNF receptor associated factor 6(TRAF6) - receptor-interacting protein 1(RIP1) complex, which leads to the activation of transforming growth factor beta activated kinase 1(TAK1) and subsequently the classical IκB kinase (IKK) complex (Sato, Sugiyama et al. 2003, Jiang, Mak et al. 2004, Meylan, Burns et al. 2004). Then, the activated IKK complex phosphorylates nuclear factor of kappa light polypeptide gene enhancer in B-cells inhibitor, alpha (IκBα) on its serine 32 and 34 and causes it to be degraded by the proteasome, which will release NF-κB dimmers. The free NF-κB dimmers enter the nucleus and turn on the transcription of the specific genes with the κB site in the promoter (Kawai and Akira 2011). On the other hand, TRIF associates with TRAF3 to activate the noncanonical IKK kinases, TBK1 and/or IKKε. The activated TBK1 and IKKε phosphorylate and activate IRF3 and IRF7. The phosphorylated IRF3 and IRF7 undergo the dimerization and then go into the nucleus to induce the production of type I and/or type III IFNs. These proinflmmatory

cytokines and IFNs serve as the first defense line against virus infection. Therefore, during virus infection, any dysregulation of TLR3 singling results in severe outcomes. For example, mice lacking TLR3 are hypersensitive to the infection of mouse cytomegalovirus (MCMV), herpes simplex virus (HSV) 2, poliovirus, encephalomyocarditis virus (EMCV), coxsackie virus B3 or B4, rotavirus etc., as it is evidenced by the significantly increased viral shedding and decreased production of antiviral and proinflmmatory cytokines(Hoebe, Du et al. 2003, Tabeta, Georgel et al. 2004, Herman, Ciancanelli et al. 2012). This *in vivo* evidence confirms the importance of TLR3 in antivirus immune response.

Similar to TLR3, TLR7 and TLR8 are also located in endosome. They recognize GU-rich and AU-rich ssRNA sequence of RNA viruses, including the human immunodeficiency virus (HIV-1), VSV, sendai virus, coxsackie B virus, coronaviruses, flaviviruses, such as HCV, dengue virus and WNV(Diebold, Kaisho et al. 2004, Heil, Hemmi et al. 2004, Lund, Alexopoulou et al. 2004). In recognition of viral-derived ssRNA in endosome, TLR7 or TLR8 utilizes MyD88-dependent pathways to activate NF-κB and IFN regulatory factor (IRF7). More specifically, the TLR7 or TLR 8 recruits interleukin-1 receptor-associated kinase (IRAK4), interleukin-1 receptor-associated kinase (IRAK1) and many E3 ubiquitin ligases, such as TRAF6 and TRAF3, through MyD88. It leads to the activation of IKKa and TAK1. TAK1 directly phosphorylates IKKβ in the IKK complex and subsequently activates NF-κB signaling pathway. In parallel, IKKα and IRAK1 phosphorylate and activate IRF7, resulting in the production of IFN alpha (Hemmi, Kaisho et al. 2002, Kawai, Sato et al. 2004, Honda, Yanai et al. 2005). Also, the tissue distribution of TLR7 and TLR8 suggests their important role in innate immunity. Different from TLR3 with wide tissue distribution ,

TLR7 is predominatly expressed in plasmacytoid dendritic cells (pDCs), B cells and monocytes/macrophages, while TLR8 is only found in monocytes/macrophages and myeloid dendritic cells(Lester and Li 2014).

TLR9 is another endocytic PRR, which recognizes unmethlated CpG motifs, a PAMP of many bacterial and viral DNA. The unmethlate CpG is always found in microbial genomes but rare in verterbrate genome, by which TLR9 can discriminate host DNA from microbe-derived DNA(Latz, Schoenemeyer et al. 2004). Besides, the intracellular localiztion of TLR9 decreases the risk responding to self DNA and developing autoimmune disease. TLR9 is expressed in many immune cells including macrophage, B cells, myeloid dendritic cells, classical dendritic cells(cDCs) and pDCs. Similar to TLR7 and TLR8, TLR9 utilizes MyD88-dependent pathways to activate IRF7 and NF-κB. Mice with TLR9 deficiency are hypersusceptible to many double-stranded DNA virus infection, including mouse cytomegalovirus (MCMV), HSV 1 and HSV 2, and poxviruses(Lund, Sato et al. 2003, Krug, Luker et al. 2004, Tabeta, Georgel et al. 2004).

Unlike endocytotic TLRs, TLR2 and TLR4 are located in cell membrane, which recognize viral envelop proteins or viral proteins that are released to extracellular milieu. For example, TLR2 recognizes the core and NS3 proteins of HCV, the glycoproteins B and H of human cytomegalovirus, the glycoproteins, such as gH/gL and gB of HSV, the UTPase of EBV and hemagglutinin(HA) protein of measles virus and nsp4 of rotavirus(Bieback, Lien et al. 2002, Compton, Kurt-Jones et al. 2003, Boehme, Guerrero et al. 2006, Ariza, Glaser et al. 2009, Leoni, Gianni et al. 2012). TLR4 recognizes the VSV-G protein of VSV, the GP protein of Ebola virus, the envelop protein of MMTV and so on (Georgel, Jiang et al. 2007,

Ariza, Glaser et al. 2009, Okumura, Pitha et al. 2010). After engagement of ligands, TLR2 and TLR4 activate downstream signal pathways in different manners. Specifically, TLR2 dimmerizes with other TLRs such as TLR1 or TLR6 on the cell membrane. Then, TLR2 initiates MyD88-dependent pathways to activate NF-κB. The role of TLR2 in IFN production seems controversial, which may depend on the cells type and virus types. Different from TLR2, TLR4 does not form a heterodimer with other TLRs. TLR4 signal on the cell membrane is transduced via MyD88- and TRIF- dependent pathways. In TLR4 signaling, the activation of early-phase NF-κB is linked to MyD88-dependent pathways, while the late phase NF-κB and IRF3/7 are activated by TRIF-dependent pathways(Lester and Li 2014).

These TLRs sense diverse virus-derived PAMPs and constitute a powerful antiviral innate immune system to quickly react to invading viruses(Lester and Li 2014).

1.2 RIG-I and MAVS signaling pathway

The innate immunity utilizes not only TLRs but also RIG-I- like family receptors (RLRs) in the cytoplasmic compartments to detect viral infection. Upon activation, RIG-I initiates distinct signaling pathways to produce type I IFN and other proinflmmatory cytokines (e.g., TNFα and IL-6), which quickly limit virus infection and activate the adaptive immune system (Akira, Uematsu et al. 2006, Kawai and Akira 2006).

Previous studies have identified several RLR family members, including RIG-I, melanoma differentiation associated gene 5(MDA5), and laboratory of genetics and physiology 2(LGP2). All of the three RLRs are DExD/H box RNA helicases and share very

similar domains, including the central DExD/H box RNA helicase domain with ATPase activity and the C-terminal domain (CTD). Different from LGP2, RIG-I and MDA5 contain the N-terminal domain (NTD) consisting of tandem CASPASE activation and recruitment domains (CARDs). Without CARD domains, LGP2 serves as a regulatory but not an essential component in RIG-I/MDA5/mitochondrial antiviral-signaling protein (MAVS) signaling pathway (Satoh, Kato et al. 2010).

These functional domains contribute to the overall function of a protein. Among RLRs family proteins, only the structures of "active" and "silence" RIG-I have been well studied, therefore, we will take RIG-I as an example to interpret the function of domains in RLRs family proteins. In resting cells, the N-terminal CARD domains are bound to the central helicase domain of the protein and thus, are not available for their function. After RNA virus infection, the "free" CTD senses viral RNA and interacts with blunt-ended 5'ppp-dsRNA.Then, the CTD competes with the CARD domains to interact with central helicase domain and release CARD domains. After that, the "free" CARD domains become potentially available for downstream adaptors, for example, MAVS. RIG-I interacts with MAVS through the CARD domains, which activates MAVS to form prion -like structure. Then, the aggregated MAVS works as a platform in the mitochondrial to recruit the IKK and TBK1 complex to activate NF-κB and IRF3 signaling pathways, respectively (Hou, Sun et al. 2011)(Fig. 2). Followed by ATP hydrolysis and phosphate release, the helicase domain no longer interacts with the CTD but binds to the CARD domain again. It results in the

dissociation of RIG-I from MAVS and stops the activation of signaling pathways (Zeng, Sun et al. 2010, Kolakofsky, Kowalinski et al. 2012).

Although three RLRs share very similar protein structure, they do have some functional difference. For example, RIG-I and MDA5 can recognize different RNA viruses. RIG-I is essential for innate immunity to many ssRNA viruses, including influenza A and B virus, NDV, Sendai virus (SeV), respiratory syncytial virus, measles virus, VSV, rabies virus, HCV and Japanese encephalitis virus. After transcription of AT-rich DNA genome of DNA virus, RIG-I can recognize some DNA viruses including adenovirus, HSV1, and EBV (Sumpter, Loo et al. 2005, Hornung, Ellegast et al. 2006, Kato, Takeuchi et al. 2006, Samanta, Iwakiri et al. 2006, Plumet, Herschke et al. 2007, Saito, Hirai et al. 2007, Loo, Fornek et al. 2008, Ablasser, Bauernfeind et al. 2009, Chiu, Macmillan et al. 2009). Different from RIG-I, MDA5 protects host from the infection of EMCV, Theiler's virus, mengovirus, murine norovirus, and murine hepatitis virus(Kato, Takeuchi et al. 2006, McCartney, Thackray et al. 2008, Roth-Cross, Bender et al. 2008). Recognition of different viruses suggests that RIG-I and MDA can detect distinct features of RNA viruses. 5'-triphosphate RNA as well as short (<2 kbp) dsRNAs is the ligand for RIG-I, while MDA5 can be activated by transfection of a long (>2 kbp), synthetic dsRNA analog of artificial sequence, namely polyinosinic:polycytidylic [poly(I:C)](Hornung, Ellegast et al. 2006). Additionally, LGP2 is different from other family members. Without CARD domain, LGP2 cannot interact with adaptor protein MAVS and thereby, play a negative role in regulating RIG-I and MDA5-mediated antiviral response (Satoh, Kato et al. 2010).

MAVS mediates antiviral response as an adapter protein for RLRs. MAVS was first identified by the four independent labs almost at the same time in 2005. Therefore, MAVS is also known as virus-induced signaling adapter (VISA), IFN-β promoter stimulator 1(IPS-1) and CARD adapter inducing IFN beta (Cardif) (Kawai, Takahashi et al. 2005, Meylan, Curran et al. 2005, Seth, Sun et al. 2005, Xu, Wang et al. 2005). Different from mice with loss of RIG-I, MAVS-deficient mice were viable and fertile. However, the knock-out mice fail to produce type I- IFN in response to poly (I:C) stimulation and increase mortality during virus infection. It suggests the important role of MAVS in innate immunity against viral infection (Sun, Sun et al. 2006). MAVS contains an N-terminal CARD followed by a proline-rich region and a transmembrane domain (TMD). These domains together contribute to the overall function of protein. The N-terminal CARD is important for MAVS interaction with upstream RLRs. The prolin-rich region in MAVS is required for the recruitment of many E3 ligases including TRAF2, TRAF5 and TRAF6. The TMD domain is important for MAVS mitochondrial localization. Being activated, MAVS forms a prion-like structure in the mitochondrial outer membrane and works as a platform to assembly a MAVS signalosome including TRAF2, TRAF3, TRAF6, TRAF family member-associated NF-κB activator (TANK), TNFR1-associated death domain protein (TRADD). The formation of a MAVS signaling complex leads to the activation of NF-κB and IRF3 to produce pro-inflammation cytokines and type I IFNs. These secreted proteins become the first defense line against virus infection(Fig. 2)(Jacobs and Coyne 2013).

1.3 IFN and antivirus response

After virus infection, host cells quickly releases IFNs, which provides the first defense line against virus invasion (Colonna, Krug et al. 2002). The IFNs were firstly discovered at the early 1950. It was found that virus-infected cells were resistant to the second virus infection under some conditions. However, people did not identify the substrate or agent responsible for this phenomenon at that time (Henle 1950). In 1957, Issacs and Lindenmann coined the term "IFN" to describe the substrate secreted by the cells to interfere the virus infection (Isaacs and Lindenmann 1957, Isaacs, Lindenmann et al. 1957). Twenty years later, the IFNs were firstly purified from the medium of stimulated human white blood cells (Cantell, Hirvonen et al. 1981, Cantell, Hirvonen et al. 1981). After the refinement of purification schemes, it was found that IFN was not one but a family of different proteins(Cantell, Hirvonen et al. 1981). Until now, more than 20 distinct IFNs have been identified in animal, including humans(Schneider, Chevillotte et al. 2014).

IFNs belong to a large family of cytokines. After virus infection, IFNs produced by cells are released into extracellular milieu, where they can be recognized by different IFN receptors(Schneider, Chevillotte et al. 2014). Based on different receptors, the IFNs are divided into three different classes, type I IFN, type II IFN and type III IFN. Type I IFN is the largest group in IFN family, including IFNα, IFNβ, IFNε, IFNκ and IFNω in humans(Schneider, Chevillotte et al. 2014). All type I IFN proteins are recognized by the type I IFN heterodimeric receptors, which consist of IFNα receptors 1(IFNAR1) and IFNα receptors 2 (IFNAR2). Type I IFN proteins can be produced by nearly all types of cells. Consistently, IFN receptors are ubiquitously expressed. Wide tissue distribution of IFNs with

their receptors suggests their important role in antiviral innate immunity(Schneider, Chevillotte et al. 2014). Different from type I IFNs, there are only one type II IFN, IFNγ. In the recognition of IFNγ, the type II IFN receptor forms a complex with interaction between two IFNγ receptor 1(IFNGR1) subunits and two IFNγ receptor 2(IFNGR2), which results in the activation of the receptors(Walter, Windsor et al. 1995). Although the type II IFN receptor is expressed on the cell surface of all cell types, the IFNγ is only produced by the cells of immune system and plays an important role in both innate and adaptive immunity(McLaren and Ramji 2009, Zaidi and Merlino 2011). In 2003, the type III IFN class was identified by two different groups (Kotenko, Gallagher et al. 2003, Sheppard, Kindsvogel et al. 2003). Until now, four different members have been identified. They are IFNL1, IFNL2, IFNL3 and IFNL4 (also known as IFN-λ1, IFN-λ2, IFN-λ3 and IFN-λ4) (Fox, Sheppard et al. 2009, Prokunina-Olsson, Muchmore et al. 2013). The structure of these proteins is similar to the proteins of the IL-10 cytokine family. Therefore, the type III IFNs bind to IL-10 receptor 2 with low-affinity. Additionally, the types III IFNs interact with type III IFN receptor with high affinity and activate downstream signaling pathways(Fox, Sheppard et al. 2009). Together, IFNs and their receptors constitute an immune system in response to virus infection (Fig. 3).

Although distinct IFNs can be recognized by different receptors, they share janus kinases (JAKs)- signal transducers and activators of transcription(STATs) signaling pathway to increase the transcription of IFN-stimulated genes (ISGs)(Stark and Darnell 2012). In resting cells, the JAKs interact with the cytoplasmic domain of each IFN receptor subunits in an inactive form. Upon ligand stimulation, receptor chains undergo conformational change to

bring the kinase domains of JAKs into close proximity, where JAK are autophosphorylated and subsequently activated. Then, the “active” JAKs in turn phosphorylate the cytoplasmic part of IFN receptors on some conserved tyrosine residues, which works as the docking sites for STAT proteins. The Src homology domain2 (SH2) on STAT is responsible for STAT-receptor interaction. The receptor-recruitment of STAT proteins is essential for phosphorylation and activation of STAT proteins. After phosphorylation, STAT proteins undergo conformational change and form a homo-(type II IFN) or heterodimer (type I and type III IFN). Then, STAT dimmers are released from IFN receptors and enter the nucleus, where they serve as transcriptional factor to drive expression of ISGs (Schindler, Shuai et al. 1992, Shuai, Schindler et al. 1992, Greenlund, Morales et al. 1995, Heim, Kerr et al. 1995, Sekimoto, Imamoto et al. 1997, Melen, Kinnunen et al. 2001, Fagerlund, Melen et al. 2002, McBride, Banninger et al. 2002, van Boxel-Dezaire, Rani et al. 2006) (Fig. 3).

ISGs are involved in a wide of cellular activities. They limit virus infection by directly targeting proteins or functions involved in the virus life cycles. In absence of virus, ISGs are kept in a low level. After virus infection, the induction of ISGs takes places through PRRs-triggered signaling pathways to reinforce the IFN response and prime antiviral immune response(Schneider, Chevillotte et al. 2014).

Virus relies on host cells to complete their life cycle, which includes cellular entry of virus, translation and replication of viral genomes and viral shedding(Schneider, Chevillotte et al. 2014). ISGs target these stages of viral life cycle through different mechanisms. For example, the murine myxovirus resistance 1 and 2(Mx1 and Mx2) are two important ISGs targeting the cellular entry of virus. Both of them are small guanosine

triphosphatases(GTPase)(Schneider, Chevillotte et al. 2014). Mx1 traps uncoating of ribonuclocapsids and thereby, interferes endocytic traffic of incoming virus particles (Gao, von der Malsburg et al. 2010). In this way, MX1 prevents viral components from reaching their cellular destination and inhibits the translation and replication of viral genome. Similarly, MX2 inhibits the replication cycle of HIV-1 by preventing viral reverse-transcribed genome from reaching its nuclear destination (Kane, Yadav et al. 2013). Another set of ISGs inhibits viral replication and translation, such as the IFN-induced protein with tetratricopeptide repeats (IFIT) family, the OAS-RNaseL pathway, PKR and zinc-finger antiviral protein (ZAP) (Goff 2004, Kok and Jin 2013, Munir and Berg 2013). Furthermore, many ISGs execute their inhibitory functions at the last stage of virus life cycle. Viperin and tetberin are two good examples. Upon influenza or HIV infection, the amount of viperin was induced, which affected plasma membrane fluidity through disrupting lipid rafts. The lipid rafts with appropriate membrane fluidity is perquisite for influenza or HIV shedding. By disrupting lipid rafts, viperin blocks virus shedding (Wang, Hinson et al. 2007, Nasr, Maddocks et al. 2012). Different from viperin, tetberin directly traps virus particles on the plasma membrane through utilizing two membrane anchors (Perez-Caballero, Zang et al. 2009).

Another important role of ISGs is to desensitize cellular IFN response. IFN response not only renders cells resistance to virus infection but also triggers inflammation. Under some conditions, the sustained IFN response leads to apoptosis. Therefore, in some cases, the hyperactivation of IFN signaling pathway can cause severe outcomes. To return cellular homeostasis, many ISGs reduce the activation of the JAK-STAT signaling pathway to

negatively regulate IFN signal(Schneider, Chevillotte et al. 2014). Among them, suppressor of cytokine signaling proteins (SOCS) and ubiquitin-specific peptidase 18(USP18) undergo intensive investigation. SOCS directly interacts with IFN receptors or the JAK proteins and serves as pseudosubstrates of the kinase. Therefore, it inhibits the activation of JAK-STAT signaling pathway(Hong and Carmichael 2013). The induction of USP18 results in a more sustained inhibition of IFN signaling. USP18 interacts with the cytoplasmic part of IFNα receptor2 (IFNAR2), which leads to the conformational changes of the extracellular domain of IFNAR2. It keeps the IFNAR from binding with IFNα and shut down the JAK-STAT signaling cascade. In contrast, USP18 also interacts with IFNβ receptor but cannot inhibit the signaling cascade, which may due to the IFNβ interact with its receptor with high affinity. It seems that USP18 specifically inhibits IFNα signaling, since it does not interact with type II and type III IFN receptors(Schneider, Chevillotte et al. 2014).

In sum, ISGs play an important role in regulating the antiviral immune responses and keeping cellular homeostasis, which is important for the host cells to survival and control the infection of pathogen.

1.4 NF-κB signaling pathway and CARMA family members

The prototype of NF-κB is referred as p65 and p50 heterodimer. They belong to a family of transcription factors that regulate the transcription of various genes involved in diverse cellular activities including inflammation, immune response, cell growth, apoptosis, differentiation and etc. The NF-κB family has five members, which are NF-κB1 (p105/p50),

NF-κB2 (p100/p52), RELA (p65), RELB and c-Rel. All NF-κB proteins contain Rel homology domain (RHD) in their N-terminus, which plays an important role in NF-κB protein's dimerization and DNA binding. The difference among members lies in their transcription domain. According to the presence of transcription domain, the NF-κB family proteins are classified into two groups. The first group consists of RELA, RELB and c-Rel. They contain a transactivation domain in their C-terminal and are synthesized as mature proteins. The second group includes NF-κB1 and NF-κB2. They do not have a transactivation domain but instead C-terminal ankyrin repeats. They are large precursors and undergo processing through the ubiquitin/proteasome pathway to generate the mature proteins, p50 and p52 respectively. This processing is to selectively degrade NF-κB1 and NF-κB2's C-terminal regions. (Hayden and Ghosh 2004, Natoli 2010).

Two distinct NF-κB signaling pathways have been characterized, namely the canonical and non-canonical pathway. In the canonical NF-κB signaling pathway, in quiescence cells, NF-κB dimmers are associated with IκB proteins that block the NF-κB nuclear localization domains and thereby, preventing translocation of NF-κB into the nucleus. The canonical NF-κB signaling pathway is activated by a wide variety of receptors, including receptors for proinflammatory cytokines, such as tumor necrosis factor α (TNFα) and interleukin-1β (IL-1β), TLRs, TCRs, growth factor receptors, such as epithelial growth factor receptor family members, and G protein-coupled receptors (GPCR). Upon receipt of appropriate signals, many signaling cascades are activated, leading to activation of the IκB kinase (IKK) complex. Activation of the IKK complex results in IκBα phosphorylation at Ser32 and Ser36, ubiquitination, and degradation, which frees the NF-κB dimers. Then, the free NF-κB

dimmer translocates from the cytoplasm into the nucleus and facilitates transcription of its target genes (Hayden and Ghosh 2004, Perkins 2007).

Different from the canonical NF-κB signaling pathways, the non-canonical NF-κB signaling pathway is thought to mainly mediate the adaptive immune functions. The activation of non-canonical NF-κB pathway relies on the stabilization of NF-κB inducing kinase (NIK). In resting cells, NIK is constantly degraded in a TRAF3-dependent manner. In brief, inhibitor of apoptosis (cIAP) proteins target NIK for ubiquitination and continuous proteasomal degradation through tumour necrosis factor receptor associated factor 2 (TRAF2) and TRAF3. TRAF3 serve as an adaptor that directly brings NIK to the TRAF2–cIAP complex through TRAF3 interaction with TRAF2(Gyrd-Hansen and Meier 2010). Upon receiving appropriate signals, TRAF3 undergoes K-48 linked ubiquitination and consequent degradation, which frees NIK from its E3 complexes. Then, the NIK is stabilized and activates its downstream kinase IKKα. The activated IKKα phosphorylates S866 and S870 on the NIK-responsive domain of p100. These two phosphorylation residues, S866 and S870 sites, serve as docking sites of the $SCF^{\beta TrCP}$ ubiquitin ligase complexes. The upstream lysine (K) residue, K856, on p100 works as the ubiquitin acceptor site. The phosphorylation and ubiquitination of p100 facilitate its proteasomal processing to p52 through the deletion of c-terminal of p100(Oeckinghaus and Ghosh 2009). Then, p52 and RelB heterodimers enter the nucleus and regulate the expression of genes, including cxcl12, cxcl13 and etc. These genes play an important in B cell homeostasis and lymph node(Oeckinghaus and Ghosh 2009).

Recent studies have revealed the unexpected role of non-canonical NF-κB signaling pathway in innate immunity (Jin, Hu et al. 2014). Mice and cells with genetic deficiencies in

non-canonical NF-κB components produced more type I IFN upon dsRNA virus infection. As a result, the mice and cells were more resistant to viral infection. Besides, the authors found that the virus-induced activation of non-canonical NF-κB suppressed the recruitment of a histone demethylase, JMJD2A and transcriptional factor RelA to the *ifnβ* promoter, which play important role in the *infβ* transcription (Jin, Hu et al. 2014). In this way, non-canonical NF-κB signaling pathway works synergistically with canonical NF-κB signaling pathway to regulate type I IFN induction and thus, is involved in host anti-virus response.

While there has been tremendous progress in revealing the NF-κB signaling pathways in the context of different situations, it still remains to be seen what is the mechanistic details regarding stimulation-specific activation of IKK complex. The scaffold complexes are thought to serve as a platform in determining NF-κB activation in different context. Among different scaffold proteins, members from Caspase Recruitment domain(CARD)- and membrane-associated guanylate kinase-like domain-containing protein (CARMA) , play an important role in regulating IKK activities(Blonska and Lin 2011).

CAMAR family has three members, CARMA1, CARMA2 and CARMA3, which are encoded by different genes. They are conservative among different species and share very similar structure homology. There is an N-terminal CARD domain, followed with a coiled-coil domain(C-C), a PDZ domain, an SH3 domain, and a the C-terminal guanylate kinase-like (GUK) domain in all family members. Each domain has its own unique function and together contributes to overall protein functions. Since the functions of CARMA1 are well studied, we will take CARMA1 as an example to introduce the function of domains located in CARMA family proteins. Original study suggested that CARMA1 was required for T cell

receptor (TCR)-induced NF-κB activation (Gaide, Favier et al. 2002, Wang, You et al. 2002, Blonska and Lin 2011). In resting status, CARMA1 is kept in the inhibitory conformation. Upon stimulation, CARMA1 is recruited into the immunological synapse through its MAGUK domain and its adaptor protein known as adhesion and degranulation-promoting adapter protein. In immunological synapse, PKCβ (in the B cells) or PKCθ (in the T cells) can phosphorylate CARMA1 at the linker region between the C–C and PDZ domain, which leads to the release of CARMA1 autoinhibition(Matsumoto, Wang et al. 2005, Sommer, Guo et al. 2005). Then, the "activated" CARMA1 undergoes auto-oligomerization and recruits its partner B-cell lymphoma (Bcl10) to form CARMA1/Bcl10 complex (Jiang and Lin 2012). In the complex, CARMA1 serves as nucleator of Bcl10 polymerization. Then, CARMA1/Bcl10 complex further interacts with paraCASPASE mucosa-associated lymphoid tissue lymphoma translocation protein 1(MALT1) to form CBM signalosome and regulates NF-κB activities (Qiao, Yang et al. 2013).

Although CARMA proteins shared very similar domains, they have different tissue distribution. CARMA1 is only expressed in the hematopoietic tissues, whereas CARMA3 is expressed in the non-hematopoietic tissues and CARMA2 is expressed in the placenta, skin and mucosal tissues (Bertin, Wang et al. 2001, Gaide, Martinon et al. 2001, McAllister-Lucas, Inohara et al. 2001, Wang, Guo et al. 2001). The distinct tissue distribution of CARMA proteins indicates that they may regulate NF-κB signaling pathway by forming the complex with BCL10 and MALT1 in a similar manner but in different tissues. Consistent with this concept, BCL10 and MALT1 are expressed in all tissues(Jiang and Lin 2012).

Although the role of CARMA1 in NF-κB signaling pathway had been intensively studied, the function of other CARMA proteins has not been well characterized. Original studies showed that CARMA3 interacted with Bcl10 and activated NF-κB, when they are overexpressed in the mammalian cells (Wang, Guo et al. 2001). The following studies mainly focus on the role of CARMA3 in some GPCRs signaling pathways. GPCRs are also known as seven-transmembrane domain receptors (7TM receptors), serpentine receptors, and G protein-linked receptors (GPLR), which comprises the largest integral membrane protein family encoded in the human genome with nearly 1000 members. Many of them can activate NF-κB through PKCs(Jiang and Lin 2012). Since CARMA1works downstream of PKC in antigen receptor-induced NF-κB activation, it is reasonable to hypothesize that CARMA3 plays a similar role downstream of PKC and is involved in some GPCR-induced NF-κB activation. Indeed, the researchers showed there were the defects of IKK and NF-κB activation in CARMA3 deficient mouse embryonic fibroblasts (MEFs) after exposure to lysophosphatidic acid and endothelin-1, which are ligands for two distinct GPCRs. Mechanistically, CARMA3 interacts with Nemo and regulate Nemo-associated polyubiquitination, by which CARMA3 deficiency leads to the impaired kinase activity of IKK complex(Grabiner, Blonska et al. 2007). Consistently, it has been found that Bcl10 and MATL1 also play an essential role in some GPCR-induced NF-κB activation in different cellular context (McAllister-Lucas, Ruland et al. 2007, Wang, You et al. 2007, Rehman and Wang 2009, McAllister-Lucas, Jin et al. 2010). In summary, these studies suggest that CBM complex is required for GPCR-induced NF-κB activation.

Recently, a study has revealed the important role of CARMA3 in the epidermal growth factor receptor (EGFR)-induced activation of NF-κB (Jiang, Grabiner et al. 2011). EGFR is a transmembrane tyrosine kinase receptor and belongs to the HER family of receptor. EGFR plays an essential role in regulating cell proliferation and differentiation, by which EGFR contributes to a number of malignancies. EGFR activates many downstream signaling cascades, including signaling pathway leading to activation of NF-κB signaling pathway, through its receptor tyrosine kinases (RTK). Both CARMA3 and BCL10 deficiency impairs EGF-induced activation of the IKK complex, resulting in a defect of IκBα phosphorylation and NF-κB activation. Furthermore, CARM3 and BCL10 contribute to EGFR-associated malignancy both *in vivo* and *in vitro* (Jiang, Grabiner et al. 2011). Several studies support the clinical significance of CARMA3 in different types of cancer. For example, in non-small-cell lung cancer (NSCLC), the overexpression of CARMA3 correlates with cancer progression, EGFR mutation and overexpression (Li, Qu et al. 2012). Besides, in colon cancer, CARMA3 is overexpressed, which facilitates the disease progression by regulating NF-κB mediated transcription of cyclin D1 (Miao, Zhao et al. 2012).

Although significant progresses have been made to understand the function of CARMA3 in NF-κB signaling pathway, the precise mechanism remains largely unknown. Future investigations are needed to answer these questions: 1) how is CARMA3 activated in different cellular context? 2) How is the CARMA3 linked for the receptors? 3) Which PKCs is involved in regulating CARMA3 complex? 4) Does CARMA3 contribute to other signaling pathways or diseases? These studies will provide us the insight into the molecular

mechanism of CARMA3 in NF-κB signaling pathway, by which the researchers can develop interference therapeutic targeting CARMA3 for cancer and other diseases.

1.5 Influenza and VSV

Influenza or flu is an infectious disease caused by viruses, which are capable of infecting many animals including birds and mammals. Seasonal influenza virus in humans leads to widespread epidemics and is a serious public health problem. For example, the 1918 flu pandemic was the most lethal and famous outback. 1918 influenza pandemic lasted from 1918 to 1919. Although the exact number of people who died from the disease was unknown, it was estimated that 50 to 100 million people died during the flu outbreak. The death of millions people might be due to the high infection rate and extreme severity of the symptoms, which may be caused by virus-induced cytokine storm(Patterson and Pyle 1991). Even in modern society, the influenza pandemic endangers people lives. The threat of influenza virus to public health urges researchers to better understand influenza virus and its-related host immune response, which may facilitate developing the corresponding therapeutic interference.

Influenza virus is RNA virus, which belongs to the family of Orthomyxoviridae. The influenza virus is classified into three types, A, B and C. Among them, influenza A virus is the most common one and usually causes the most serious problems in humans(Medina and Garcia-Sastre 2011). Additionally, our research mainly focused on influenza A virus and its

related host immune response. Therefore, in the following sections of this chapter, we will mainly focus on influenza A virus.

Influenza A viruses are negative-sense, single-stranded RNA virus. Its segmented genome consists of eight single-stranded negative-sense RNA molecules encoding 11 or 12 viral proteins. These viral proteins are nuclear export protein(NS2), the host antiviral response antagonist non-structural protein 1(NS1), the matrix protein M1, the ion channel M2, the receptor-binding protein haemagglutinin (HA), the sialic acid-destroying enzyme neuraminidase(NA), nucleoprotein(NP), the components of the RNA-dependent RNA polymerase complex(PB1, PB2 and PA) and N40(Wise, Foeglein et al. 2009, Medina and Garcia-Sastre 2011).

These viral proteins play several roles for virus to complete its life cycle in host cells. Specifically, HA proteins on the viral envelop interact with host cell receptors containing terminal α-2,6-linked or α-2-3 linked sialic acid moieties, by which viruses are attached to the host cells(Wagner, Matrosovich et al. 2002). Then, HA proteins are cleaved by cellular protease to expose HA peptide, which is prerequisite for the fusion between viral envelop and the cellular endosomal membrane(Steinhauer 1999). In this way, HA proteins determine host tropism and systematic spread, affecting disease severity. When viruses enter cellular endosome, the acidification of the vesicles opens the minor virus envelop protein M2, which leads to acidification of the core of the virion(Pinto and Lamb 2006, Bouvier and Palese 2008, Liu, Zhang et al. 2012). The process is required for uncoating and cytoplasmic release of the ribonucleoprotein complex (RNP), where viral RNA genome is wrapped around NP. Then, the complex is transported to the nucleus, when the negative-sense viral RNA((-) VRNA) is

transcribed and replicated by the RNA-dependent RNA polymerase. During this process, three different types of RNA molecules are generated, including the complementary positive-sense RNA((+)cRNA), negative-sense small viral RNAs(svRNAs) and the viral mRNAs. cRNA severs as a template to replicate more vRNA(Cros and Palese 2003). svRNAs play an important role in regulating the change from transcription to replication(Perez, Varble et al. 2010). The viral mRNAs either are transferred to the cytoplasm for the translation of viral protein or remain in nucleus. Some newly synthesized viral proteins are secreted onto the cell surface through the Golgi apparatus, such as NA and HA and M2. Some viral proteins are transferred into the nucleus to wrap progeny viral genome to form RNP complex for virus packaging. Other viral proteins have multiple functions in host cells, including repressing the IFN-mediated antiviral response, degrading cellular mRNA, and etc. In plasma membrane, the influenza virus M1 protein facilitates the formation of virus particles. Then, budding occurs and detaches from cells. The neuraminidase activity of NA is essential for budding, by which the SA of the cellular and viral glycoproteins is destroyed. After virus completes its life cycle in host cells, the host cells die(Medina and Garcia-Sastre 2011).

HA and NA not only play crucial roles in virus life cycle but also determine virus serotypes. Until now, 18 known types of HA proteins and 11 known types of NA proteins have been identified (Tong, Li et al. 2012). Base on the types of HA and NA protein on the surface of the viruses, the influenza A virus are divided into different subtypes. For example, H1N1 virus designates an influenza virus subtypes with a type 1 HA protein and a type 5 NA proteins. Theoretically, there are possible 198 combinations of HA and NA proteins with their corresponding virus subtype. In fact, virus strains circulating in birds are from 16 HA

subtypes and nine NA subtypes, while virus strains circulating among humans are H1N1, H1N2 and H3N2. H1N1 is responsible for “Spanish flu” and the 2009 swine flu outbreak, H2N2 leads to the pandemic of “Asian flu” in the late 1950. H3N2 results in the Hong Kong flu in the late 1960s (Air 1981, Nobusawa, Aoyama et al. 1991, Russell, Gamblin et al. 2004, Fouchier, Munster et al. 2005).

Since HA and NA determines serotypes of influenza virus, any change in two proteins affects host susceptibility and pathogenesis. Changes in HA and NA proteins occur through two different ways. One is antigenic drift, which is characterized by the amino acid changes in HA and NA proteins of new virus strains. The antigenic drift is caused by the virus' RNA polymerase with no proofreading mechanism, which results in an error rate between 1×10^{-3} and 8×10^{-3} substitutions per site per year during the replication of viral genome replication. Therefore, most of newly synthesized viruses are mutants, which partially overcome the protective immunity and are mainly responsible for seasonal influenza pandemic. Another way is antigenic shifts, which is characterized by the dramatic change in HA subtype. Antigenic shifts help viruses to quickly overcome the protective immunity and to infect new host species, leading to the emergence of new pandemics(Medina and Garcia-Sastre 2011).

VSV is a negative strand RNA virus too, which belongs to the rhabdovirus family, and has been widely used to study the host innate immune response against single strand RNA virus. VSV genome is a single molecule of negative-sense RNA with 11,161 nucleotides long, encoding five major viral proteins. These viral proteins are nucleoprotein, matrix protein(M), phosphoprotein, large protein(L) and G protein(Lichty, Power et al. 2004).

Those proteins play several roles in different stages of viral life cycle and facilitate virus to complete its life cycle in host cells. Specifically, VSVG is required for viral entry by mediating virus attachment to an LDLR family member present on the cell surface. Following viral attachment, the VSV-LDLR complex undergoes quick endocytosis, where the viral envelope is fused with endosomal membrane and releases viral genome to the cytoplasm. In cytoplasm, the virus genome is either replicated with the facilitation of viral protein VSV L protein and phosphoprotein or translated for new viral proteins(Finkelshtein, Werman et al. 2013).The mature viral protein and new virus genome are packaged into a new virus budding from the host cells.

Since VSVG has a broad host range, VSV is capable of infecting many distinct mammalian and nonmammalian cell types. Therefore, VSV can infect many species including cattle, horses, pigs, insects and humans. In some cases, it can cause flu-like symptom in infected humans (Lichty, Power et al. 2004). Therefore, VSV is a good experimental tool for investigating host innate immune responses against RNA virus infection.

.

CHAPTER 2: MATERIALS AND METHODS

2.1. Antibodies, Plasmids, and Reagents

Antibodies against p-TBK1(Ser172)(#5483), p-IRF3(Ser396)(#4947), TBK1(#3013), RIG-I(#4743), IκBα(#4814) were purchased from Cell Signaling Technology. Antibodies against IRF3 (FL-425), BCL10 (H-197), TRAF6 (H-274), ACTIN (#8432, clone C-2), HA (sc-805), OctA-probe (D-8) (FLAG: sc-807), were from Santa Cruz Biotechnology. The specific CARMA3 antibody was generated by immunizing rabbits with the small peptide VRGRILQEQARLVWVEC, matching to the C terminus of human and mouse CARMA3. Then, the antibody was purified by the same peptide-conjugated columns. The MAVS antibody was a kind gift from Dr. Zhijian "James" Chen's Lab. NF-κB or OCT-1binding-site-specific probes were obtained from Promega. TRIzol reagent (15596-026), Lipofectamine 2000 Transfection Reagent (11668-019), Superscript III First-Strand Synthesis system (18080-051) were obtained from Invitrogen. Fast SYBR Green Master Mix was purchased from Applied Biosystems (4385612). Mouse IFN Beta ELISA Kit was obtained from PBL Assay Science (42400-2) , while Mouse IL-6 ELISA Ready-SET-Go KIT was purchased from Affymetrix bioscience(88-7064-86). Poly (I:C) LMW(tlrl-picw-250), 5'ppp-dsRNA(tlrl-3prna-100) and 5ppp-dsRNA control(tlrl-3prna) were purchased from InvivoGen. Influenza A/PR/8/34(H1N1) was purchased from Charles River. NF-κB Inhibitors (213546-53-3), polybrene (sc-134220) was obtained from Santa Cruz. Cycloheximide was purchased from Sigma (C7698). PCMV-Tag4-CARMA3 and its

derivatives (CD-CC, ΔCD-CC, ΔSH3-GUK, ΔGUK) that encode Flag-tagged CARMA3 WT or mutants have been described previously (Sun and Lin 2008). RIG-I, IKKε, MAVS and TBK1 plasmids were obtained from Addgene. Myc-tagged BCL10 has been described previously (Blonska, Pappu et al. 2007). shRNA against GFP, CARMA3 or BCL10 were obtained from Sigma.

2.2. Cell Cultures

WT, CARMA3 deficient, BCL10 deficient and MALT1 deficient mouse embryonic fibroblasts (MEF) cells were isolated from mouse embryos from corresponding knockout mice and prepared as previously described (Grabiner, Blonska et al. 2007). MEF cells, human neuroblastoma SKNAS cells and human lung adenocarcinoma epithelial A549 cells were cultured in Dulbecco's modified Eagle medium (DMEM) supplemented with 10% fetal bovine serum, 100 U/ml penicillin, and 100 mg/ml streptomycin. MEF cells were grown in 8.5% CO_2 at 37°C and passaged every three days. SKNAS and A549 cells were grown in 5% CO_2 at 37°C and passaged every two days.

2.3. Electrophoretic Mobility Shift Assay (EMSA)

Nuclear extraction and EMSA were performed as described previously (Grabiner, Blonska et al. 2007). Briefly, nuclear extracts were isolated from 1×10^6 cells stimulated for appropriate times with different agents. Then, nuclear extracts (1–10 μg) were incubated with ^{32}P-labeled NF-κB and OCT-1 probes at room temperature for 15 minutes. After incubation,

the mixed samples were loaded into a native 10% acrylamide gel (1×Tris-borate-EDTA) and run for 85 minutes at 220V. The gels were dried in a vacuum gel drying system and then exposed to X-ray film.

2.4. Western Blotting and Immunoprecipitation

Various types of cells were lysed in a lysis buffer containing 50 mM HEPES (pH 7.4), 150mM NaCl(or in the range of 50–250 mM NaCl), 1 mM EDTA, 1% NP-40, 1 mM Na_3VO_4, 1mM PMSF, 1 mM NaF, 1mM DTT, and 1×protease inhibitor cocktail (Roche Diagnostics). The cell lysates were subjected with immunoblotting by the indicated antibodies or immunoprecipitated with various antibodies-conjugated beads. For immunoprecipitation, the antibodies-conjugated beads were incubated with the cell lysate overnight at 4˚. After incubation, the beads were washed with cold 1×PBS. Then, the precipitates were eluted by 2×loading buffer and were subjected to SDS-PAGE and immunoblot.

2.5. Quantitative RT-PCR (qRT-PCR)

Total RNA isolation was isolated using TRIzol reagent (Invitrogen) according to the manufacturer's instructions. Reverse transcription was performed by the SuperScriptIII First-Strand Synthesis System with 1 μg of total RNA according to the manufacturer's instructions with 50 μM oligo(dT) or random hexanucleotides. Then, qRT-PCRs were performed using

the cDNA with gene-specific oligonucleotide primers (10 pM each). The primers used are listed in Table 2.

2.6. Lentivirus Infection for shRNA Knockdown

Lentivirus encoding control shRNA, CARMA3 shRNA and BCL10 shRNA was generated as previously described (Jiang, Grabiner et al. 2011). Briefly, HEK 293 cells were transfected with Lentivirus plasmids with packaging vectors encoding VSV-G and Dr.82 to generate viruses. At 12 hours after transfection, the supernatant was replaced with the fresh medium. The supernatant was collected from the HEK 293 cells at 48 hours after transfection and centrifuged at 2000×g for 10 minutes to get rid of any cell debris. Then, the supernatant was incubated with target cells for infection in presence of 8 μM polybrene overnight. One day after virus infection, the infectious medium was replaced with media containing 1 μg/ml puromycin for the selection. Four days after puromycin selection, the resultant pools were used for experiments.

2.7. Semidenaturing Detergent Agarose Gel Electrophoresis(SDD-AGE)

SDD-AGE was performed as previously described (Hou, Sun et al. 2011). In brief, crude mitochondrial were isolated from cells stimulated for appropriate time with various reagents. Then, the crude mitochondrial were resuspended in 1×sample buffer containing 0.5×TBE, 10% glycerol, 2% SDS, and 0.0025% bromophenol blue. The mixed samples

were separated in a vertical 1.5% agarose gel in the running buffer (1×TBE and 0.1% SDS) for 35 min with a constant voltage of 100 V on ice. After running, the proteins were transferred to nitrocellulose membranes (Bio-Rad) for immunoblotting by indicated antibodies.

2.8. VSV and Influenza virus mouse model

Groups of six 4–6 weeks old WT and CARMA3 or BCL10 deficient mice were intranasally inoculated with 20 µl of H1N1 influenza virus at pfu=600 in PBS under isofluorane sedation. Mice survival and body weight were measured daily until 14 days post-infection (dpi). Moribund mice were considered as losing body weight >20% of their initial or exhibiting severe disease. Moribund mice were humanely sacrificed.

Groups of 4–6 weeks old WT and CARMA3 or CARMA1 mice were intranasally inoculated with 20 µl of VSV at pfu=1×10^7 in PBS under isofluorane sedation. Mice serum was harvested at 24 hours after infection, while different tissues (lung, brain and spleen) were harvested at 2 days after infection.

2.9. Influenza $TCID_{50}$ Assay

MDCK cells were cultured in high glucose DMEM containing 10% FBS and 1% Pen-Strep in a T75 at 37°C. One day before $TCID_{50}$ assay, 2×10^3 cells were seeded in 96 well plates with 150µL of medium. In next day morning, influenza samples were thawed and

homogenized on ice with 600µl medium, which was transferred into the 1st tube of the dilution series and then serially dilute 184 µL across the tubes on ice. 100 µL of diluting sample was incubated with cells at 37^{o}C for 1 hour in the presence of 1ug/ml TPCK treated trypsin. After incubation, the infectious medium was replaced with fresh 150uL DMEM with 1µg/ml TPCK treated trypsin. After 3 days of incubation, the medium was aspirated off and replaced with 200 uL of a crystal violet working stock (40 mL 1% Crystal Violet, 80 mL Methanol, 300 mL H_2O). Cells were stained with crystal violet working stock for 1 hour and rinsed with tap-water.

2.10. Luciferase Reporter Assay

Luciferase assays were performed as described previously (44). In brief, HEK 293 cells were seeded in triplicates in 12-well plates and transfected with 100 ng of NF-κB-responsive luciferase and IFNβ promoter-dependent luciferase constructs encodes the firefly luciferase and 10 ng of EF1α promoter-dependent Renilla luciferase reporter together(as a transfection control) with 1.5 µg of expression vectors for different proteins or vector controls. At 16 hours after transfection, the cells were harvested and lysed to detect luciferase activities by dual-luciferase kit (Promega).

2.11. VSV plaque assay

The medium containing virus was diluted with DMEM and prepared for VSV plaque assay. The tissue samples were homogenized and the supernatant was used for VSV plaque assay. The VSV plaque assay protocol was previously described. Briefly, at 1 hour after infection, the infectious medium in cells was replaced with complete medium containing 0.5% methylcellulose (Sigma-Aldrich) for 48 hrs. Then, BHK cells were fixed in fixation solution and stained with crystal violet working solution. Virus titers were expressed as PFU per milliliter, which counts the plaques in well. VSV plaque assay for each sample was triplicated, and the averages of the virus titers were calculated.

2.12. Isolation of crude mitochondria

Crude mitochondrial was isolated as described previously (Hou, Sun et al. 2011). Briefly, cells simulated with appropriate reagents for indicated time were washed with ice-cold PBS twice and harvested by centrifuging at 600g for 3 minutes. Hypotonic buffer was used to swell the cells for 2.5 minutes at 4°C. Hypotonic buffer contains 10mM KCl, 0.5mM EGTA, 10mM Tris-Cl, pH7.5, 1.5mM $MgCl_2$, 1mM PMSF, and 1x EDTA-free protease cocktail. Then, the swollen cells were homogenized for 40 strokes in a tight-fitting Douncer Homogenizer at 4°C. The supernatant was centrifuged at 600g for 5 minutes to remove the insoluble parts. The resulting supernatant was centrifuged at higher speed to collect the mitochondria. The crude mitochondria was resuspended in mitochondria resuspend buffer (MRB) ,containing 0.5mM EGTA, 1mM PMSF, 20mM HEPES-KOH, pH7.4, 1x EDTA-free protease cocktail, 0.8M sucrose and then, centrifuged at 7,000g for 10 minutes. The pellet

was resuspended and centrifuged again. The resulting pellet was resuspended in MRB buffer with 2% CHAPs and was incubated in ice bath for 15 min. The mitochondria lysates were mixed with 2X loading dye (1 × TBE, 10% glycerol, 4% SDS, and 0.005% bromophenol blue) containing no reduction reagents.

2.13. Bone marrow-derived macrophage (BMDM) preparation.

Primary cultures of BMDMs from WT or CARMA1 deficient mice were isolated from tibias and femurs of WT or CARMA1−/− mice as previously described (Bi, Gojestani et al. 2010, Gorjestani, Yu et al. 2011). In brief, after isolation, the mix cells were incubated in hypotonic solution for 10 minutes to get rid of erythrocytes. The resulting cells were cultured in DMEM containing 20% FBS, 55 μM β-mercaptoethanol, 100 μg/ml streptomycin, 100 U/ml penicillin, and 30% conditioned media from L929 cells expressing macrophage CSF (M-CSF) for 7 days. At 3 days after isolation, the medium was replaced with the fresh one to remove non-adherent cells. After 1 wk of cultures, cells was stained with combinations of fluorescence-conjugated monoclonal antibodies (CD11b+ and F4/80+) and analyzed by flow cytometry to assess the cellular purity. Cell population contained 86–95% CD11b+ F4/80+cells.

2.14. Splenocyte Isolation and Staining

Splenocytes were isolated from the spleen of different types of mice. Briefly, the spleens were transferred into the cell strainer in the Petri dish and washed with 1ml pre-cold PBS. The spleen was mashed by the black rubber end of 2ml syringe to relase the splenocytes into the Pertri dish. The homogenized cell suspension was transferred to a new tubes and was collected by centrifuge at 400×g for 10 minutes. The resulting cells was washed with 1ml pre-cold PBS once and were incubated with hypotonic solution for 15 minutes to get rid of erythrocytes. The resulting cells were washed with PBS again and were ready to stain with the fluorescence-conjugated monoclonal antibodies(CD11c+).

2.15. Stable isotope labeling by amino acids(SILAC) experiments

All SILAC experiment-related reagents were bought from Pierce (Thermo Scientific). SILAC-DMEM medium deficient in lysine and arginine were supplemented with L-lysine, L-arginine, 10% dialyzed fetal bovine serum, 100 U/ml penicillin, and 100 mg/ml streptomycin. HEK 293T cells expressing empty vector were cultured in the "light" medium supplemented with Lys0 (12C6) and Arg0 (12C6), while HEK293T cells transiently expressing CARMA3-FLAG were culture in the 'heavy' culture with Lys8 (13C6) and Arg10 (13C6). 48 Hours after transfection, cells were lysed in a lysis buffer containing 50 mM Tris (pH 7.4), 150mM NaCl, 1 mM EDTA, 2% DDM, and 1×protease inhibitor cocktail (Roche Diagnostics). The same amounts of cell lysates of more than 1 mg were immunoprecipitated with FLAG antibodies-conjugated beads. The proteins-bead were washed 3 times with cold lysis buffer. The proteins were eluted with FLAG peptides(100μg/ml) and merged together before subjecting to SDS-PAGE and silver staining. Then, gel slices from SDS-PAGE lanes were excised and digested with trypsin. Peptides generated by protease digestion were fractionated on a analytical column (75 μm ID, 100 mm in length) packed with C18 resin by Dionex Ultimate 3000 nanoLC system (Thermo Scientific). The

column was coupled in-line to a Q Exactive mass spectrometer (Thermo Scientific) equipped with a nano-electrospray ion source. MS/MS spectra (resolution: 17,500 at m/z = 200) were acquired in a data-dependent mode, whereby the top 15 most abundant parent ions were subjected to further fragmentation by higher energy collision induced dissociation (CID). MS raw data was searched against Swissprot database(Homo Sapiens) using mascot searching engine and was quantified with mascot distiller. The MS tolerance was set to 15 ppm, and the MS/MS tolerance was set to 20 mmu. To define a reliable peptide, the score should exceed the identity threshold given by Mascot, meanwhile, the false discovery rate (FDR) at protein levels was set to 0.01. For the quantification of the identified proteins, Mascot Distiller software (Version 2.5.1.0) was used to calculate the ratios between the heavy- and light-labeled IP products (H/L) at both peptides and proteins level. For the quality control, the threshold of standard error for each XIC pair was set to 0.1, and the threshold of correlation coefficient between the predicted and observed precursor isotope distributions was set to 0.7. Only peptides exceeding the homology threshold were used for the quantification.

CHAPTER 3: RESULTS

3.1.CARMA3 deficiency caused mouse to be more resistant to influenza infection.

Using collaborative cross (CC) mouse model of influenza infection, the researchers found that genetic variations in CARMA3 regulated differential response phenotypes to influenza infection(Ferris, Aylor et al. 2013). However, the role of CARMA3 in influenza infection remains largely unknown. To confirm the important role of CARMA3 in influenza infection, we infected WT and CARMA3 deficient mice with H1N1 influenza virus at pfu=600. Then, we measured the change of mice bodyweight daily until 14 days after virus infection. We found that WT mice lose more body weight than CARMA3 deficient mice until the end of experiments (Fig.5A). Next, we decided to detect the virus replication in mice. The WT, CARMA3+/- and CARMA3 deficient mice were intranasally injected with influenza at pfu=500. Two days later, we harvested the lungs from mice. The influenza virus titer in lungs was measured by tissue culture infectious dose ($TCID_{50}$) assays. We found that there was less virus titer in lungs from CARMA3 deficient mice than that from WT or CARMA3 Het mice. It might explain why WT mice losed more body weight than CARMA3 deficient mice during the experiments (Fig.5B). These data suggested that CARAM3 deficiency caused mice more resistant to influenza infection.

After influenza virus infection, its RNA genome is recognized by PRRs to trigger the production of proinflmmatory cytokines and type I IFNs(Medina and Garcia-Sastre 2011).

Among them, IL6 and IFNβ are the important cytokines. The transcription of IL6 is controlled by transcription factor NF-κB, while the expression of IFNβ is mainly mediated by the transcriptional factor IRF3 (Sato, Suemori et al. 2000, Xiao, Hodge et al. 2004, Honda, Yanai et al. 2005). The lung and serum were harvested from the infected mice 3 days after infection. The level of serum IL6 and lung IFNβ were measured by ELISA and qRT-PCR, respectively. We found that CARMA3 deficient mice had more lung IFNβ but less the serum IL6 after virus infection (Fig.6).

3.2.CARMA3 deficiency caused mice to be resistant to VSV infection.

VSV also is a negative single-stranded RNA virus. To check whether CARMA3 contributes to the variable host responses to RNA virus infection, we challenged WT and CARMA3 deficient mice intranasally with VSV-GFP at 1×10^7 pfu. We harvested serum and tissues at 24 hrs and 48 hrs after infection, respectively. The virus titer in different tissues was measured by viral plaque assay. The level of serum IL6 and IFNβ were measured by ELISA. There was less virus titer in the CARMA3 deficient mice than that in WT mice in different tissues including spleens, olfactory bulbs (OB) and lungs, which suggested the negative role of CARMA3 in VSV infection *in vivo*(Fig.7). Next, we decided to check the level of serum IL6 and IFNβ. Surprisingly, the level of serum IL6 and IFNβ was comparable between WT and CARMA3 deficient mice. Since the CARMA3 is only expressed in non-hematopoietic tissues, we decided to further check the local IFNβ and IL6 production by

qPCR in OB(Jiang and Lin 2012). We found that there was more IFNβ in the OBs from CARAM3 deficiency mice than those from WT mice (Fig.8).

To check the negative role of CARMA3 in VSV infection *in vitro*, we infected primary WT and CARMA3 deficient MEF cells with VSV at MOI=10. One hour after infection, the infectious medium was replaced with fresh medium to get rid of uninfected virus. At 24 hrs after infection, we measured the virus titer in supernatant using viral plaque assay. We found that there was less viral titer in supernatant from CARAM3 deficient cells than that from WT cells. Next, we obtained lentivirus constructions encoding control shRNA and CARMA3 shRNA, which significantly inhibited CARMA3 mRNA transcription. We infected different cell lines, such as A431, Hela with lentivirus construction encoding control shRNA or CARMA3 shRNA. Then, we examined the virus titer from supernatant using the protocol as described previously. We found that there was less viruses in the supernatant from CARMA3 knockdown cells than that from control knockdown cells (Fig.11). It suggested that CARMA3 deficiency or knockdown caused cells more resistant to VSV infection.

3.3. The activation of NF-κB signaling pathway was reduced in CARMA3 deficient cells after VSV infection.

It was found that the CARMA3 was required for NF-κB activation induced by some GPCRs and receptor tyrosine kinases in non-hematopoietic tissues (Grabiner, Blonska et al. 2007, Klemm, Zimmermann et al. 2007, McAllister-Lucas, Ruland et al. 2007, Mahanivong, Chen et al. 2008). To determine whether CARMA3 was involved in VSV-induced NF-κB

activation, we first infected WT and CARMA3 deficient MEF cells with VSV at MOI=3. We detected the activation of NF-κB signaling pathway by EMSA at different time points. We found the activation of VSV-induced NF-κB was decreased in CARMA3 deficient MEF cells, compared to WT cells. It suggested that CARMA3 played a positive role in VSV-induced NF-κB activation (Fig.9A). To further confirm the positive role of CARMR3 in VSV-induced NF-κB activation, we decided to check the production of IL6 in WT and CARAM3 deficient MEF cells upon VSV infection, since the transcription of IL6 is controlled by NF-κB (Xiao, Hodge et al. 2004). The level of IL6 was measured at 6,12 hours after virus infection by both qPCR and ELISA. We found there was less production of IL6 in CARAM3 deficient MEF cells than that in WT cells (Fig.9 B&C).

3.4. CARMA3 deficient cells increased IFN-β production after VSV infection.

IFNβ secreted by cells plays an important role in inhibiting virus infection(Schneider, Chevillotte et al. 2014). Since previous data showed that tissues in CARMA3 deficient mice produced more IFNβ after virus infection, we decided to detect the production of IFNβ in cells after virus infection. WT and CARMA3 deficient MEF cells were infected with VSV at MOI=3. At the different time points, the production of IFNβ was measured by qPCR or ELISA. We found that CARMA3 deficient cells produced more IFNβ after virus infection, compared to WT cells (Fig.10 A&B).

It has been established that the production of IFNβ was controlled by TBK1-IRF3 signaling pathway. Since there was increased production of IFNβ in CARMA3 deficient cells

after VSV infection, we decided to check the activation of TBK1-IRF3 signaling pathway in different cell types after virus infection. The WT and CARMA3 deficient MEF cells were infected with VSV at MOI=3. The activation of TBK1-IRF3 signaling pathway was measured by immunoblotting using specific p-TBK1 (Ser 172) and p-IRF3 (Ser 396) antibodies. We found that the phosphorylation of TBK1 and IRF3 were increased in CARMA3 deficient MEF cells. It suggested that the activation of TBK1-IRF3 signaling cascade was enhanced in CARMA3 deficient cell (Fig.10C). These data suggested that CARMA3 played a negative role in the virus-induced activation of TBK1-IRF3 signaling pathway.

3.5 CARMA3-deficient MEF cells had decreased activation of NF-κB signaling pathway and thereby, produced less IL6 after poly(I:C) transfection.

Both VSV and influenza are ssRNA viruses. When they infect cells, their RNA genome are recognized by both TLR3 and RIG-I(Jacobs and Coyne 2013). To specify the role of CARMA3 in RIG-I/MAVS signaling pathway, we decided to transfect cells with specific ligands of the RIG-I/MAVS signaling pathway such as poly (I:C) and 5'ppp-dsRNA. Poly (I:C) is a synthetic analog of dsRNA, a PAMP associated with RNA virus infection. Naked poly(I:C) is recognized by TLR3 on the cell surface(Lester and Li 2014). However, when poly (I:C) is transfected into cells, it can be specifically recognized by cytoplasmic RIG-I and MDA5 receptors in a cell-dependent manner(Kato, Sato et al. 2005, Gitlin, Barchet et al. 2006). WT and CARAM3 deficient MEF cells were transfected with 1 ug/ml poly(I:C) by

lipotofactamine 2000. We measured the activation of NF-κB by EMSA and the production of IL6 by qPCR and ELISA. Both the activation of NF-κB and the production of IL6 were decreased in CARMA3 deficient cells after poly(I:C) transfection at the different time points. It suggested the positive role of CARMA3 in RIG-I/MAVS-mediated NF-κB signaling pathway (Fig.12).

3.6 CARMA3-deficient MEF cells had increased activation of IRF3 signaling pathway and thereby, produced more IFNβ after poly (I:C) transfection.

WT and CARMA3 deficient MEF cells were transfected with poly (I:C) with lipotofactamine 2000. The activation of TBK1-IRF3 signaling pathway was measured by immunoblotting using the specific p-IRF3 (Ser396) antibodies. We found that IRF3 signaling pathway was activated in WT cells after poly (I:C) transfection, but the activation was increased in CARMA3 deficient MEF cells (Fig.13D). Consistently, the production of type I IFNs in CARAM3 deficient MEF was more than that in WT cells after poly(I:C) transfection. It suggested that CARMA3 negatively regulated RIG-I-mediated TBK1-IRF3 signaling pathway (Fig.13 A, B and C).

3.7 CARMA3-deficient MEF cells produced less IL6 but more IFNβ after dsRNA transfection.

To verify the role of CARMA3 in RIG-I/MAVS signaling pathway, we decided to use another specific ligand: 5' ppp-dsRNA. 5' ppp-dsRNA is a synthetic ligand specific for RIG-I. The WT and CARMA3 deficient MEF cells were transfected with 1ug/ml 5' ppp-dsRNA by lipofectamine 2000. We measured the production of type I IFNs and IL6 by qPCR and ELISA. We found that CARMA3 deficiency impaired 5' ppp-dsRNA-induced IL6 production (Fig.14). On the other hand, CARMA3-deficient cells produced more type I IFNs after ligand transfection (Fig.15). Together, these data suggested the dual role of CARMA3 in RIG-I/MAVS-mediated activation of NF-κB and IRF3 signaling pathways. Specifically, CARMA3 played a positive role in RIG-I/MAVS-mediated NF-κB signaling pathway, but a negative role in TBK1-IRF3 signaling pathway.

3.8 BCL10 deficient cells had decreased activation of NF-κB signaling pathway, but increased activation of TBK1-IRF3 signaling pathway after virus infection and poly (I:C) transfection.

Previous studies demonstrated that CARMA3 interacted with BCL10 and MALT1 to form CBM complex, which regulated the activities of IKK complex through mediating NEMO-associating polyubiquitination (Grabiner, Blonska et al. 2007). Therefore, we hypothesized that BCL10 is involved in RIG-I-mediated NF-κB activation. To test the hypothesis, we treated WT and BCL10 deficient MEF cells with VSV infection or poly (I:C) transfection. The production of IL6 was measured by both qPCR and ELISA. We found that BCL10 deficiency impaired both virus infection and poly (I:C) transfection-induced IL6

production (Fig.18). It suggested that BCL10 played a positive role in RIG-I /MAVS-mediated NF-κB signaling pathway, which was similar to CARMA3.

Next, we decided to test the role of BCL10 in RIG/MAVS-mediated TBK1-IRF3 signaling pathway. We treated WT and BCL10 deficient MEF cells with VSV infection and poly (I:C) transfection. We detected the activation of TBK1-IRF3 signaling pathway and the production of type I IFNs, using the methods as described previously.BCL10 deficiency caused cells to produce more type I IFNs after both VSV infection and poly(I:C) transfection. Consistently, the activation of TBK1-IRF3 signaling pathways was enhanced in BCL10-deficienct cells after treatments. It suggested that BCL10 played a negative role in the activation of RIG-I/MAVS-mediated TBK1-IRF3 signaling pathway, which is similar to CARAM3 (Fig.17).

To further demonstrate the role of CARMA3 and BCL10 in RIG-I/MAVS signaling pathways, we obtained three different lentivirus constructions encoding control shRNA, CARAM3 shRNA and BCL10 shRNA. We infected A549 cells with different lentiviruses to significantly suppress the expression of CARMA3 or BCL10. We compared the activation of NF-κB and IRF3 signaling pathway among cells stably expressing control shRNA, CARMA3 shRNA and BCL10 shRNA upon VSV infection or poly (I:C) transfection. Cells with control knockdown produced IL6 and IFNβ after VSV infection or poly (I:C) transfection, whereas cells with CARMA3 or BCL10 knockdown produced more IFNβ, but less IL6 after treatments(Fig.20). Consistently, the activation of TBK1-IRF3 signaling pathway was enhanced in cells with CARMA3 or BCL10 shRNA, compared to cells with control knockdown (Fig.19).

3.9 BCL10 deficiency caused mice to be more resistant to VSV infection.

Our previous data suggested that CARMA3 deficiency led to mice more resistant to VSV infection. Since BCL10 always functions together with CARAM3 to form a complex, we hypothesized that BCL10 deficiency also causes mice to be more resistant to VSV infection (Grabiner, Blonska et al. 2007). Groups of 6-8 weeks WT and BCL10 deficient mice were intranasally injected with VSV-GFP at pfu=1×10^7. The virus titer in different tissues was measured by viral plaque assay. WT mice had more virus titer in different tissues than BCL10 deficient mice did. It suggested that BCL10 deficiency caused mice to be more resistant to VSV infection, which is similar to CARAM3 deficient mice (Fig.21).

Together, our data suggested that BCL10 functioned as a partner with CARMA3 to regulate RIG-I/MAVS-mediated signaling pathways.

3.10 MALT1 deficiency did not impair VSV infection or poly (I:C) transfection-induced NF-κB activation.

Previous study showed that MALT1 was an important component of CBM complex, which regulated NF-κB signaling pathway through IKK complex (Grabiner, Blonska et al. 2007). Therefore, we hypothesized that MALT1 contributes to VSV-induced NF-κB activation. We treated WT and MALT1 deficient MFE cells with VSV infection. We found that the activation of NF-κB and the production of IL6 were comparable between two cells

types after virus infection (Fig.22C& Fig.23). It suggested that MALT1 deficiency did not impair RIG-I/MAVS-mediated NF-κB activation.

3.11 MALT1 deficiency did not enhanced VSV or poly (I:C) transfection-induced IRF3 activation.

Our previous data showed that both CARMA3 and BCL10 play a negative role in VSV infection and poly (I:C) transfection-induced IRF3 activation. Additionally, MALT1 always forms a complex with CARMA3 and BCL10 in context of NF-κB signaling pathway. Therefore, we hypothesized that MALT1 plays a negative role in RIG-I/MAVS-mediated IRF3 activation. To test the hypothesis, we infected the WT and MATL1 deficient MEF cells with VSV. We measured the activation of TBK1-IRF3 signaling pathway and the production of type I IFNs according to protocols previously described. We found the activation of IRF3 signaling pathway and the production of type I IFNs were comparable between WT and MALT1 deficient MEF cells(Fig.22 A and B& Fig. 24). It suggested that MALT1 did not play a role in RIG-I/MAVS-mediated IRF3 activation.

3.12 The inhibition of NF-κB signaling pathway did not enhance the activation of IRF3.

Both NF-κB and IRF3 are transcription factors. When they are active, they enhance expression of genes in response to different stimulus(Oeckinghaus and Ghosh 2009).

Additionally, based on our data, we found that NF-κB signaling pathway acted prior to TBK1-IRF3 signaling pathway. Therefore, we hypothesized that NF-κB target genes inhibit the activation of IRF3. To test the hypothesis, we pretreated the primary MEF with NF-κB inhibitors and then infected the cells with VSV at MOI=3. The NF-κB inhibitor is a small peptide, which specially targets the nuclear translocation signals in p50 and thereby, blocks the nuclear translocation of the active NF-κB dimmers. The activation of NF-κB signaling pathway was measured by EMSA, while the activation of IRF3 was measured by immunoblotting using specific p-IRF3 antibody. NF-κB signaling pathway was activated by VSV infection at different time points, whereas the activation was partially blocked by the treatment of NF-κB inhibitor. It suggested that the NF-κB inhibitor worked well in the experiments. On the other hand, the IRF3 was phosphorylated at different time points after VSV infection. However, the IRF3 phosphorylation was not enhanced with the treatment of NF-κB inhibitor during VSV infection. It suggested that NF-κB target genes did not inhibit IRF3 activation (Fig.25). In other words, crosstalk between NF-κB and IRF3 signaling pathway was not critical for the increased activation of IRF3 signaling pathway in CARMA3 deficient cells.

3.13 The inhibition of new protein synthesis did not rescue the enhanced activation of TBK1-IRF3 signaling pathway in CARAM3 deficient cells

To further confirm it, we decided to pretreat primary MEF cells with 10 μg/ml

cycloheximide (CHX) to block new protein synthesis. Then, cells were transfected with 1μg/ml poly (I:C) by lipofectamine 2000. At the different time points, the activation of IRF3 was measured by immunoblotting using specific p-IRF3 antibody. Compared to WT MEF cells, the phosphorylation of IRF3 was increased in CARMA3 deficient MEF cells. The enhancement cannot be blocked by CHX treatment. It suggested that CARMA3 and BCL10 directly regulated RIG-I/MAVS-mediated signaling pathways, not through the secondary effect (Fig.26).

3.14 In RIG-I/MAVS signaling pathway, CARAM3 worked together with MAVS.

Our previous data suggested that CARMA3 and BCL10 were directly involved in RIG-I/MAVS signaling pathways. Next, we decided to investigate how CAMRA3 and BCL10 regulated IRF3 or NF-κB signaling network. To do that, we infected HEK 293 cells with lentivirus encoding control shRNA, CARMA3 shRNA or Bcl10 shRNA. Then, we overexpressed MAVS-FLAG in those cells together with NF-κB-responsive luciferase construct or IFNβ luciferase reporter plasmids. The overexpression of MAVS could activate both NF-κB and IRF3 signaling pathways in cells with control knockdown. There is hyperactivation of IRF3 and hypoactivation of NF-κB in cells with CARMA3 or BCL10 knockdown. It suggested that CARMA3 and Bcl10 worked together with MAVS (Fig.27A).

3.15 In MAVS/RIG-I signaling pathway, CARAM3 worked upstream of TBK1 and IKKε

Next, we overexpressed TBK1-FLAG or IKKε-FLAG in HEK 293 cells stably expressing control shRNA, CARMA3 shRNA or BCL10 shRNA, together with NF-κB-responsive luciferase constructs or IFNβ luciferase reporter plasmids. Overexpression of TBK1-Flag induced the activation of both NF-κB and IRF3 signaling pathway in cells with control knockdown, while the activation of these two signaling pathways was comparable in cells with CARMA3 and BCL10 knockdown. When it came to IKKε overexpression, we found the similar results. It suggested that CARMA3 worked upstream of TBK1 and IKKε in MAVS/RIG-I signaling pathway (Fig.27 B, C&D).

Together, our data suggested that CAMRA3 worked downstream of MAVS, but upstream of TBK1 and IKKε.

3.16 CARMA3 interacted with MAVS.

Similar to CARMA3, MAVS and RIG-I proteins contain CARD domain. It was established that CARD domain was important for the interaction between CARD-domain containing proteins(Blonska and Lin 2011). Additionally, our previous data showed that CARMA3 worked downstream of MAVS. Therefore, we hypothesized that CARMA3 interacts with MAVS. To test the hypothesis, we decided to firstly detect the interaction between CARMA3 and MAVS, when they are overexpressed in HEK 293 cells. We

overexpressed CARMA3-HA with MAVS-FLAG or RIG-I-FLAG in HEK 293 cells. At 24 hours after transfection, we immunoprecipitated(IP) MAVS or RIG-I using anti-Flag antibody conjugated beads. The immunoprecipitated complex and cell lysates were subject to immunoblotting using indicated antibodies. We found that both CARMA3 and BCL10 interacted with MAVS, while BCL10 not CARMA3 was associated with RIG-I (Fig.28A).

To further confirm MAVS's interaction with CARMA3, we decided to check the endogenous interaction between CARMA3 and MAVS. We infected immortalized CARMA3 deficient MEF with lentivirus constructions encoding CARMA3-HA. Then, we infected cells stably expressing CARMA3-HA with VSV at MOI=3. At different time points, we immunoprecipitated CARMA3-HA using specific anti-HA antibody-conjugated beads or control anti IgG-conjugated beads. The immunoprecipitated complex and cell lysates were subject to immunoblotting using indicated antibodies. We found that CARMA3 inducibly interacts with MAVS and BCL10 at 3 and 4 hours after virus infection (Fig.29A).

Besides, we found that CARMA3 was cleaved after virus infection. The immortalized CARMA3 deficient cells stably expressing CARMA3-HA were infected with VSV at MOI=3. We detected two bands at 3 hours after virus infection using anti-HA antibody. The upper band was decreased, while the lower band was increased during virus infection. To confirm the cleavage of CARMA3, we used specific anti-CARMA3 antibody, which raised against the small peptides from both N-terminal and C-terminal of protein. We detected one lower cleaved band. It suggested that CARMA3 was cleaved in the middle of protein (Fig.29A).

3.17 BCL10 interacted with MAVS and RIG-I.

Next, we decided to check the interaction between BCL10 and MAVS. We firstly overexpressed BCL10-MYC and MAVS-FLAG or RIG-I-FLAG in HEK 293 cells and then immuniprecipitated MAVS or RIG-I using anti-FLAG antibody conjugated beads. The immunoprecipitated complex and cell lysates were subject to immunoblotting with the indicated antibodies. We found that Bcl10 interacted with both MAVS and RIG-I, when they were overexpressed (Fig.28B).

To further confirm the interaction between MAVS and BCL10, we decided to detect the endogenous interaction between two proteins. The HEK 293 cells were transfected with 1μg/ml poly (I:C) by lipofectamine 2000. At the different time points, we immunoprecipitated BCL10 and detected its interaction with MAVS. We found that BCL10 inducibly interacted with MAVS at 1 hour after poly (I:C) transfection. We cannot see the interaction between BCL10 and MAVS at 2 and 3 hours after poly (I:C) transfection(Fig.29B).

3.18 CARMA3 and BCL10 competed with RIG-I in binding with MAVS

It was found that RIG-I interacted with MAVS and triggered MAVS to form prion-like structure after virus infection (Hou, Sun et al. 2011). Our previous data showed that CARMA3 and BCL10 interacted with MAVS. Therefore, we hypothesized that CARMA3 or BCL10 competes with RIG-I in binding with MAVS. To test the hypothesis, we

overexpressed MAVS-His and RIG-I-FLAG in presence of CARMA3-HA or BCL10-Myc in HEK 293 cells. At 24 hours after infection, we immunoprecipitated MAVS using Ni-NTA beads and detected its interaction with RIG-I, CARMA3 and BCL10 by immunoblotting. We found that RIG-I interacted with MAVS in the absence of CARMA3 or BCL10. After the overexpression of CARAM3 or BCL10, the interaction between MAVS and RIG-I was blocked in a dose-dependent manner. In contrast, MAVS was associated with CARMA3 or BCL10 even in the presence of RIG-I. Together, our data suggested that CARMA3 and BCL10 competed with RIG-I in binding with MAVS (Fig.30).

3.19 CARMA3 interacted with CASPASE-3, CASPASE-8 and CASPASE -9.

There is a CARD domain at the N-terminal of CARAM3. CARD domain originates from proteins involved in regulation of CASPASE proteins' activation and recruitment(Jiang and Lin 2012). CARMA3 was cleaved after virus infection. The cleavage sites might be located in the middle of CARMA3. By sequence analyses, we identified a potential CASPASE 8 cutting site in the middle of protein. Therefore, we hypothesized that CARMA3 interacts with CASPASE proteins after virus infection. To test the hypothesis, we infected A431 cells with VSV at MOI=3. At the different time points after infection, we immunoprecipitated CASPASE3, 8 and 9 using their specific antibodies-conjugated beads. CARMA3 constitutively interacted with CASPASE 3, 8 and 9. They interacted with each other with the highest affinity at 4 hours after virus infection. At 8 hours after infection, we can only detect the weak interaction between CARMA3 and CASPASE 3, while CASPASE 8 and 9 were

dissociated from CARMA3 (Fig.38). The interaction between CARMA3 and CASPASE proteins raised the possibility that CARMA3 was cleaved by CASPASE proteins. More studies are needed to test the hypothesis.

3.20 The aggregation of MAVS was required for NF-κB and IRF3 activation

Previous studies showed that MAVS was aggregated to form a prion-like structure after SeV infection. The prion-like structure of MAVS was important for MAVS to recruit many different E3 ligases, such as TRAF6, TRAF2/5, linear ubiquitin assembly complex (Lubac) complex, which work together to activate NF-κB and IRF3 (Hou, Sun et al. 2011). To confirm it, we obtained two plasmids encoding MAVS WT or MAVS E26A and overexpressed them with NF-κB-luc and IFN-luc in HEK 293 cells. It was found that MAVS WT but not MAVS E26A formed prion-like structure, when they were overexpressed (Hou, Sun et al. 2011). MAVS WT induced the activation of both signaling pathways, while the mutant cannot. Next, we detected the level of these two proteins by immunoblotting. We found that the level of these two proteins were comparable. Our data suggested that the aggregation of MAVS was required for both NF-κB and IRF3 activation (Fig.31).

3.21 CARMA3 and BCL10 overexpression inhibited MAVS to form prion-like structure.

Our previous data showed that CARMA3 and BCL10 interacted with MAVS and regulated MAVS function. Additionally, MAVS aggregation was essential for both NF-κB and IRF3 activation. Therefore, we hypothesized that CARMA3 or BCL10 overexpression inhibits MAVS aggregation. To test the hypothesis, we overexpressed different doses of CARMA3-FLAG together with RIG-I-FLAG in HEK 293 cells. Then, we isolated mitochondrial from transfected cells and analyzed MAVS aggregation by SDD-AGE assay. We found that overexpression of RIG-FLAG led to MAVS aggregation, while the MAVS aggregation was inhibited with increasing amount of CAMRA3 in mitochondrial (Fig.32).

Next, we decided to check the role of BCL10 in regulating MAVS aggregation. We overexpressed different doses of BCL10 together with RIG-I-FLAG in HEK 293 cells. Then, we decided to detect the MAVS aggregation using the methods as described before. We found that BCL10 overexpression inhibited MAVS aggregation in a dose-dependent manner (Fig.32).

Together, our data suggested that CAMRA3 and BCL10 overexpression inhibited MAVS from aggregated form.

3.22 After virus infection, MAVS aggregation more easily occurred in cells with CARMA3 deficiency.

To further confirm the negative role of CARMA3 in MAVS aggregation, we infected WT and CARAM3 deficient MEF cells with VSV at MOI=3. At the different time points, we measured the MAVS aggregation using the method as described previously. One hour after

virus infection, MAVS did not undergo aggregation in WT cells, but MAVS aggregation occurred in CARMA3 deficient cells. This trend became more obvious at 6 hours after virus infection. Next, we checked the level of MAVS in WT and CARMA3 deficient MEF cells in mitochondrial. We found that the level of MAVS was comparable between two cell types. Therefore, our data suggested the negative role of CARMA3 in MAVS aggregation (Fig.33).

3.23 Schematic model of CARMA3 and BCL10-mediating MAVS aggregation and MAVS-mediating signaling pathway.

Based on our previous data, we propose a model to describe how CARMA3 and BCL10 regulate MAVS aggregation in RIG-I/MAVS signaling pathways. In resting cells with no virus infection, MAVS was kept as an individual form. After virus infection, RIG-I interacted with MAVS and triggered the MAVS to form a prion-like structure. During the process, CAMRA3 and BCL10 complex interacted with MAVS and was involved in the activation of NF-κB signaling pathway. In the meantime, the CARMA3 and BCL10 complex inhibited MAVS from more aggregated form. In CARMA3 deficient cells, virus infection triggered the quick and easy MAVS aggregation. Therefore, in CARMA3 deficient cells, there was more activation of TBK1-IRF3 signaling pathway. Since CARAM3 and BCL10 are involved in NF-κB through unknown mechanism, there was partially defective of virus-induced NF-κB activation (Fig.34).

3.24 Compared to WT mice, CARMA1-deficient mice had less serum IFNβ and IL6 levels after VSV-GFP infection

CARMA1 is another CARMA family member. Different from CARMA3, the CARMA1 is only expressed in the hematopoietic tissues. However, CARMA1 shared a high degree of sequence and structural homology with CARMA3(Jiang and Lin 2012). Furthermore, CARMA3 had an ability to rescue TCR-induced NF-κB activation in CARMA1-deficient T cells, which suggested that CARMA3 and CARMA1 regulate the same signaling pathway in a similar manner but in different tissues (Matsumoto, Wang et al. 2005). Therefore, we hypothesized that CARMA1 contributes to the variable host responses to VSV infection, similar to CARMA3. To test it, we challenged WT and CARMA3 deficient mice intranasally with VSV-GFP infection. We checked cytokine production in serum and virus titer in brain. We found that virus titer in CARMA1 deficient mice exhibits modestly decreased virus titer, compared to WT mice. (Fig.35A). However, we surprisingly found that the serum IL6 and IFNβ was significantly decreased in CARMA1 deficient mice at 24 and 48 hours after infection, but the level of serum IFNε is comparable between two types of mice (Fig.35B). It suggested that CARMA1 specifically regulated VSV-induced the production of IL6 and IFNβ.

3.25 CARMA1 contributed to VSV-induced the production of IFNβ in splenocyte and CD11c^{+} cells.

Our previous data showed that the serum IL6 and IFNβ was decreased in CARMA1 deficient mice at 24 or 48 hours after VSV infection. It suggested that CARMA1 mainly contributed to the innate immunity against VSV infection. Additionally, multiple dendritic cell types served as major IFNs producing cells *in vivo* in response to RNA virus infection(Colonna, Krug et al. 2002, Diebold, Montoya et al. 2003). Therefore, we hypothesized that CARMA1 contributes to VSV-induced IL6 and type I interferons production in dendritic cells *in vivo*. To do that, we directly sorted $CD11c^+$ from the spleen of infected WT and infected CARMA1 mice. Before sorting, one part of cells from spleen was kept. Then, we detected the cellular production of IFNβ by RT-PCR. We found that the production of INFβ in splenocytes from CAMRA3 deficient mice is nearly 10 folds less than WT mice, while the difference goes up to nearly 20 fold in $CD11c^+$ cells(Fig.36). It suggested that CARMA1 contributed to VSV-induced the production of IFNβ in splenocyte and $CD11c^+$ cells.

3.26 CARMA1 deficiency did not affect VSV-induced the production of IL6 and IFNβ in BMDMs.

Next, we decided to study the role of CARMA1 in VSV-induced the production of IL6 and IFNβ in macrophage. To test the hypothesis, we cultured primary BMDMs isolated from WT or CARMA1 deficient mice as previously described. Then, we infected the primary cultures of BMDMs with VSV at MOI=3 and detected the production of IL6 and type I IFNs.

We found the production of either IL6 or type I IFNs is comparable in BMDMs from both types of mice after infection (Fig.37 A, B&C). Consistently, the activation of TBK1-IRF3 was also similar in BMDMs from both types of mice (Fig.37D). It suggested that CARMA1 deficiency did not affect VSV-induced the production of IL6 and IFNβ in macrophage.

3.27 Identification of CARMR3 binding partners by SILAC experiment.

To further characterize the CARMA3 signaling complex, we preformed SILAC experiment to identify proteins that interact with CARMA3.Extraction from HEK 293T cells expressing vector was labeled with 'light' isotopes, while extraction from HEK 293T cells expressing CARMA3-FLAG was labelled with 'heavy' isotopes. After immunoprecipitation with FLAG antibody conjugated beads, the precipitates from the heavy and light samples were subject to SDS-PAGE and silver staining. The precipitates were excited from the gel and digested with trypsin. The peptides were analyzed by nano liquid chromatography tandem mass spectrometry(nanoLC-MS/MS). 512 different proteins were identified by analyses of nanoLC-MS/MS (Figure 39B). 25 proteins enriched in the heavy sample were considered as CARMA3 binding partners (Table 3). Among them, we found that CARMA3 has highest mass score, suggesting the success of the whole SILAC experiment (Figure 39C). Gene ontology(GO) analysis was performed using Uniprot. We found that GO terms for cellular process, metabolic process, biological regulation and single-organism process were enriched in CARMA3 binding partners. We also found that CARMA3 interacts with Zinc

finger CCCH-type antiviral protein 1(ZAP), which prevents infection by retroviruses (Gao, Guo et al. 2002).

Table 1 TLRs and some of their important ligands

Receptors	Virus	Bacteria	Fungi	Endogenous Ligands	Small/Synthetic molecular
TLR1/TLR2		Triacylated lipopeptides	Yeast/Zymosan		Pam_3CSK_4
TLR2/TLR2	Haemagglutinin	Peptidoglycan	Phospholipomannan	HMGB1	
TLR2/TLR6		LTA, diacyl lipopeptide, peptidoglycan	Yeast/Zymosan		FSL-1, MALP-2, Pam_2CSK_4
TLR3	dsRNA				Poly I:C
TLR4	VSV glycoprotein G, RSV fusion protein, MMTV envelope protein	LPS	Yeast/ glucuronoxylomannan	HSP60, HSP70, fibrinogen, HMGB1	
TLR5		Flagellin			
TLR7	ssRNA				Loxoribine, R848, imiquimod
TLR8	ssRNA				
TLR9	DNA	CpG-DNA			CpG-A, CpG-B and CpG-C ODNs
TLR10	Unknown Ligands				
TLR11		Unpathogenic Bacteria			
TLR12 or TLR13	Unknown Ligands				

Table 2 The primers used in the experiments

	Forward Primers	Backward Primers
Mouse *ifnα*	TGACCTCAACACTCAGCTCAA	AGGTGCCTGTATCTCTACCTG
Mouse *ifnβ*	CAGCTCCAAGAAAGGACGAAC	GGCAGTGTAACTCTTCTGCAT
Mouse *il6*	TCTATACCACTTCACAAGTCGGA	GAATTGCCATTGCACAACTCTTT
Mouse *gapdh*	AGGTCGGTGTGAACGGATTTG	TGTAGACCATGTAGTTGAGGTCA

Table 3 The cellular binding partners of CARMA3.

Accession	Score	Mass	H/L	Description
HEBP1_HUMAN	20	21234	1239	Heme-binding protein 1 OS=Homo sapiens GN=HEBP1 PE=1 SV=1
NB5R4_HUMAN	18	59839	263.7	Cytochrome b5 reductase 4 OS=Homo sapiens GN=CYB5R4 PE=1 SV=1
PWP1_HUMAN	131	55793	198.2	Periodic tryptophan protein 1 homolog OS=Homo sapiens GN=PWP1 PE=1 SV=1
ZN638_HUMAN	23	220488	161.3	Zinc finger protein 638 OS=Homo sapiens GN=ZNF638 PE=1 SV=2
DDX23_HUMAN	36	95524	151.8	Probable ATP-dependent RNA helicase DDX23 OS=Homo sapiens GN=DDX23 PE=1 SV=3
EXOS5_HUMAN	57	25233	128.5	Exosome complex component RRP46 OS=Homo sapiens GN=EXOSC5 PE=1 SV=1
CD043_HUMAN	96	23849	96.63	UPF0534 protein C4orf43 OS=Homo sapiens GN=C4orf43 PE=1 SV=2
EEPD1_HUMAN	16	62767	83.57	Endonuclease/exonuclease/phosphatase family domain-containing protein 1 OS=Homo sapiens GN=EEPD1 PE=1 SV=2
COR1B_HUMAN	57	54200	76.61	Coronin-1B OS=Homo sapiens GN=CORO1B PE=1 SV=1
TOP3A_HUMAN	15	113083	75.72	DNA topoisomerase 3-alpha OS=Homo sapiens GN=TOP3A PE=1 SV=1
RTC1_HUMAN	115	39311	57.1	RNA 3'-terminal phosphate cyclase OS=Homo sapiens GN=RTCD1 PE=1 SV=1
PRP4_HUMAN	135	58412	46.47	U4/U6 small nuclear ribonucleoprotein Prp4 OS=Homo sapiens GN=PRPF4 PE=1 SV=2
ZER1_HUMAN	16	88612	44.74	Protein zer-1 homolog OS=Homo sapiens GN=ZER1 PE=1 SV=1
CAR10_HUMAN	8141	115859	35.37	Caspase recruitment domain-containing protein 10 OS=Homo sapiens GN=CARD10 PE=2 SV=2
ZCCHV_HUMAN	125	101367	35.2	Zinc finger CCCH-type antiviral protein 1 OS=Homo sapiens GN=ZC3HAV1 PE=1 SV=3
ASCC2_HUMAN	77	86306	25.51	Activating signal cointegrator 1 complex subunit 2 OS=Homo sapiens GN=ASCC2 PE=1 SV=3
K1C10_HUMAN	96	58792	16.78	Keratin, type I cytoskeletal 10 OS=Homo sapiens GN=KRT10 PE=1 SV=6
RBM42_HUMAN	116	50749	12.38	RNA-binding protein 42 OS=Homo sapiens GN=RBM42 PE=1 SV=1
SNUT1_HUMAN	403	90200	4.788	U4/U6.U5 tri-snRNP-associated protein 1 OS=Homo sapiens GN=SART1 PE=1 SV=1
UBF1_HUMAN	190	89350	4.37	Nucleolar transcription factor 1 OS=Homo sapiens GN=UBTF PE=1 SV=1
P5CS_HUMAN	269	87248	2.726	Delta-1-pyrroline-5-carboxylate synthase OS=Homo sapiens GN=ALDH18A1 PE=1 SV=2
XRN2_HUMAN	588	108513	2.442	5'-3' exoribonuclease 2 OS=Homo sapiens GN=XRN2 PE=1 SV=1
RLA1_HUMAN	697	11507	2.366	60S acidic ribosomal protein P1 OS=Homo sapiens GN=RPLP1 PE=1 SV=1
FUS_HUMAN	236	53394	2.125	RNA-binding protein FUS OS=Homo sapiens GN=FUS PE=1 SV=1
SFPQ_HUMAN	265	76102	2.068	Splicing factor, proline- and glutamine-rich OS=Homo sapiens GN=SFPQ PE=1 SV=2

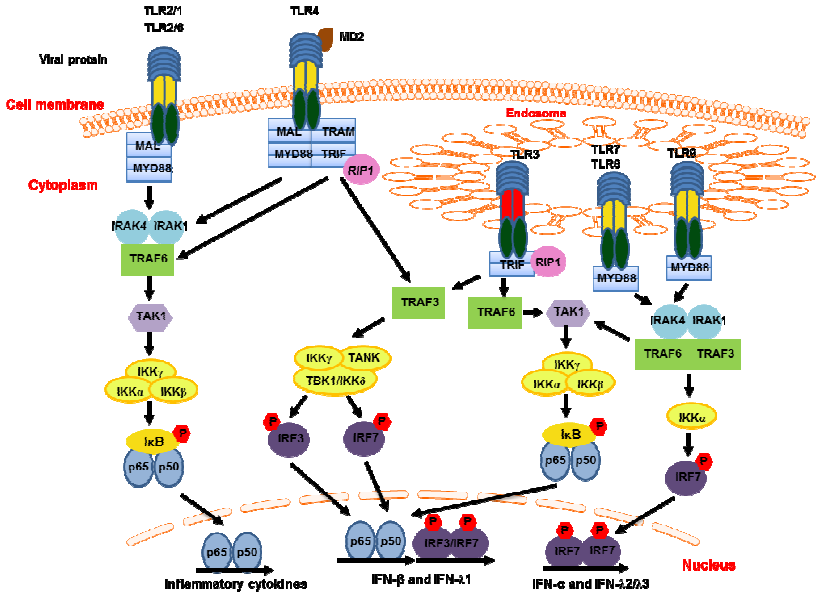

Figure 1 TLRs in antivirus response. Viral PAMPs such as dsRNA, ssRNA, CpG DNA and viral proteins are recognized by different TLRs to trigger the activation of NF-κB, AP-1and IRF3/IRF7 to produce type I /III IFNs and proinflmmatory cytokines. TLR1, TLR2 and TLR4 are present on the cell surface, which recognize viral proteins. TLR3, TLR7, TLR8 and TLR9 are located in the endosome, which is required for the recognition of virus-derived dsRNA, ssRNA and CpG. Upon ligand recognition, TLRs recruit a serious of adaptor proteins to activate downstream signaling pathways. Based on the different adapters, these signaling pathways can be divided into two types, MyD88 and TRIF-dependent pathways. TLR3 and TLR4 recruit TRIF, while others TLRs with the exception of TLR3 utilize MyD88.

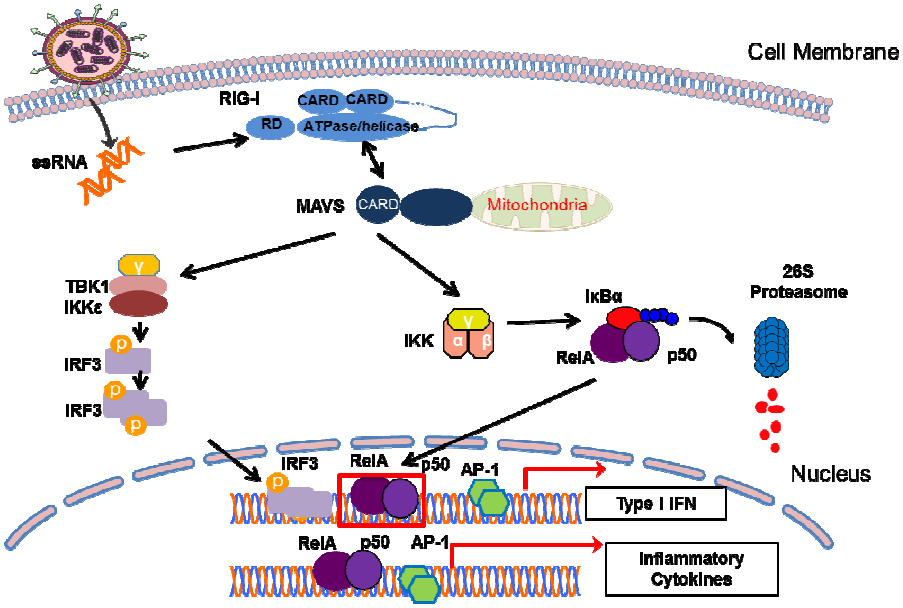

Figure 2 RIG-I/MAVS signaling pathway. After RNA virus infection, their RNA genomes are recognized by RIG-I in the cytoplasm, where RIG-I changes its conformation and exposes CARD domains. Then, the "active" RIG-I binds to and activates MAVS to form prion-like aggregates on the outer membrane of mitochondrial, which serves as a platform in activating downstream signaling pathways. For example, it activates IKK complex. The activated IKK complex phosphorylates IκBα on its serine 32 and 36, which leads to IκBα degradation by 26S proteasome. It frees NF-κB dimmer, which enters the nucleus to enhance the production of inflammatory cytokines. On the other hand, the activated MAVS recruits and activates NEMO-TBK1-IKKε complex, which phosphorylates and activates IRF3/7. The activated IRF3/7 enters into the nucleus and plays an important role in the production of type I IFNs.

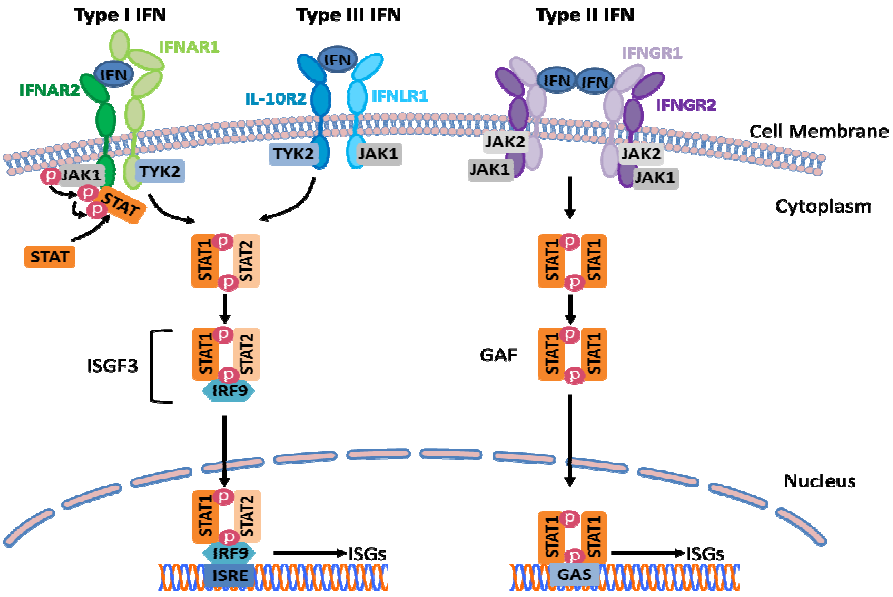

Figure 3 IFNs signaling pathway. Based on different receptors, the IFNs are divided into three different classes, type I, type II and type III IFNs. They share JAKs-STATs signaling pathway to increase the transcription of IFN-stimulated genes (ISGs). In absence of virus, the JAKs interact with the cytoplasmic domain of each IFN receptor subunits in an inactive form. Upon ligand stimulation, receptor chains undergo conformational change to bring the kinase domain of JAKs into close proximity, by which JAKs are autophosphorylated and subsequently activated. Then, the "active" JAKs in turn phosphorylate the cytoplasmic part of IFN receptors on some conserved tyrosine residues, which work as the docking sites for STAT proteins. The receptor-recruitment of STAT proteins is essential for phosphorylation and activation of STAT proteins. After phosphorylation, STAT proteins form a homo-(type II IFNs) or heterodimer (type I and type III IFNs) and are released from IFN receptors. Then, STAT proteins enter the nucleus to drive expression of ISGs.

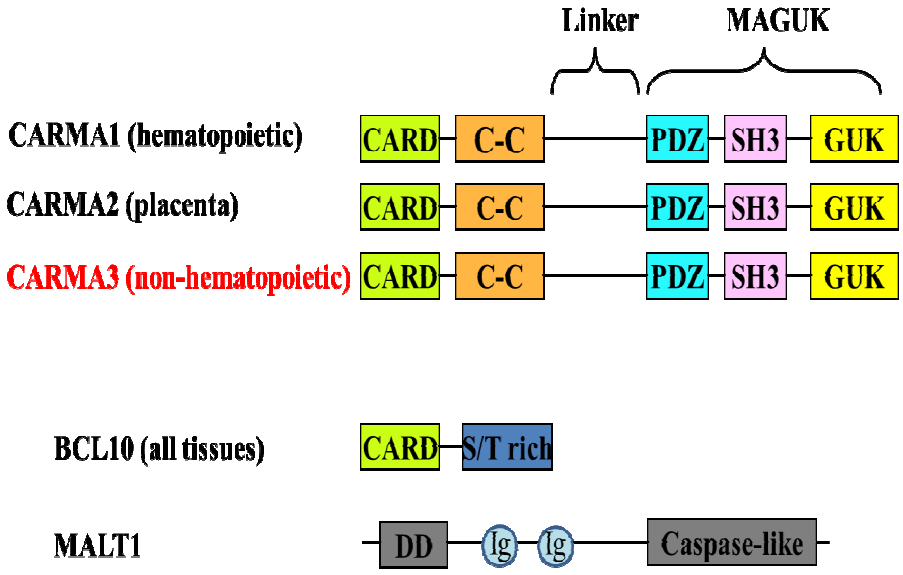

Figure 4 CARMA families of scaffold proteins. CARMA family has three proteins, CARMA1, CARMA2 and CARMA3. They share very similar structures with the same domains. These proteins all work as scaffold proteins in NF-κB signaling pathways. However, they are expressed in different tissues. CARMA1 is expressed in hematopoietic cells. CARMA2 is expressed in the placenta, skin and mucosal tissues. CARMA3 is expressed in all non-hematopoietic cells. Being activated, they will recruit partners, BCL10 and MALT1, to form a CBM complex to mediate NF-κB activation by regulating IKK activities.

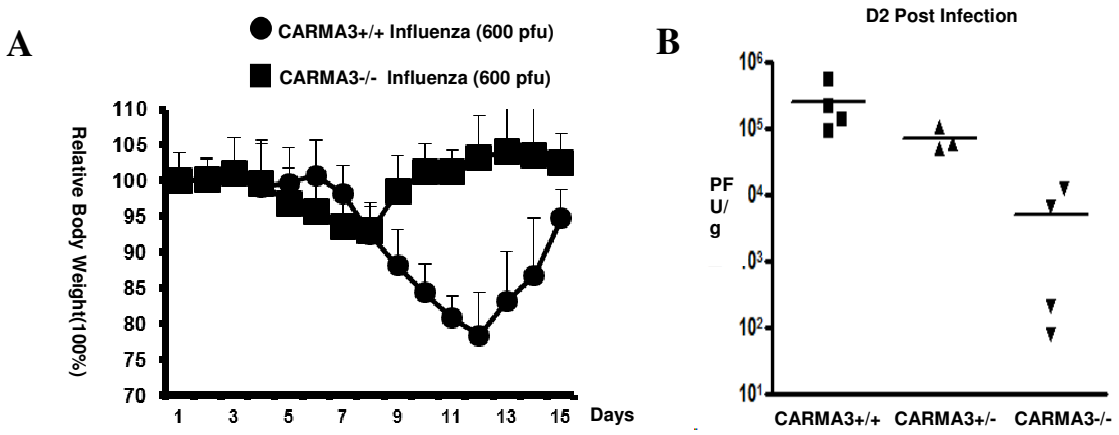

Figure 5 CARMA3 deficiency caused mice to be more resistant to the infection of H1N1 influenza virus. (A) Groups of 6-8 weeks WT or CAMRA3 deficient mice were intranasally infected with H1N1 influenza virus at pfu=600. The change of mice bodyweight had been measured daily until 2 weeks after virus infection. (B) WT, CARMA3 Het, CARMA3 deficient mice were intranasally infected with H1N1 influenza virus at pfu=500. Lungs from different mice were harvested at 2 days after virus infection. The virus titer in lungs was measured by the TCID50 assay with MDCKII cells.

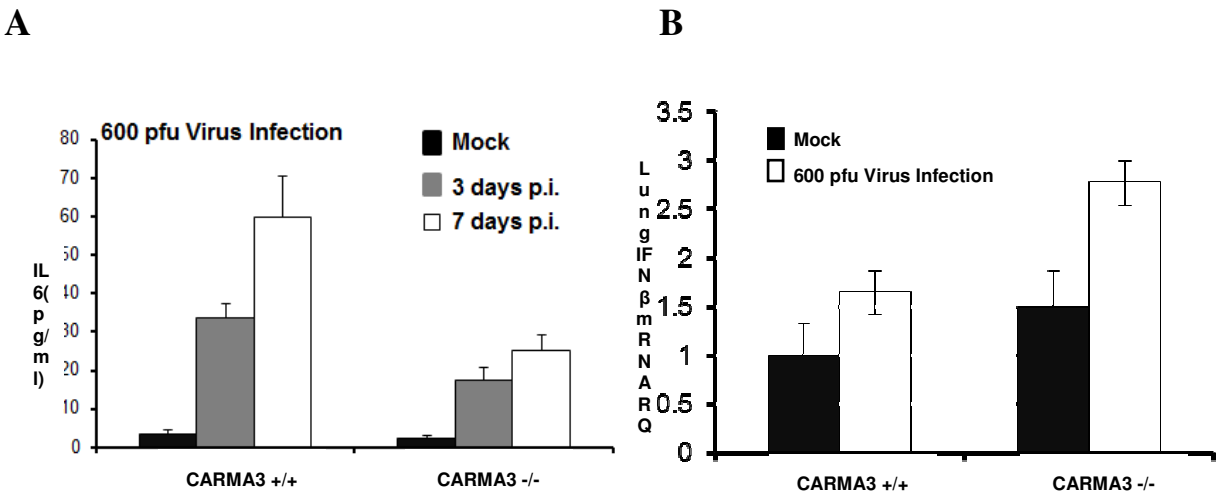

Figure 6 CARMA3 deficient mice had enhanced lung IFNβ production and decreased level of serum IL6 after the infection of H1N1 influenza virus. Groups of 6-8 weeks WT or CAMRA3 deficient mice were intranasally infected with H1N1 influenza virus at pfu=600. (A) The serum was harvested 0, 3, 6 days from WT and CARMA3 KO mice. The serum IL6 from mice was measured by ELISA. (B) The lungs form mice were harvested 3 days after infection. The mRNA was isolated from superior lobe of mice right lung using Trizol reagent. The production of IFNβ was measured by qPCR using specific mouse *ifnβ* primers.

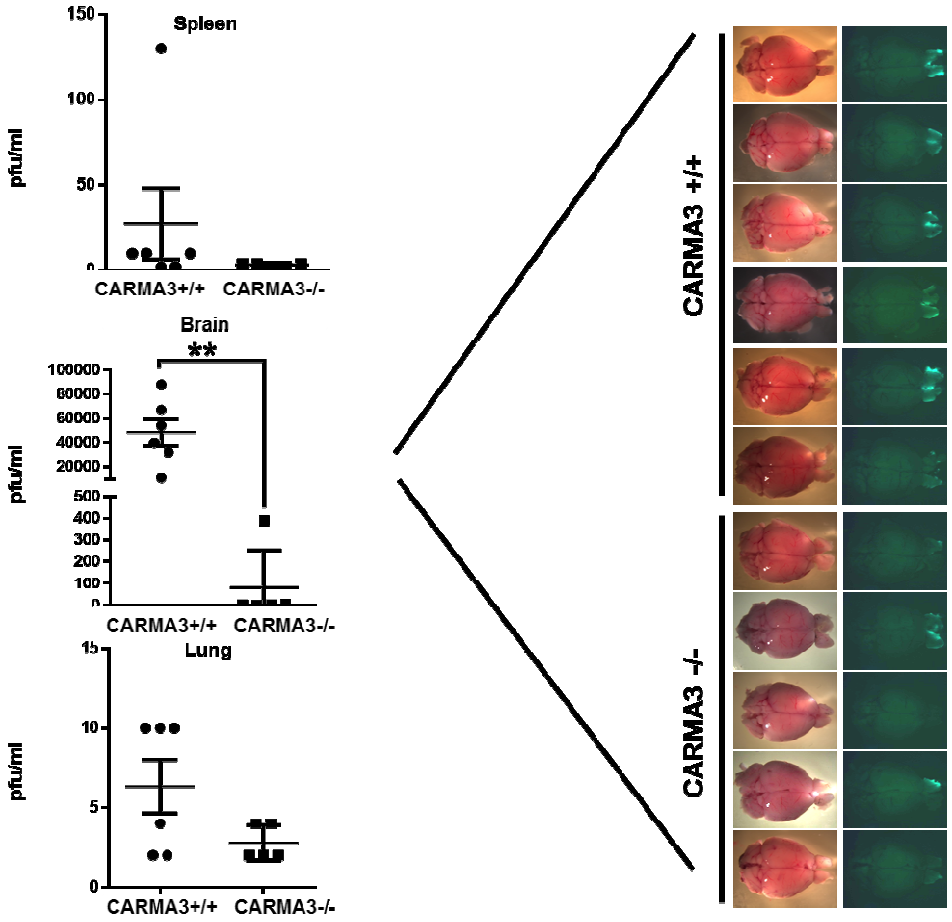

Figure7 CARMA3 deficiency caused mouse to be more resistant to VSV-GFP infection. Groups of 6-8 weeks WT or CAMRA3 deficient mice were intranasally infected with VSV at pfu=1×10^7. Spleens, brains and lungs were harvested from mice at 2 days after infection. The virus titer in different tissues was measured by viral plaque assay. The pictures of the VSV-GFP in brains were taken by fluorescence microscope.

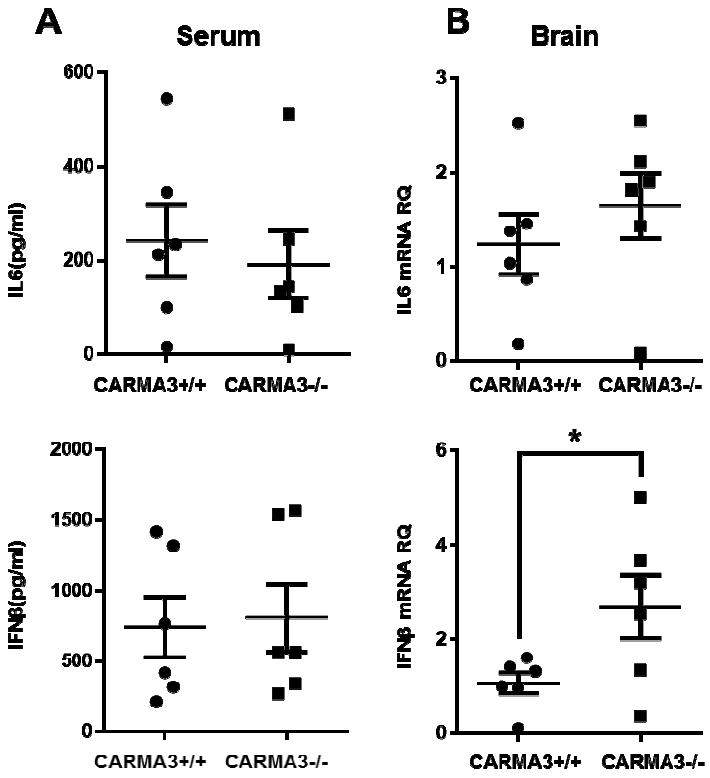

Figure 8 CARMA3 deficient mice had enhanced brain IFNβ production after VSV infection.6-8 weeks WT or CAMRA3 deficient mice were intranasally infected with VSV at pfu=1×10^7. Serum and brains were harvested from the infected mice at one day after VSV-GFP infection. (A) The serum IL6 and IFNβ were measured by ELISA. (B) The mRNA was isolated from brains using Trizol reagent. The production of IFNβ and IL6 was measured by qPCR using specific mouse *ifnβ* and *il6* primers. * indicates $P<0.05$.

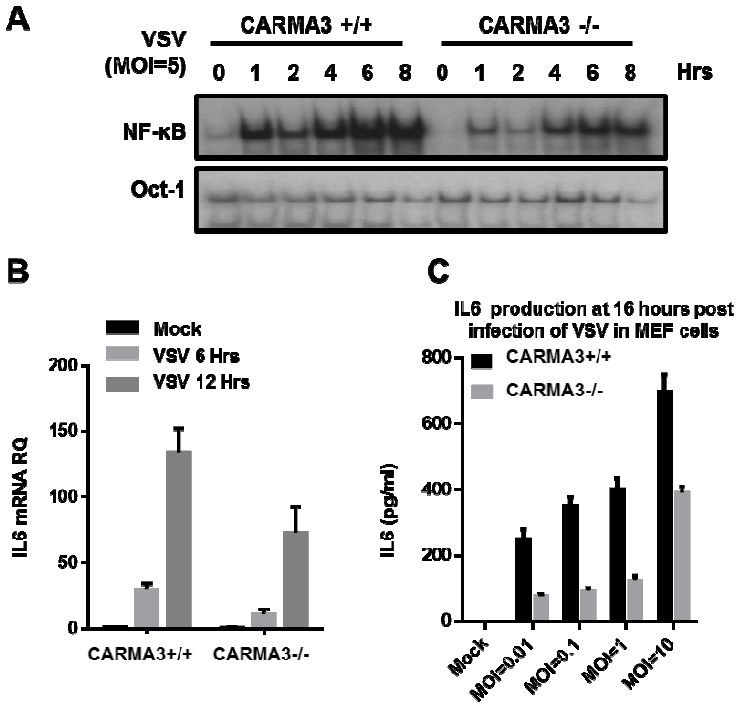

Figure 9 The activation of NF-κB signaling pathway was reduced in CARMA3 deficient cells after VSV Infection. (A)WT and CARMA3 deficient MEF cells were infected with VSV at MOI=5. At the different time points after virus infection, the nuclear proteins were isolated as previously described. The NF-κB activation was measured by EMSA using ^{32}P-labeled NF-κB and OCT-1 probe. (B) WT and CARMA3 deficient MEF cells were infected with VSV at MOI=5. At the different time points after virus infection, the mRNA was isolated from cells using Trizol. The production of IL6 was measured by qPCR with the specific mouse IL6 primers. (C) WT and CARMA3 deficient MEF cells were infected with VSV at MOI as indicated. The infectious medium was replaced with fresh medium at 1 hour after virus infection to get rid of uninfected virus. The supernatant from

both cell types was collected at 16 hours after virus infection. The protein amount of IL6 in supernatant was measured by ELISA.

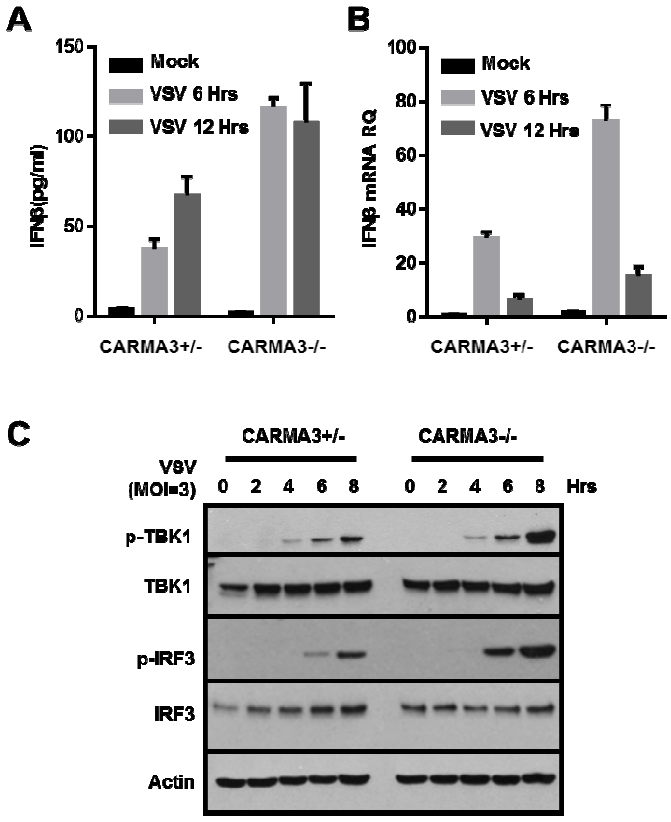

Figure 10 CARMA3-deficient cells had hyperactivation of TBK1-IRF3 signaling pathway and increased production of IFN-β after VSV Infection.(A) and (B) Primary CARMA3 Het and CARMA3 deficient MEF cells were infected with VSV at MOI=3. At the different time points, the supernatant from cell was collected for the IFNβ analyses by ELISA, whereas the cells were harvested for mRNA isolation by Trizol. The production of IFNβ was measured by both qPCR using the specific mouse IFNβ primers and ELISA. (C) Primary CARMA3 Het and CARMA3 deficient MEF cells were infected with VSV at MOI=3. The activation of TBK1-IRF3 signaling pathway was measured by immunoblotting with specific p-TBK1 and p-IRF3 antibodies. TBK1 and IRF3 were detected as a loading control.

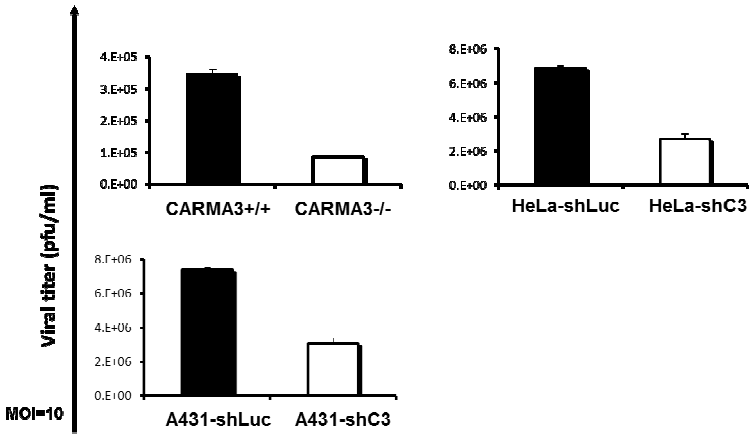

Figure 11 CARMA3 deficiency contributed to reduction in viral yield *in vitro* after VSV infection. Primary WT and CARMA3 deficient MEF cells, Hela cells with control or CARMA3 knockdown, A431 cells with control or CARMA3 knockdown were infected with VSV at MOI=10. At 1 hour after virus infection, the supernatant from each cell type was replaced with the fresh medium to get rid of uninfected virus. The virus amount in supernatant was measured using viral plaque assay at 24 hours after infection.

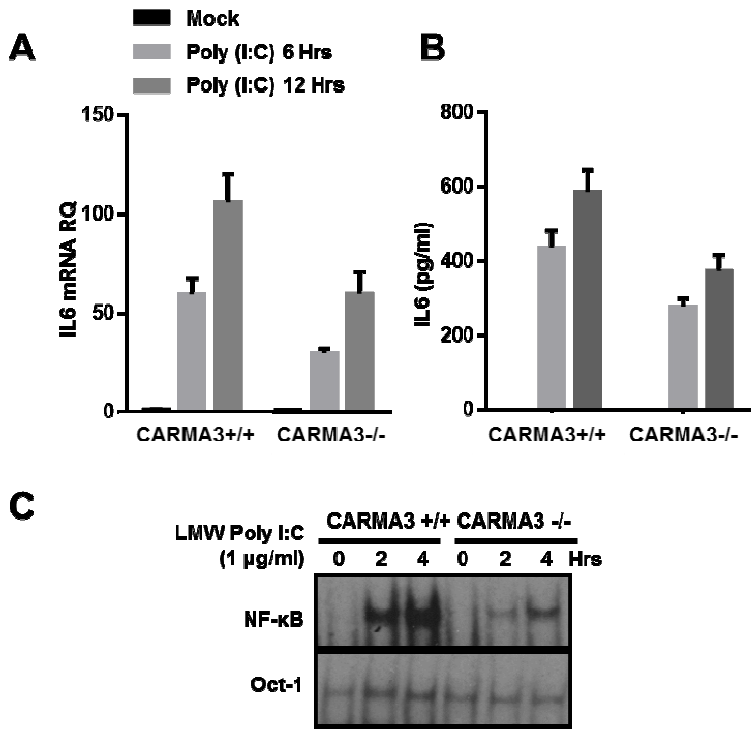

Figure 12 CARMA3-deficient MEF cells had less NF-κB activation and produced less IL6 after poly (I:C) transfection.(A) and (B) Primary WT and CARMA3 deficient MEF cells were transfected with 1µg/ml poly(I:C) by lipofectamine 2000. At the different time points after transfection, the supernatant from both cell types was collected for the ELISA analyses, whereas the cells were harvested for mRNA isolation. The production of IL6 was measured both by qPCR using the specific mouse IL6 primers and ELISA. (C) Primary WT and CARMA3 deficient MEF cells were transfected with 1µg/ml poly (I:C) by lipofectamine 2000. At the different time points after transfection, the nuclear proteins were isolated as previously described. The NF-κB activation was measured by EMSA using ^{32}P-labeled NF-κB and OCT-1 probe.

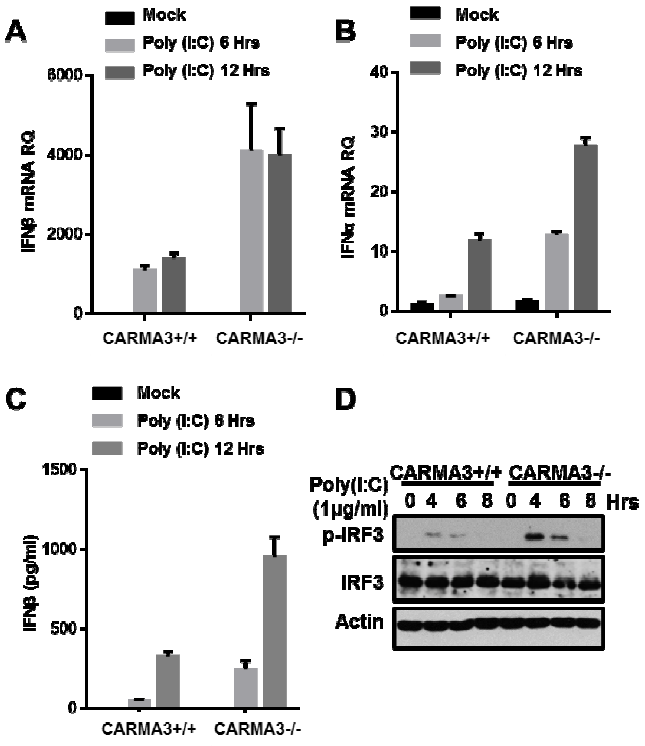

Figure13 CARMA3-deficient MEF cells had hyperactivation of TBK1-IRF3 signaling pathway and produced more type I IFNs after poly (I:C) transfection. Primary WT and CARMA3 deficient MEF cells were transfected with 1μg/ml poly (I:C) by lipofectamine2000. At the different time points after transfection, the supernatant from both cell types was collected for the ELISA analyses, whereas the cells were harvested for mRNA isolation. The nuclear proteins were isolated as previously described. (A) and (C) The production of IFNβ was measured both by qPCR using the specific mouse IFNβ primers and ELISA. (B) The production of IFNα was measured by qPCR using the specific IFNα primers. (D) The activation of TBK1-IRF3 signaling pathway was measured by immunoblotting with specific p-TBK1 and p-IRF3 antibodies. TBK1 and IRF3 were detected as a loading control.

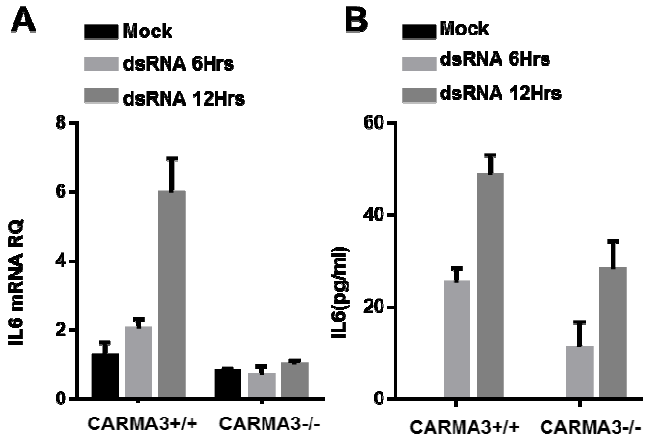

Figure 14 CARMA3-deficient MEF cells produced less IL6 after the transfection of 5' ppp-dsRNA. Primary WT and CARMA3 deficient MEF cells were transfected with 1μg/ml 5'ppp-dsRNA or its control by lipofectamine2000. At the different time points after transfection, the supernatant from both cell types was collected for the ELISA analyses, whereas the cells were harvested for mRNA isolation. (A) and (B) The production of IL6 was measured both by qPCR using the specific IL6 primers and ELISA.

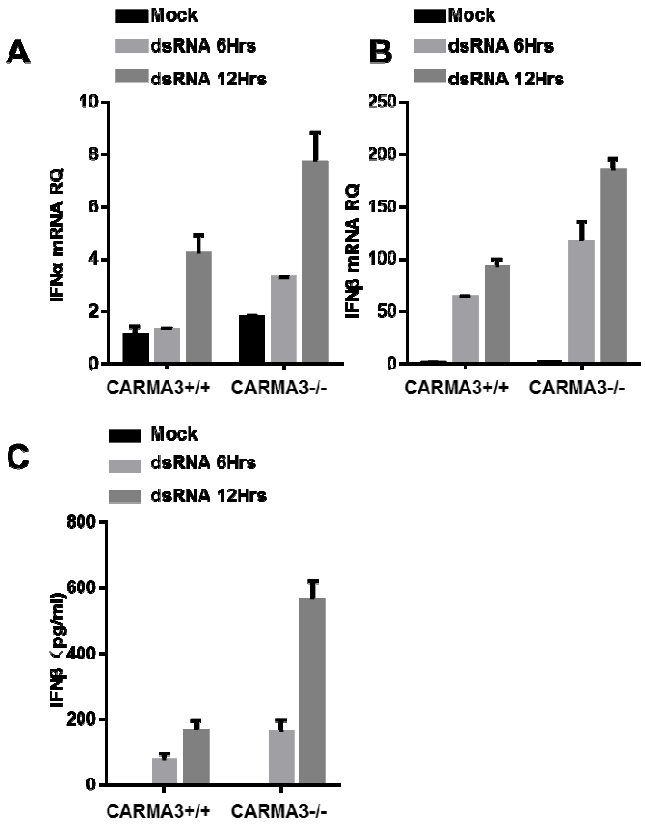

Figure 15 CARMA3-deficient MEF cells produced more IFNs after the transfection of 5' ppp-dsRNA and its control. Primary WT and CARMA3 deficient MEF cells were transfected with 1μg/ml 5'ppp-dsRNA or control by lipofectamine 2000. At the different time points after transfection, the supernatant from both cell types was collected for the ELISA analyses, whereas the cells were harvested for mRNA isolation. (A) The production of IFNα was measured by qPCR using the specific IFNα primers. (B) and (C) The production of IL6 was measured both by qPCR using the specific IL6 primers and ELISA.

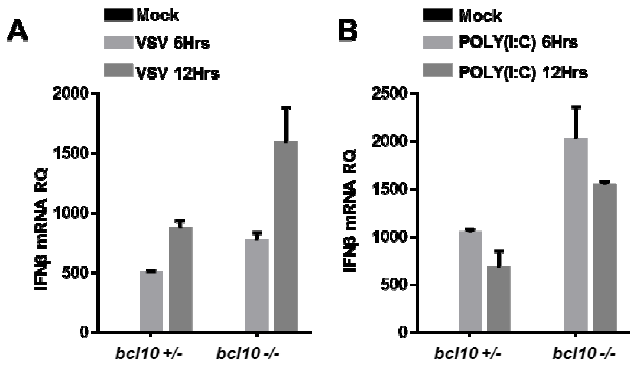

Figure 16 BCL10-deficient MEF cells produced more IFNβ after VSV infection and the poly (I:C) transfection.(A) BCL10 Het and BCL10 deficient MEF cells were infected with VSV at MOI=3.At the different time points after infection, mRNA was isolated from cells. The production of IFNβ was measured by qPCR using the specific IFNβ primers. (B) BCL10 Het and BCL10 deficient MEF cells were transfected with 1μg/ml poly (I:C) by lipofectamine2000. At the different time points after infection, mRNA was isolated from cells. The production of IFNβ was measured by qPCR using the specific IFNβ primers.

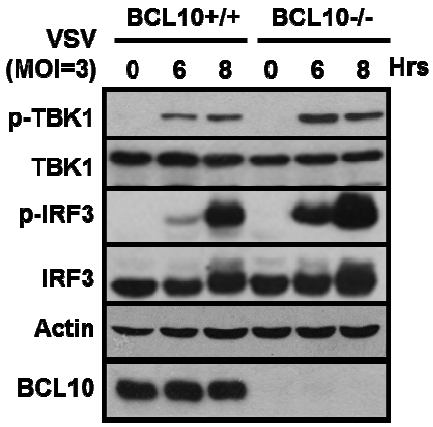

Figure 17 BCL10-deficient MEF cells had hyperactivation of TBK1-IRF3 signaling pathway after VSV infection. BCL10 Het and BCL10 deficient MEF cells were infected with VSV at MOI=3. The activation of TBK1-IRF3 signaling pathway was measured by specific p-TBK1 and p-IRF3 antibodies. TBK1 and IRF3 were detected as a loading control. BCL10 was detected as control to indicate cell types.

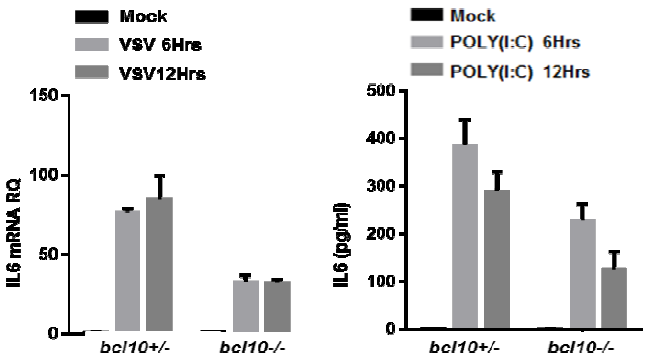

Figure 18 BCL10-deficient MEF cells produced less IL6 after VSV infection and the poly (I:C) transfection.(A) BCL10 Het and BCL10 deficient MEF cells were infected with VSV at MOI=3. At the different time points after infection, mRNA was isolated from cells. The production of IL6 was measured by qPCR using the specific IL6 primers. (B) BCL10 Het and BCL10 deficient MEF cells were transfected with 1μg/ml by lipofectaminee2000. At the different time points after infection, mRNA was isolated from cells. The production of IL6 was measured by qPCR using the specific IL6 primers.

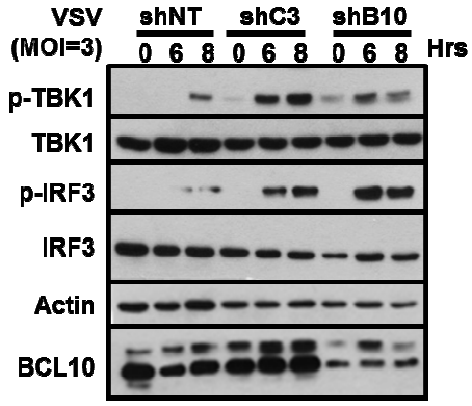

Figure 19 A549 cells stably expressing CARMA3 shRNA or BCL10 shRNA had hyperactivation of TBK1-IRF3 signaling pathway after VSV infection.A549 cells stably expressing control shRNA, CARMA3 shRNA or BCL10 shRNA were infected with VSV at MOI=3. The activation of TBK1-IRF3 signaling pathway was measured by specific p-TBK1 and p-IRF3 antibodies. TBK1 and IRF3 were detected as a loading control. BCL10 was detected as control to indicate BCL10 knockdown efficiency.

.

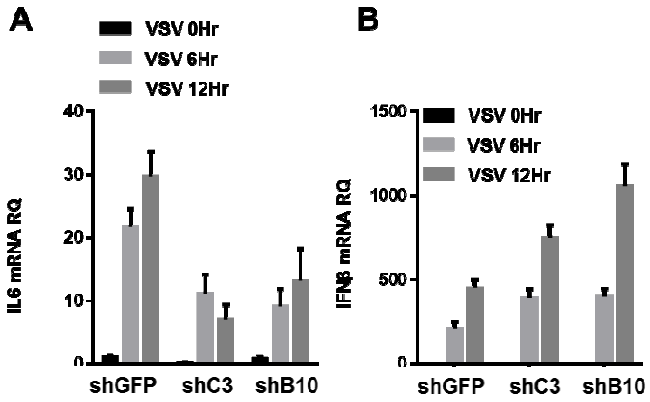

Figure 20 A549 cells stably expressing GFP shRNA,CARMA3 shRNA or BCL10 shRNA produced less IL6 and more IFNβ after VSV infection.A549 cells stably expressing GFP shRNA, CARMA3 shRNA or BCL10 shRNA were infected with VSV at MOI=3. At the different time points after infection, mRNA was isolated from cells. The production of IL6 and IFNβ was measured by qPCR using the specific IL6 and IFNβ primers

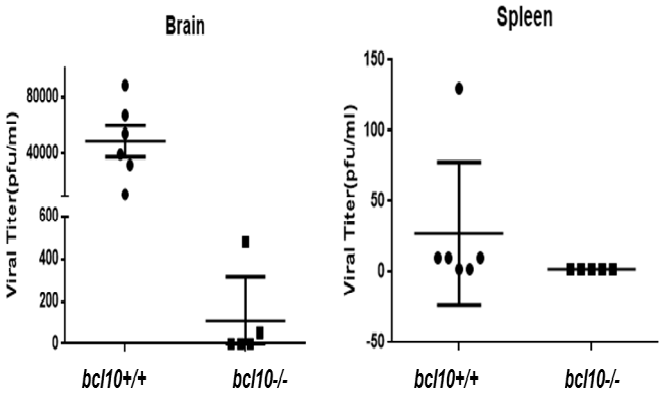

Figure 21 BCL10 deficiency caused mice to be more resistant to VSV-GFP infection.

Groups of 6-8 weeks WT or BCL10 deficient mice were intranasally infected with VSV-GFP at pfu=1×10^7. Spleens and brains were harvested from mice at 2 days after infection. The virus titer in different tissues was measured by viral plaque assay.

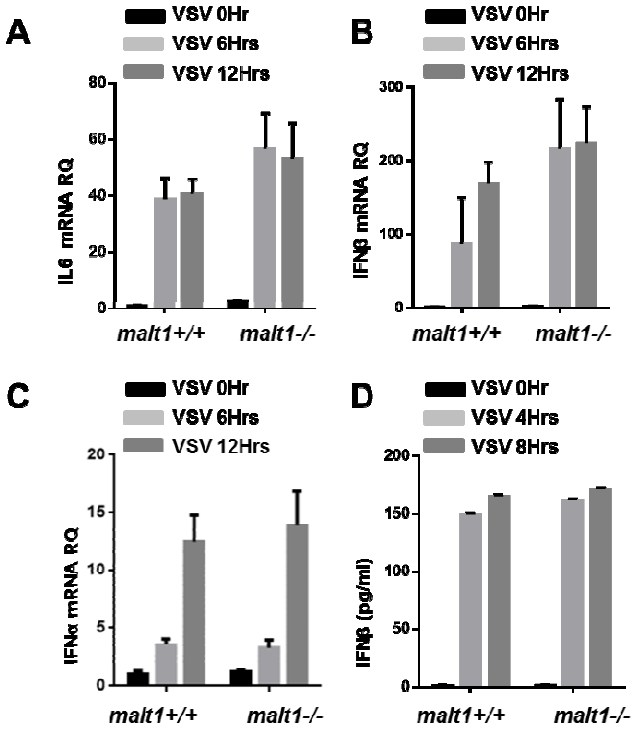

Figure 22 MALT1 deficiency did not impair VSV-induced type I IFNs production.(A), (B) and (C) Primary WT and MALT1 deficient MEF cells were infected with VSV at MOI=3.At the different time points after infection, mRNA was isolated from cells. The production of IL6 and type I IFNs were measured by qPCR using the specific IL6, IFNα and IFNβ primers.(D) Primary WT and MALT1 deficient MEF cells were infected with VSV at MOI=3.At the different time points after infection, supernatant was isolated from cells. The production of IFNβ were measured by ELISA.

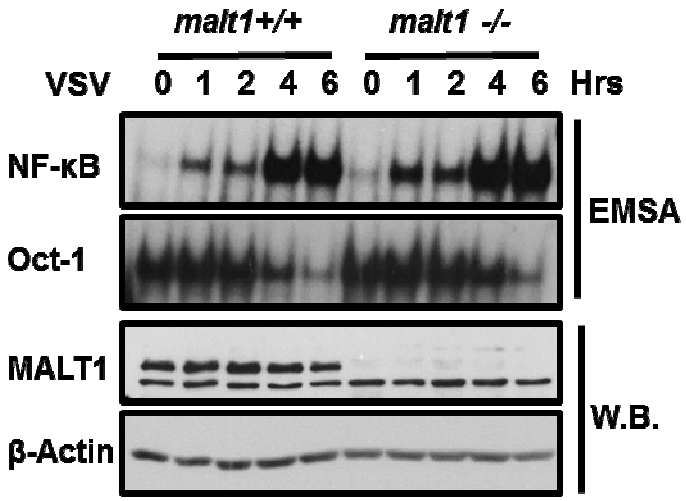

Figure 23 MALT1 deficiency did not affect VSV-induced NF-κB activation. Primary WT and MALT1 deficient MEF cells were infected with VSV at MOI=3.At the different time points after infection, the nuclear and the cytoplasmic proteins were isolated as previously described. The NF-κB activation was measured by EMSA using ^{32}P-labeled NF-κB and OCT-1 probe. The cytoplasmic proteins were subject to immunoblotting using the indicated antibodies.

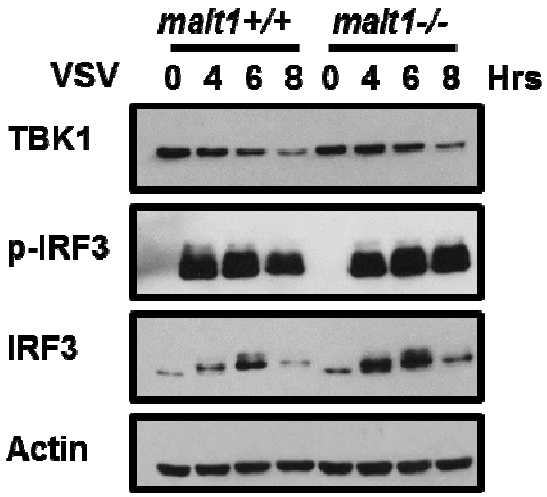

Figure 24 MALT1 deficiency did not affect VSV-induced IRF3 activation. Primary WT and MALT1 deficient MEF cells were infected with VSV at MOI=3. At the different time points after infection, the total cell lysates were isolated and subjected with immunoblotting using indicated antibodies.

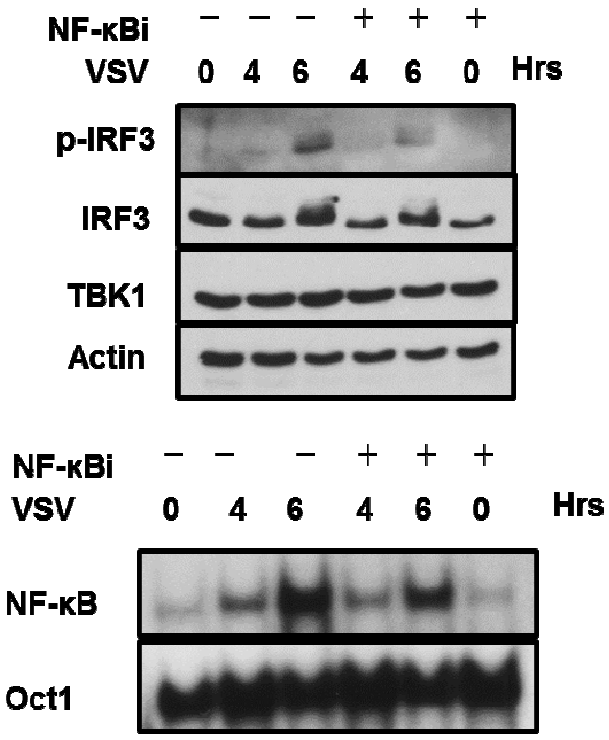

Figure 25 The inhibition of NF-κB signaling pathway did not enhance the phosphorylation of IRF3. Primary MEF cells were pretreated with NF-κB inhibitor for half an hour, which can block the translocation of p50. Then, primary MEF cells were infected with VSV at MOI=3 for indicated time. Then, one part of cells was harvested for nuclear protein extraction. Another part of cells was harvested for immunoblotting. The IRF3 activation was measured by specific p-IRF3 antibody. IRF3, TBK1 and ACTIN were detected as a loading control. The NF-κB activation was measured by EMSA.

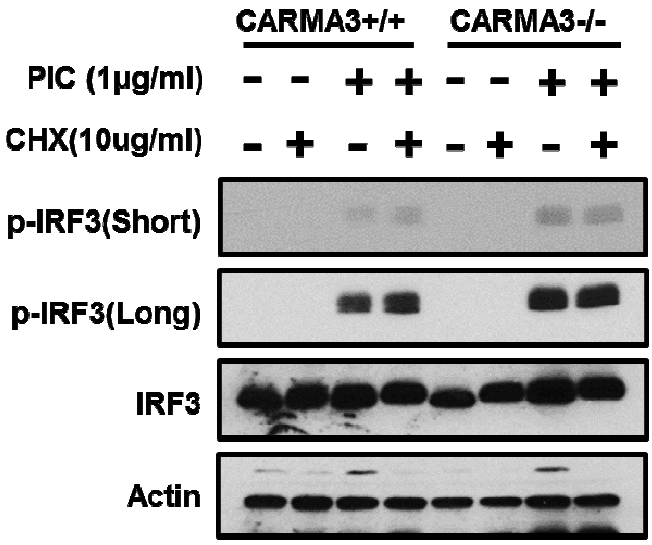

Figure 26 The inhibition of new protein synthesis did not enhance the phosphorylation of IRF3. Primary WT and CARMA3 deficient MEF cells were pretreated with 10 ug/ml cycloheximide (CHX) to block new protein synthesis. Then cells were transfected with 1 ug/ml poly (I:C) by lipofectamine2000. At the different time points, the activation of IRF3 was measured by immunoblotting using specific p-IRF3 antibody. IRF3 and ACTIN were detected as a loading control.

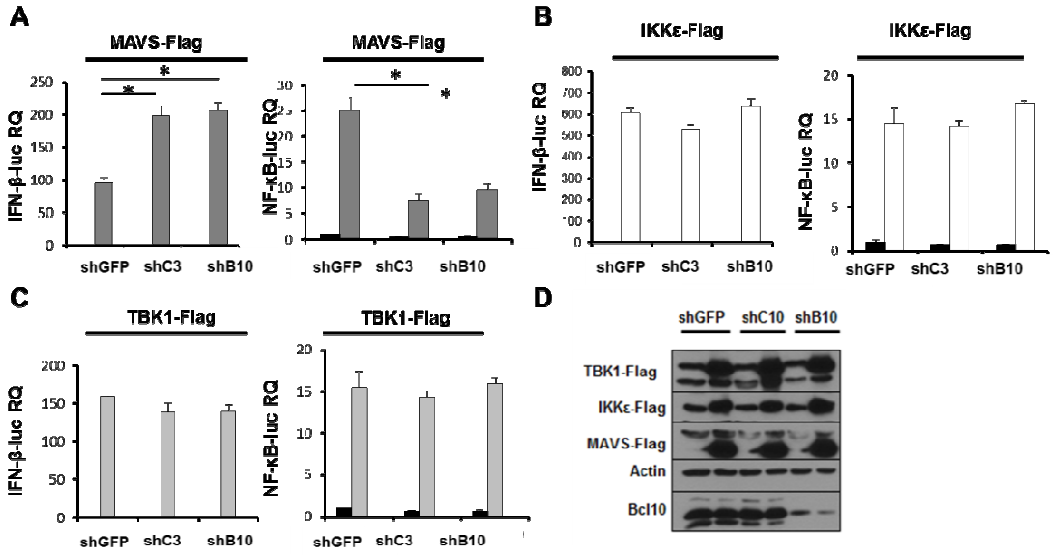

Figure 27 CARMA3 and BCL10 worked downstream of MAVS, but upstream of TBK1 or IKKε. (A) HEK 293 cells stably expressing control shRNA, CARMA3 shRNA, BCL10 shRNA were transfected with the plasmids encoding MAVS-Flag with NF-κB-luc or IFNβ-luc. At 24 hours after transfection, both NF-κB and IRF3 activation were measured by luciferase assay. (B) HEK 293 cells stably expressing control shRNA, CARMA3 shRNA or BCL10 shRNA were transfected with the plasmids encoding TBK1-Flag with NF-κB-luc or IFNβ-luc. At 24 hours after transfection, both the NF-κB and IRF3 activation were measured by luciferase assay. (C) HEK 293 cells stably expressing control shRNA, CARMA3 shRNA, BCL10 shRNA were transfected with plasmids encoding IKKε-Flag with NF-κB-luc or IFNβ-luc. At 24 hours after transfection, the NF-κB and IRF3 activation were measured by luciferase assay. (D) After transfection, cell lysates were collected and thereby, were subjected with immunoblotting using indicated antibodies.

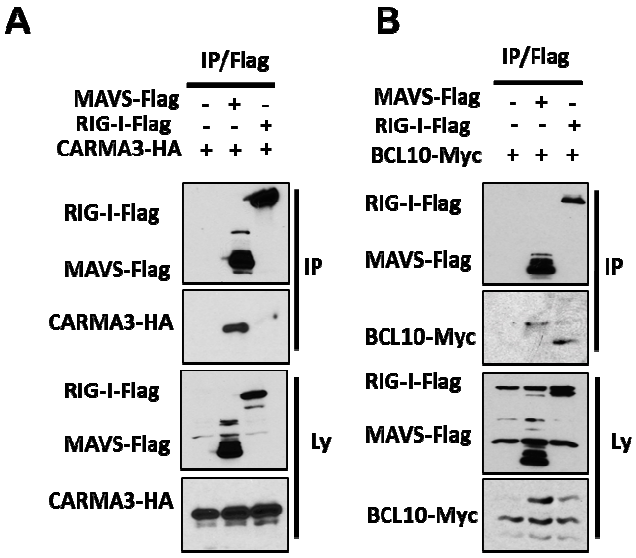

Figure 28 CARMA3 and BCL10 interacted with MAVS, when they are overexpressed in HEK 293 cells. We overexpressed the plasmids encoding CARMA3-HA (A) or BCL10-MYC (B) with MAVS-FLAG or RIG-I-FLAG in HEK 293 cells. At 24 hours after transfection, MAVS or RIG-I was immunoprecipitated using anti-Flag-conjugated beads. The immunoprecipitated complex and cell lysates were subjected with immunoblotting analysis with anti-FLAG antibody (MAVS or RIG-I), anti-HA antibody (CARMA3) and anti-MYC (BCL10) and other indicated antibodies.

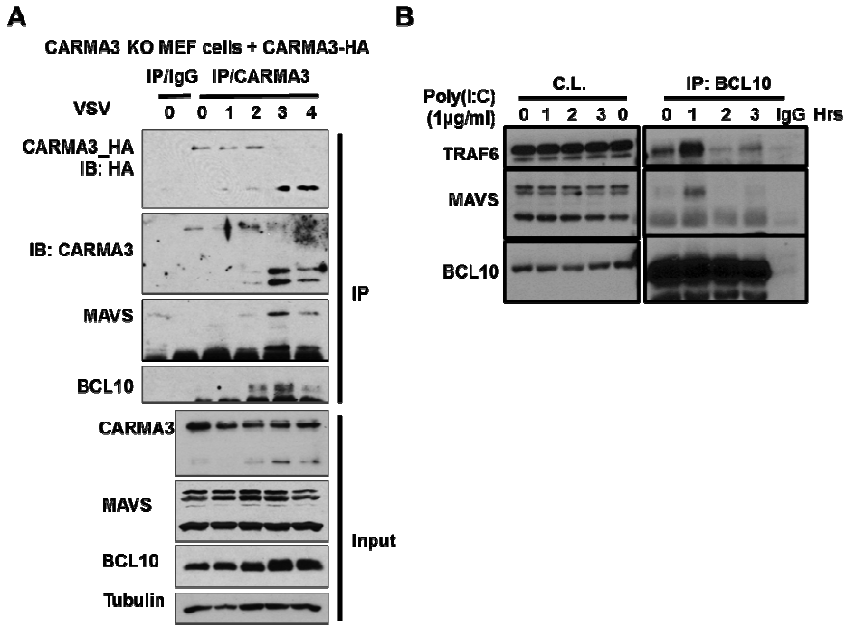

Figure 29 CARMA3 and BCL10 interacted with MAVS. (A)The immortalized CARMA3 deficient MEF cells were infected with lentivirus constructions encoding CARMA3-HA. Then, we infected cells stably expressing CARMA3-HA with VSV at MOI=3. At different time points, cell lysates were immunoprecipitated using anti-HA- or control anti-IgG-conjugated beads. The immunoprecipated complex and cell lysates were subjected with immunobloting analysis with anti-HA (CARMA3), anti-MAVS, anti-CARMA3, anti-BCL10, anti-TUBULIN antibodies. (B) HEK 293 cells were transfected with 1 ug/ml poly (I:C) with lipofectamine2000. At different time points, cell lysates were immunoprecipitated using anti-BCL10-conjugated or control anti- IgG-conjugated beads. The immunoprecipated complex and cell lysates were subjected with immunoblotting analysis with anti-BCL10, anti-MAVS, anti-TRAF6 antibodies.

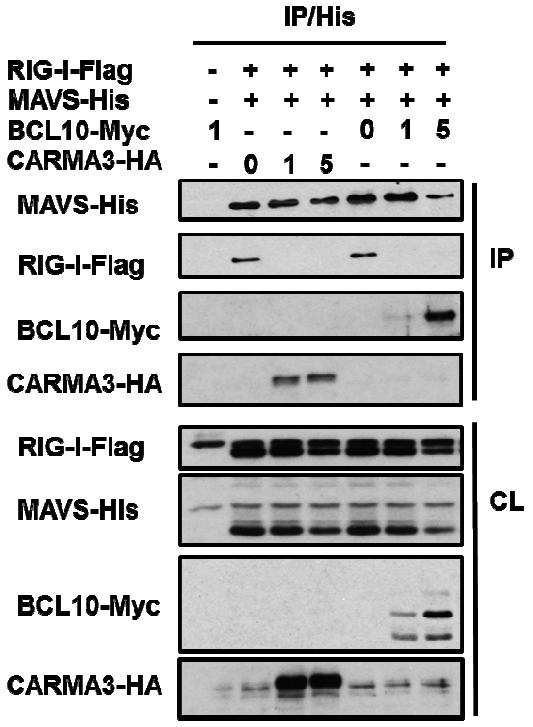

Figure 30 CARMA3 and BCL10 competed with RIG-I in binding with MAVS.MAVS-His and RIG-I-FLAG were overexpressed in presence of different doses of CARMA3-HA or BCL10-MYC in HEK 293 cells. At 24 hours after infection, cell lysates were precipitated using Ni-NTA magnetic beads. The precipitated complex and cell lysates were subjected with immunoblotting analysis with anti-HIS (MAVS), anti-FLAG (RIG-I), anti-MYC (BCL10), anti-HA (CARMA3) antibodies.

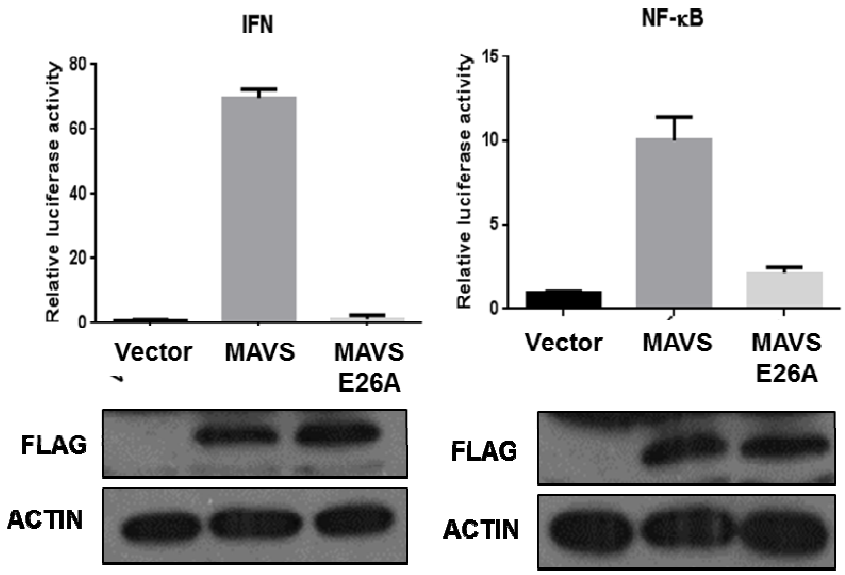

Figure 31 The aggregation of MAVS was required for NF-κB and IRF3 activation.

HEK 293 cells were transfected with plasmids overexpressing MAVS WT-FLAG or MAVS E26A-FLAG in presence of plasmids encoding NF-κB-luc or IFNβ-luc. The NF-κB and IRF3 activation were measured by luciferase assay. Cell lysates from transfected cells were subjected with immunoblotting analysis with anti-FLAG (MAVS WT and MAVS E26A), anti-ACTIN antibodies.

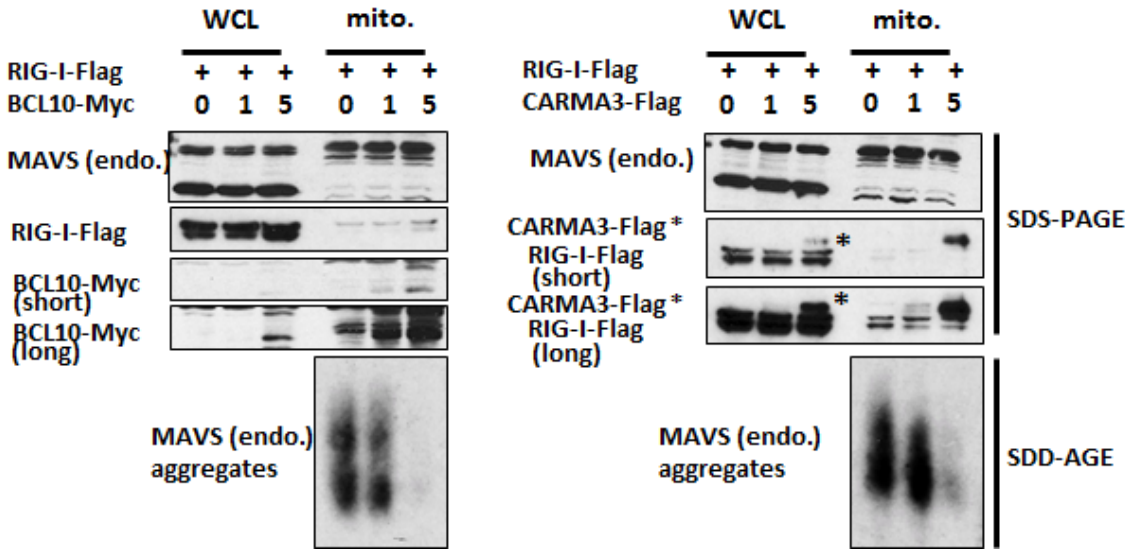

Figure 32 The interaction between CARMA3 or BCL10 with MVAS inhibited MAVS to form prion-like structure. HEK 293 cells were transfected with plasmids overexpressing RIG-I-FLAG and different dose of BCL10-MYC (A) or CARMA3-FLAG (B). 24 Hours after transfection, mitochondrial and cell lysates were isolated from transfected cells. Then mitochondrial were lysed and subjected with SDD-AGE to detect MAVS aggregates. Cell lysates were subjected with immunoblotting with the indicated antibodies.

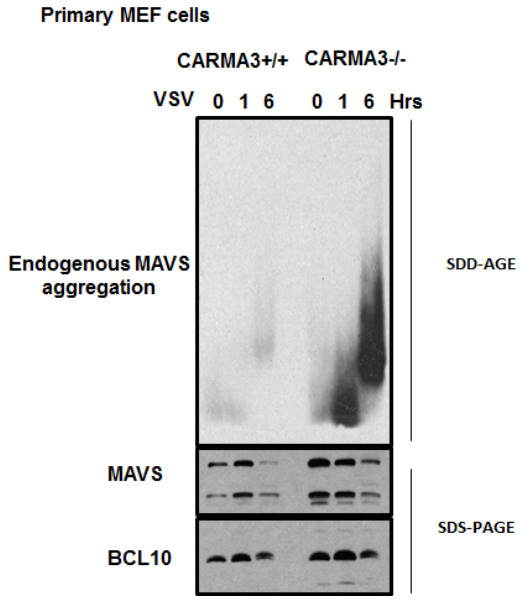

Figure 33 CARMA3 deficiency in cells led to increased aggregation of MAVS after virus infection. Primary WT and CARMA3 deficient MEF cells were infected with VSV at MOI=3. At the different time points after infection, mitochondrial and cell lysates were isolated from cells. Then, mitochondrial were lysed and subjected with SDD-AGE to detect MAVS aggregates. Cell lysates were subject to immunoblotting with the indicated antibodies.

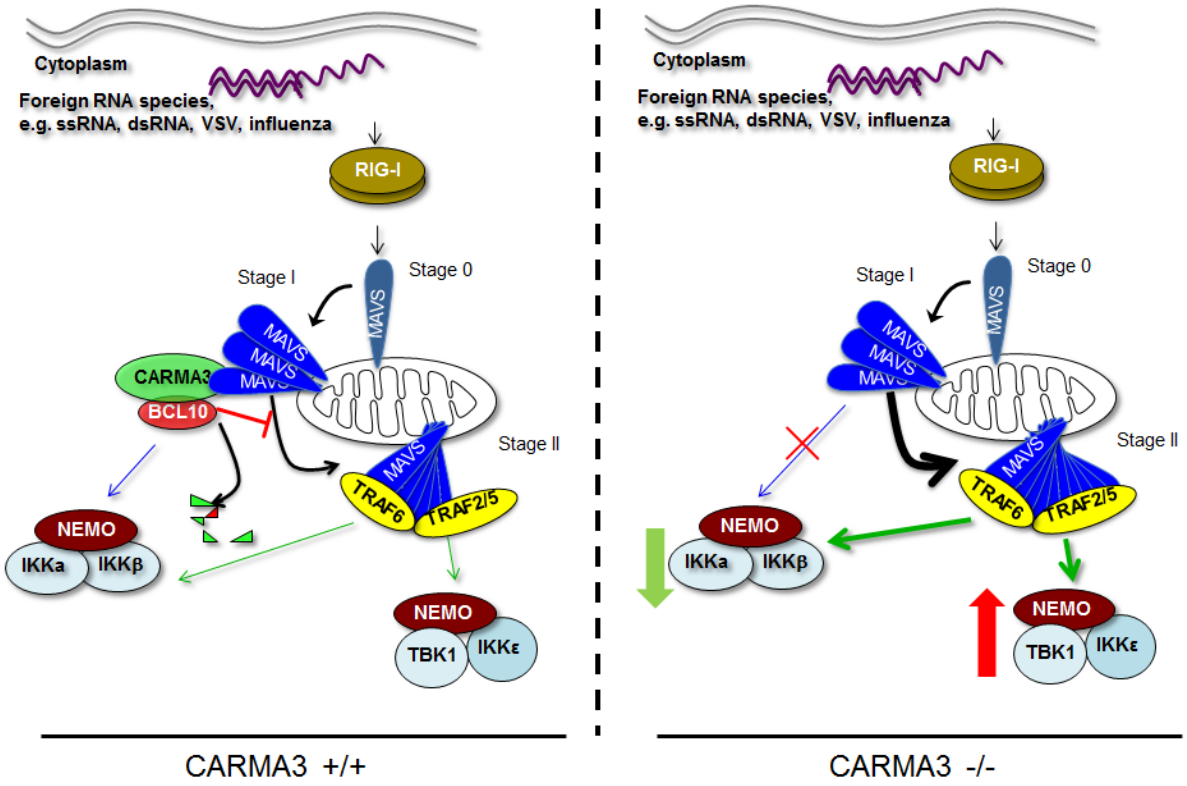

Figure 34 Schematic models of CARMA3 and BCL10-mediating MAVS aggregation and MAVS-mediating signaling pathway

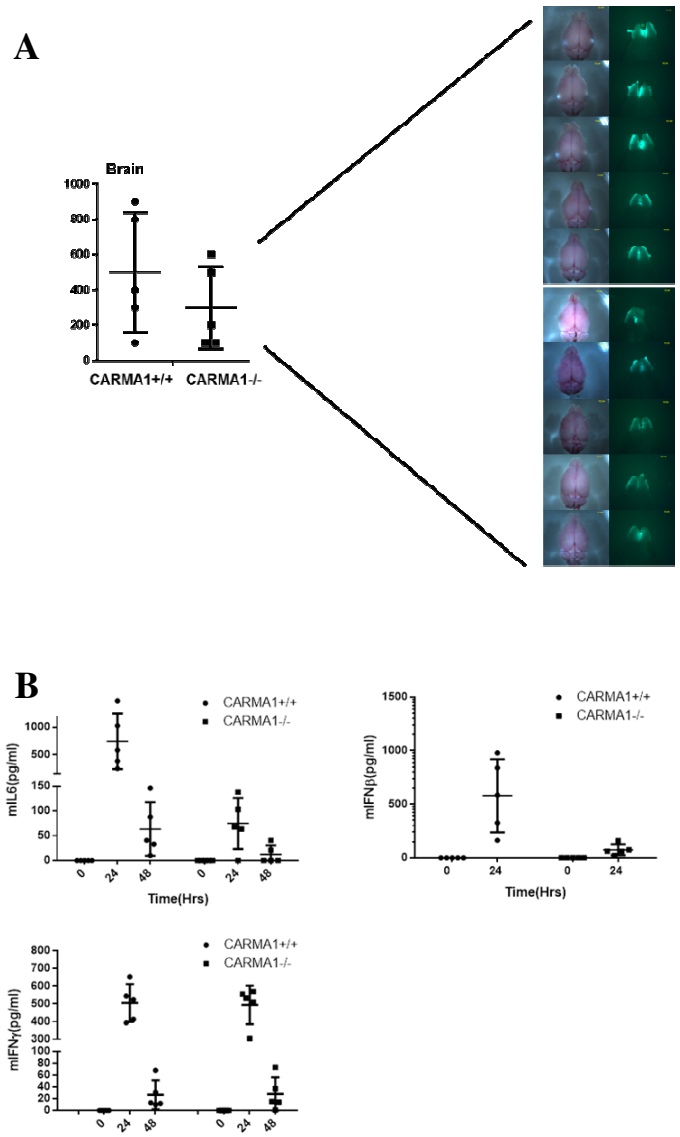

Figure 35 Compared to WT mice, CARMA1-deficient mice had less serum IFNβ and IL6 after VSV infection. Groups of 6-8 weeks WT or CAMRA1 deficient mice were intranasally infected with VSV at pfu=1×10^7. Serum or brains were harvested from the infected mice at 24 or 48 hours after VSV-GFP infection. (A) The pictures of the VSV-GFP in brains were taken by fluorescence microscope. (B) Serum IL6, IFNβ and IFNγ were measured by ELISA.

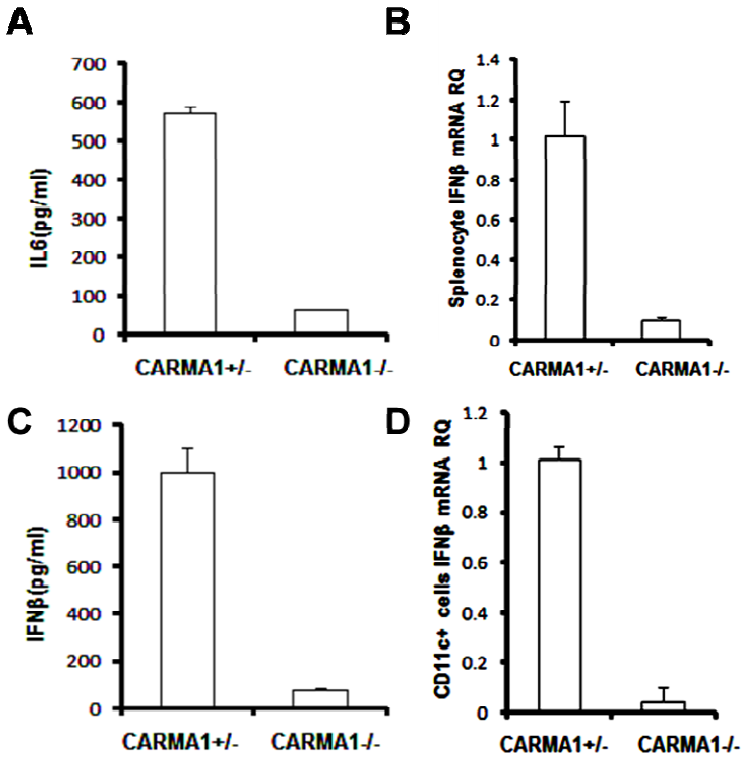

Figure 36 CARMA1 contributed to VSV-induced the production of IFNβ in splenocyte and CD11c$^+$ cells.6-8 weeks WT or CAMRA1 deficient mice were intranasally infected with VSV at pfu=1×10^7. Serum, splenocyte and CD11c$^+$ cells from splenocyte were harvested from the infected mice at 24 hours after VSV-GFP infection. (A) The serum IFNβ and IL6 were measured by the corresponding ELISA kits. (B) The production of IFNβ from different types of cells was measured by RT-PCR.

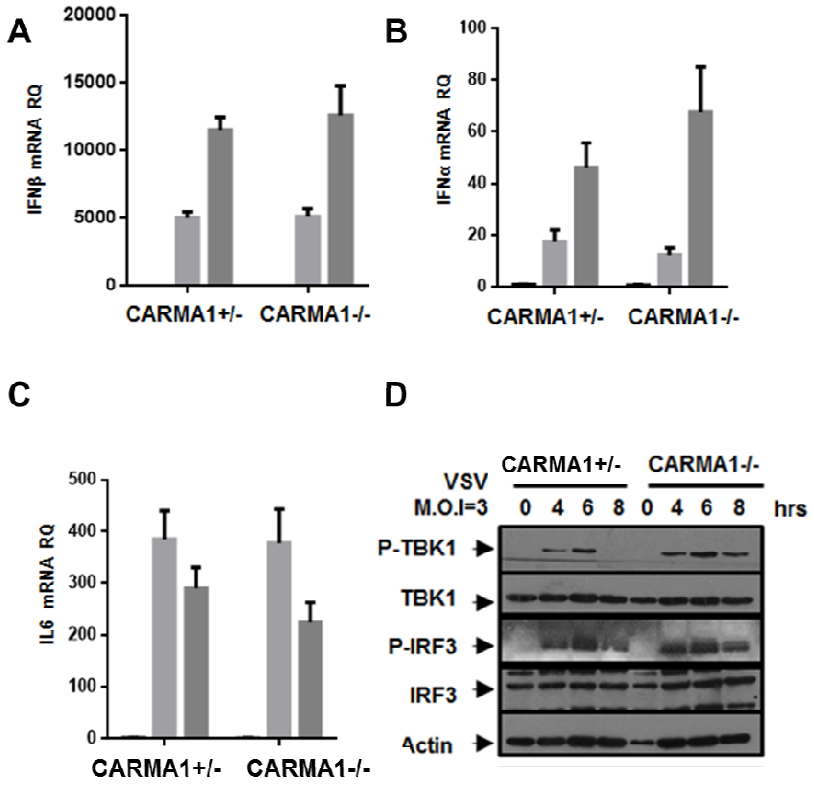

Figure 37 CARMA1 deficiency did not affect VSV-induced the production of IL6 and IFNβ in BMDMs. BMDM was harvested from different types of mice. WT and CARMA1 deficient BMDMs were infected with VSV at pfu=3. (A) The production of type I IFNs was measured by RT-PCR. (B) The production of IL6 was measured by RT-PCR. (C) Cell lysates from infected cells were subject to immunoblotting using indicated antibodies.

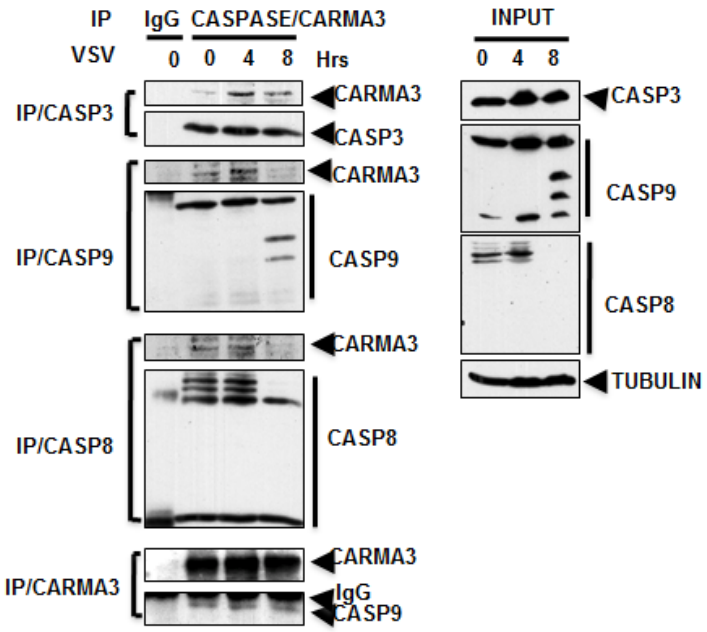

Figure 38 CARMA3 interacted with CASPASE-3, CASPASE-8 and capase-9.A431 cells were infected with VSV at pfu=3. At different time points, cell lysates were subjected with immunoblotting using indicated antibodies or immunoprecipitated using anti-CARMA3, CASPASE8, CASPASE9 or CASPASE3 antibodies-conjugated beads. The immunoprecipitated complexes were subjected with immunoblotting using indicated antibodies.

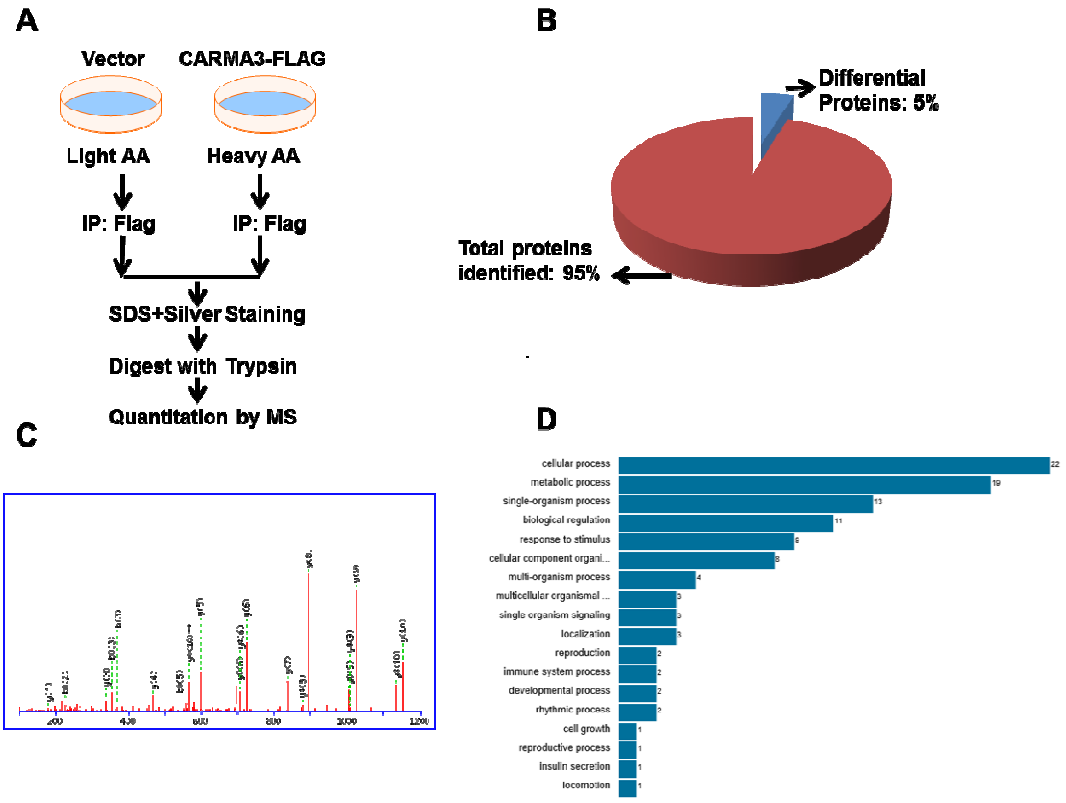

Figure 39 SILAC experiments to identify CARMA3's binding partners in cells. (A) Workflow chart of the SILAC experiment. (B) Numbers of differential proteins and total proteins identified. The pie chart showed percentages of differential proteins and total proteins identified. (C) A representative spectrum assigned to CARMA3. (D) Gene ontology(GO) analysis was performed using Uniprot.

CHAPTER 4: DISCUSSION

Using WT MEF cells and CARAM3 or BCL10 deficient cells, we showed that CARMA3 and BCL10 played a positive role in RIG-I/MAVS-mediated NF-κB activation, whereas a negative role in RIG-I/MAVS-mediated IRF3 activation. As a result, CARMA3 or BCL10-deficient cells produced less IL6, but more type I IFNs than WT cells did, upon VSV infection or specific ligands transfection. It was found that type I IFNs produced by cells constituted the host first defense line against virus infection(Schneider, Chevillotte et al. 2014). Therefore, we found that CARMA3 deficient cells had less VSV replication after infection. VSV and influenza mice model also confirmed the negative role of CARMA3 and BCL10 during virus infection. Both in VSV and influenza mice model, CARMA3 deficient mice had less virus titer than WT mice did. Furthermore, CARMA3 deficient mice had more local IFNβ production after virus infection. Mechanistic study showed that CARMA3 and BCL10 interacted with MAVS and directly regulated MAVS activities. CARMA3 and BCL10 overexpression inhibited MAVS aggregation triggered by RIG-I overexpression. Furthermore, MAVS more easily underwent aggregation in CARMA3 deficient cells, compared to the WT cells. Together, these findings provided a strong evidence to show the important role of the CARMA3 and BCL10 in orchestrating NF-κB and IRF3 activation.

Seasonal influenza virus outbreak in human results in about 3~5 million cases of severe illness and around 500,000 deaths worldwide (Lozano, Naghavi et al. 2012). H1N1, H2N2and H3N2 are the best-known IAVs currently circulating in humans. Additionally,

avian influenza strains, such as H5N1 and H7N9, are emerging highly pathogenic strains with significant pandemic potential and post a serious threat to global public health (Yen and Webster 2009, Lam, Wang et al. 2013). Therefore, it is critical to study the host immune response against IAV, which may facilitate the rational design of interference therapeutic.

It has been found that genetic diversity contributes to broad host responses and outcomes upon IAV infection. Revealing genetic variations will provide the important information for our understanding of antiviral immune responses. It is well known that genetic variations between different mouse strains contribute to diverse phenotypic responses to IAV infection. Therefore, it is reasonable to use mouse models to reveal genetic diversity for host susceptibility to IAV infections and thereby, to identify many important genes associated with host responses, for example, the landmark discovery of TLR4(Poltorak, He et al. 1998). Recently, Ferris et al has been identified three novel quantitative trait loci (QTL) that may contribute to the mice susceptibility for IAV infection, using incipient lines of mice with highly genetical diversity. CARD10 that encodes CARMA3 was found within one of QTL. However, the role of CARMA3 during IAV infection remains largely unknown. Previous studies from our lab and others indicate the important role of CARMA3 in NF-κB signaling pathway (Grabiner, Blonska et al. 2007, McAllister-Lucas, Ruland et al. 2007, Jiang, Grabiner et al. 2011). However, the role CARMA3 in response to virus infection has not been investigated before. In the study, we studied the role of CARMA3 and BCL10 in RIG-I/MAVS signaling pathway for the first time, which suggests that CARMA3/Card10 may be the genes contributing to the observed phenotype found in the study by Ferris et al (Ferris, Aylor et al. 2013). It was found that influenza NS1 protein interacted with some PDZ-

containing proteins and inhibited the cellular anti-virus response, for example, the production of IFNβ(Medina and Garcia-Sastre 2011). CARMA3 contains a PDZ domain and plays an important role in anti-virus response. It would be interest to study whether CARAM3 is one of host protein targeted by virus protein. Establishing these new paradigm will provide the molecular basis for our future research to investigate whether the differential mutations or SNP of CARMA3 (and its associated complex) contributes to the distinct response in human patients to IAV (or other respiratory viruses) infection.

Our data suggested that CARMA3 and BCL10 played a positive role in RIG-I/MAVS-mediated NF-κB activation, but a negative role in RIG-I/MAVS-mediated IRF3 activation. Therefore, CARMA3 or BCL10 served as a "switch" to orchestrate NF-κB and IRF3 activation in RIG-I/MAVS signaling pathway, which was different from other regulators. Most of them only had a unique role in both pathways. For example, the nucleotide-binding domain and leucine-rich repeat containing family member 1(NLRX1) inhibited the interaction between MAVS and RIG-I and thereby, inhibiting both NF-κB and IRF3 activation (Allen, Moore et al. 2011). Similarly, focal adhesion kinase(FAK) interacted with MAVS on the outer membrane of mitochondrial in a virus-dependent manner and inhibited the MAVS signaling(Bozym, Delorme-Axford et al. 2012). Another example is laboratory of genetics and physiology 2 (LGP2), which serves a negative role in RLR pathway by interfering the interaction between MAVS and downstream many E3 ligases (Komuro and Horvath 2006, Tang and Wang 2009).

Similar to CARAM3 and BCL10, the linear ubiquitin assembly complex (LUBAC) also plays a dual role in MAVS signaling. LUBAC consists of the E3 ligases HOIL-1L, HOIP and

the accessory protein SHARPIN, which functions to stabilize the whole complex. After virus infection, SHARPIN-deficient cells (cpdm) produced more type I IFNs, but decreased NF-κB activation and less VSV replication. LUBAC induced linear ubiquitination of NEMO, which led to NEMO's association with TRAF3 and thereby, disrupted MAVS-TRAF3 interaction. In this way, LUBAC served as a "switch" in both NF-κB and IRF3 signaling pathways by regulating the linear ubiquitination of NEMO. The similarity in cellular response during virus infection suggested that CARMA3 and LUBAC might share the similar mechanism to regulate MAVS signaling. Interestingly, previous studies in our lab showed the CARMA3 physically interacted with NEMO and regulated IKK activities through NEMO-associating ubiquitination. Additionally, linear ubiquitination of NEMO has been shown to play an important role in activation of IKK complex in response to different stimulus (Belgnaoui, Paz et al. 2012). It may explain why the NF-κB signaling pathway is partially defective in CARMA3 deficient cells. More studied are needed to test the hypothesis. All studies suggested the complicated regulating mechanisms in RIG-I/MAVS signaling pathways.

NF-κB signaling pathway can be activated by many viruses throughout different mechanisms(Santoro, Rossi et al. 2003). However, it remains controversial that NF-κB activity is beneficial to host. On one hand, NF-κB target genes play important roles in the activation of the host immune and inflammatory response(Pahl 1999). For example, the NF-κB activation induced the expression of many genes including many enzymes such as cyclooxygenase 2, the inducible form of nitric oxide synthase, a variety of cytokines and chemokines, receptors responsible for immune recognition, receptors involved in neutrophil adhesion an transmigration across blood vessel walls, proteins required for antigen

presentation and etc(Pahl 1999). Additionally, NF-κB activation does not required new protein synthesis. Therefore, NF-κB activation is a rapid event that occurs within minutes after virus infection, which constitutes the first host defense line against virus infection(Hoesel and Schmid 2013). Consistent with this, mice with the deficiency of NF-κB family members exhibit susceptible to virus infection. On the other hand, many viruses evolve different strategies to hijack NF-κB, including HIV-1, HTLV-1, influenza virus, hepatitis B and C virus, Herpes virus and etc(Santoro, Rossi et al. 2003). For example, functionally important NF-κB-binding sites have been identified in the genome of several viruses, including HIV-1, SV40 and different members of herpesvirus. These viruses utilize NF-κB to drive the expression of many viral proteins (Sassone-Corsi, Wildeman et al. 1985, Nabel and Baltimore 1987, Cherrington and Mocarski 1989, Rong, Libermann et al. 1992). Additionally, the NF-κB is a transcription factor regulating the expression of many anti-apoptotic genes such as members of the Bcl2 family, cellular inhibitors of apoptosis -1, 2, TRAF proteins, and the FLICE-inhibitory protein(Hoesel and Schmid 2013). Therefore, NF-κB activation improves cellular survival after virus infection, which is prerequisite for completion of entire virus life cycle. Moreover, sometimes, aberrant NF-κB activation sometimes caused chronic inflammation and leads to tissue damage, which is harmful to the host. Therefore, virus-induced NF-κB activation is double-edged sword for both host and pathogen survival.

During RNA virus infection, NF-κB was activated through both TLR-dependent and MAVS/RIG-I signaling pathways. It was well established that CARMA3 is not required for

TLR-induced NF-κB activation (Jiang, Grabiner et al. 2011, Pan and Lin 2013). In this study, we found loss of CARMA3 impaired poly (I:C) and 5'ppp-dsRNA transfection induced NF-κB activation. This suggests that CARMA3 and BCL10 play a specific role in by RIG-I/MAVS signaling but not TLR-dependent NF-κB activation. However, in mice model, both TLR and RIG-I-dependent signaling pathways contributed to NF-κB activation in immune cells. This may explain why we don't observe significant effect of CARMA3 deficiency in systematic IL-6 mRNA at 24 hours post infection of VSV infection.

CARMA3 deficient cells enhanced the production of IFNβ but decreased NF-κB activation after virus infection. It suggested that NF-κB did not play an essential role in IFNβ production. Earlier studies revealed that NF-κB could bind to positive regulatory domains II (PRDII) in IFN promoter and is required for the assemble of IFNβ enhanceosome. Single base substitutions in κB sites in IFN promoter impaired inducibility of the IFN beta. However, there is no endogenous evidence to show the essential role of NF-κB in the IFNs induction at that time (Thanos and Maniatis 1995, Merika, Williams et al. 1998, Agalioti, Lomvardas et al. 2000). Later, using $p65^{-/-}$, $p50^{-/-}p65^{-/-}$ MFE cells, the researchers showed that the production of type I IFNs was modest decreased after virus infection(Wang, Hussain et al. 2007). Consistently, using p65-/- MFE cells, another two groups confirmed the essential role of NF-κB in the early, but not late IFNs induction. It was found p65 deficient cells produced less type I IFNs after virus infection at the early time points, but not later time points (Basagoudanavar, Thapa et al. 2011). One reasonable explanation is the activation of IRF3 or IRF7. The essential role of IRF3 and IRF7 has been demonstrated using mouse

model. More importantly, high activation of IRF3 only sufficiently induced the type I IFNs in p65-/- MEF cells (Wang, Basagoudanavar et al. 2010, Basagoudanavar, Thapa et al. 2011). In our studies, the NF-κB activation was decreased in CARMA3 deficient MEF cell, whereas IRF3 activation was enhanced, which resulted in the increased production of type I IFNs.

CARMA3 and BCL10 may provide a better drug target, considering their dual role in MAVS signaling. On one hands, drugs targeting CARMA3 and BCL10 manipulate the production of type I IFNs, which inhibit virus proliferation by targeting proteins or functions involved in virus life cycle. On the other hands, it suppresses the inflammation by inhibiting NF-κB activation, which is double-edged sword during virus infection. Therefore, the balance between NF-κB activation and antiviral response is key events for host to survive. Drugs targeting CARMA3 and BCL10 may meet the scenario.

Currently, the prevail view is that the "activated" MAVS undergoes self-aggregation to form prion-like structure, which severs as a platform on mitochondrial to recruit many E3 ligases, including TRAF6, TRAF2, TRAF5 and LUBAC. These E3 ligases play essential roles in activating both NF-κB and IRF3. Therefore, the MAVS polymerization is essential for both pathways (Hou, Sun et al. 2011). There is something in common between our model and prevailing model. We also confirmed the importance of MAVS self-aggregation in both pathways by luciferase assay using plasmids encoding WT MAVA and MVAS E26A. The difference between two models lies in different state of MAVS aggregates. Our model shows that MAVS self-aggregation was a dynamic process. Less aggregated MAVS interacts with CAMRA3 and BCL10, which is important for NF-κB activation and blocks the formation of more aggregated MAVS. After CARMA3 is cleaved, the MAVS undergoes further

aggregation to activate both the IRF3 and NF-κB. Compared to previous model, our model can explain that NF-κB activates prior to IRF3 activation. Also, 1M GA can block the IRF3 activation, but cannot block the degradation of IKBα. Furthermore, the data from Liu's paper also supported our model. Using agarose gradient assay, the researchers found the activated MAVS exited in complex with different molecular weight. It suggested that MAVS had different aggregated status (Hou, Sun et al. 2011). Additionally, there is IKKβ only in the complex with low molecular weight.

CARMA family has three members, CARMA1, CARMA2, CARMA3, which share similar domains structure but with different tissue distribution(Jiang and Lin 2012). It suggests that CARMA1 and CARMA3 may regulate the same signaling pathway in a similar manner but in different tissues (Grabiner, Blonska et al. 2007). Consistent with this, previous studies showed that CARMA1 was the counterpart of CARMA3 in hematopoietic cells (Matsumoto, Wang et al. 2005). However, we surprisingly found that CARMA1 played a positive role in VSV-induced the production of both IL6 and IFNβ *in vivo*, which is different form CARMA3. CARMA1 deficient mice had less serum IL6 and IFNβ than WT mice did at 24 hours after virus infection. In contrast, the level of serum IFNγ is similar between WT and CARAM1 mice. While in CARMA3 deficient mice, the level of serum IL6 and IFNβ is comparable with WT mice. It is well known that IFNs with their receptors are important for host immune system against virus infection(Schneider, Chevillotte et al. 2014).Therefore, CARMA1 contributed to the innate immunity against virus infection by regulating the production of IFNβ.

Previous studies mainly focused on revealing the role of CARMA1 in NF-κB activation in T cell or B cells and thereby, in adaptive immunity. Therefore, it would be interesting to study the role of CARMA1 in innate immunity. Dendritic cells would be a candidate cell type used in our future studies, since they are the main IFN producing cells *in vivo* after RNA virus infection(Colonna, Krug et al. 2002). Additionally, using the $CD11c^+$ cells from spleen from WT and CARAM1 deficient mice, we found that VSV-induced IL6 and IFNβ production is decreased in CARMA1 deficient cells. It suggested that CARMA1 contributed to the production of these two cytokines in dendritic cells. More studies are needed to study how CARMA1 contributed to observed phenotype. We will investigate the role of CARMA1 in RIG-I-and TLR-dependent signaling pathway in dendritic cells, respectively, since RIG-I and TLR system exert antiviral response in a cell type dependent manner. For example, RIG-I is required for the production of type I IFNs in conventional dendritic cells (DCs). In contrast, plasmacytoid DCs utilized the TLR system rather than RIG-I for viral detection (Kato, Sato et al. 2005). It may explain that CARMA1 plays a positive role in VSV-induced the production of cytokines, which is different from CARMA3.

Using bone marrow derived-macrophages, we found that CARMA1 deficiency did not affect VSV-induced the production of IL6 and IFNβ in macrophage, since the production of two cytokines is similar in cells from WT or CARMA1-deficient mice. Consistent with this, the activation of TBK1-IRF3 was also similar in BMDMs from both types of mice. One possible explanation for this observation is that other CARD domain containing proteins may substitute the CARMA1's role in macrophage. CARD9 may be the best candidacy. CARD9 is structurally similar to CARMA family members with N-terminal CARD and a CC domain.

However, it lacks the C-terminal MAGUK domain, which is important for plasma membrane localization(Blonska and Lin 2011). Without MAGUK domain, CARD9 may reside in cytosol and be recruited to signaling complex after activation. Different from CARMA family proteins, the CARD9 expression seems to be restricted to myeloid cells such as macrophages, dendritic cells and neutrophils(Bertin, Guo et al. 2000, Gross, Gewies et al. 2006). More recent studies have revealed the important role of CARD9 in RIG-I/MAVS signaling pathway (Poeck, Bscheider et al. 2010). The authors found that CARD9-deficient myeloid cells produced less IL6 and pro-IL-1β after transfection of RIG-I ligands or dsRNA virus infection. Since the transcription of *il6* and pro-IL-1β are controlled by NF-κB signaling pathway, CARD9 may contribute to RIG-I-mediated NF-κB activation in macrophage, which may substitute CARMA1's role in the same signaling pathway (Poeck, Bscheider et al. 2010).

Although serum IFNβ level is decreased in CARMA1 mice after VSV infection, the virus burden in brains of CARMA1 deficient mice is similar to that of WT mice (Fig.35 A&B). In contrast, the virus burden in brains of CARMA3 deficient mice is less than that of WT mice, while serum IFNβ level is comparable with mice (Fig8 A&B).These dates suggest that serum IFNβ level does not correlate with VSV spread in brains. It may due to the fact that the peripheral type I IFN would not easily go through blood brain barrier (BBB) to reach brain (Detje, Lienenklaus et al. 2014). Besides, VSV spread in brain is efficiently arrested by the local type I interferon (Detje, Meyer et al. 2009). Consistently, using qPCR, we can detect more production of IFNβ in brain from CARAM3 deficient mice than that from WT mice (Fig8 B), which decreased VSV spread in brain.

There are limitations in the present study. Firstly, our experiments relied too much on primary MEF cells to study antivirus response, although MAVS and RIG-I had wide tissue distribution and shared a similar signaling pathway to activate NF-κB and IRF3 in many types except plasmacytoid dendritic cells (Sun, Sun et al. 2006). It is well known that cellular antiviral response is determined by both the cell type and virus type. For example, VSV is capable of infecting many different types of cells, whereas the main targets of influenza virus are epithelial cells. More importantly, the majority of data generated using VSV may not be extended to IAV. In this case, we will isolate and differentiate primary lung and airway epithelial cells (LECs) from WT and CARMA3 deficient mice, and then infect cells with IAV or VSV to measure NF-κB by and TBK1/IRF3 activation as well as the production of IFNβ and IL6. Also, we are going to detect virus replication in WT and CARMA3 KO cells and the sensitivity of two cell types to virus infection.

Our study suggests a dual role of the CARMA3-BCL10 complex in RIG-I/MAVS-mediated NF-κB and IRF3 activation and elucidates the mechanism of how CAMRA3 and BCL10 regulate MAVS signaling, which may facilitate the development of the corresponding methods to manipulate the antivirus response and the production of inflammatory cytokines.

CHAPTER 5: FUTURE DIRECTION AND PERSPECTIVE SECTION

As a scaffold protein, CARMA3 contains multiple domains for protein-protein interaction including CARD domain and PDZ-domain. Here we found that CARMA3 interacted with MAVS and negatively regulated the formation of MAVS aggregates and IRF3 activation. It would be interesting to know which domains and/or residues are required for the interaction between CARMA3 and MAVS and thereby, are important for mediating RIG-I/MAVS signaling. Fine mapping of CARMA3 will provide insights for further studies and drug development. Since there is no cure and effective vaccine available for many RNA viruses, it will be important to develop medicine that help reduce inflammation while enhance anti-viral response. CARMA3 is such a good target that meets both criteria.

Furthermore, it was interesting to find that CARMA3 protein level was gradually turned over or CARMA3 was cleaved during VSV infection, which may serve as a feedback to enhance the IRF3 activation, and meanwhile, to shut down NF-κB activation. The presence of CARMA3 during early time of infection inhibited the function of MAVS in mediating IRF3 activation. With CARMA3 gradual turnover or cleavage, this inhibitory effect weakens and IRF3 activation is activated. Therefore, in the absence of CARMA3 from the beginning of virus infection, IRF3 can be activated at greater level and maybe at earlier time points as well. Further studies are necessary to address what causes this CARMA3 turnover or cleaved and how? CASPASE 8 might be a potential protein cleaving CARMA3, since we found that CASPASE8 interacted with CARMA3. Additionally, we identified one

cleaved band using antibody targeting C-terminal of protein. Using antibody targeting both ends of the protein, we identified two cleaved bands. It suggested the cleaved site was located in the middle of proteins. Then, based on sequence analyses, we found there was one potential CASPASE8 cutting site in the middle of CARMA3. More studies are needed to study the role of CASPASE 8 in the cleavage of CARMA3, since it may reveal the role of CASPASE 8 in RIG-I/MAVS signaling pathways.

By SILAC experiment, we identified 25 potential CARMA3 binding partners. Among them, ZAP aroused our great interests. ZAP was initially discovered by screening genes that prevent retrovirus infection in a cDNA library. Later, the functional studies of ZAP protein revealed that the expression of ZAP inhibited the expression of viral genes in the cytoplasm without affecting the level of nuclear mRNAs (Gao, Guo et al. 2002). The following studies showed that ZAP directly interacted with viral mRNA at ZAP-responsive elements through its four CCCH zinc-finger motifs(Jeong, Kim et al. 2010). Then, it recruited polyA-specific ribonuclease PARN, 3'-5' exoribonuclease complex, DCP1-DCP2 decapping complex to degrade the RNA body from both 5' and 3'-ends(Zhu, Chen et al. 2011). ZAP targeting viruses includes HIV-1, moloney and murine leukemia virus, xenotropic MuLV-related virus, ebola virus, marburg virus, sindbis virus and Ross river virus. Among them, HIV-1 and Ebola also were RIG-I target viruses (Spiropoulou, Ranjan et al. 2009, Wang, Wang et al. 2013). As a CARAM3 binding partner, ZAP might work together with CARAM3 in the RIG-I/MAVS signaling pathway. More studies are needed to test this hypothesis.

By GO analysis, we found that most of CARMA3 binding partners were involved in metabolic process (Figure 39D). Additionally, both CARMA3 and BCL10 reside in the

mitochondrial (Figure 32&33). The mitochondrial have been shown to play an important role in metabolic pathways including carbohydrate metabolism, fatty acid oxidation, urea cycle (Demine, Reddy et al. 2014) . Therefore, in future studies, we are going to investigate the role of CAMRA3 in these metabolic pathways.

In this study, we found that CARMA3 deficient mice showed reduced disease symptoms and/or better survival, when challenged with VSV or influenza. These viruses represent negative, single-stranded RNA viruses. It will be interesting to see if CARMA3 indeed play a general effect in response to other RNA viruses. And can this expend to DNA viruses?

CHAPTER 6: BIBLIOGRAPHY

Ablasser, A., F. Bauernfeind, G. Hartmann, E. Latz, K. A. Fitzgerald and V. Hornung (2009). "RIG-I-dependent sensing of poly(dA:dT) through the induction of an RNA polymerase III-transcribed RNA intermediate." Nat Immunol **10**(10): 1065-1072.

Agalioti, T., S. Lomvardas, B. Parekh, J. Yie, T. Maniatis and D. Thanos (2000). "Ordered recruitment of chromatin modifying and general transcription factors to the IFN-beta promoter." Cell **103**(4): 667-678.

Air, G. M. (1981). "Sequence relationships among the hemagglutinin genes of 12 subtypes of influenza A virus." Proc Natl Acad Sci U S A **78**(12): 7639-7643.

Akira, S., S. Uematsu and O. Takeuchi (2006). "Pathogen recognition and innate immunity." Cell **124**(4): 783-801.

Alexopoulou, L., A. C. Holt, R. Medzhitov and R. A. Flavell (2001). "Recognition of double-stranded RNA and activation of NF-kappaB by Toll-like receptor 3." Nature **413**(6857): 732-738.

Allen, I. C., C. B. Moore, M. Schneider, Y. Lei, B. K. Davis, M. A. Scull, D. Gris, K. E. Roney, A. G. Zimmermann, J. B. Bowzard, P. Ranjan, K. M. Monroe, R. J. Pickles, S. Sambhara and J. P. Ting (2011). "NLRX1 protein attenuates inflammatory responses to infection by interfering with the RIG-I-MAVS and TRAF6-NF-kappaB signaling pathways." Immunity **34**(6): 854-865.

Ariza, M. E., R. Glaser, P. T. Kaumaya, C. Jones and M. V. Williams (2009). "The EBV-encoded dUTPase activates NF-kappa B through the TLR2 and MyD88-dependent signaling pathway." J Immunol **182**(2): 851-859.

Basagoudanavar, S. H., R. J. Thapa, S. Nogusa, J. Wang, A. A. Beg and S. Balachandran (2011). "Distinct roles for the NF-kappa B RelA subunit during antiviral innate immune responses." J Virol **85**(6): 2599-2610.

Belgnaoui, S. M., S. Paz, S. Samuel, M. L. Goulet, Q. Sun, M. Kikkert, K. Iwai, I. Dikic, J. Hiscott and R. Lin (2012). "Linear ubiquitination of NEMO negatively regulates the interferon antiviral response through disruption of the MAVS-TRAF3 complex." Cell Host Microbe **12**(2): 211-222.

Bertin, J., Y. Guo, L. Wang, S. M. Srinivasula, M. D. Jacobson, J. L. Poyet, S. Merriam, M. Q. Du, M. J. Dyer, K. E. Robison, P. S. DiStefano and E. S. Alnemri (2000). "CARD9 is a novel caspase recruitment domain-containing protein that interacts with BCL10/CLAP and activates NF-kappa B." J Biol Chem **275**(52): 41082-41086.

Bertin, J., L. Wang, Y. Guo, M. D. Jacobson, J. L. Poyet, S. M. Srinivasula, S. Merriam, P. S. DiStefano and E. S. Alnemri (2001). "CARD11 and CARD14 are novel caspase recruitment domain (CARD)/membrane-associated guanylate kinase (MAGUK) family members that interact with BCL10 and activate NF-kappa B." J Biol Chem **276**(15): 11877-11882.

Bi, L., S. Gojestani, W. Wu, Y. M. Hsu, J. Zhu, K. Ariizumi and X. Lin (2010). "CARD9 mediates dectin-2-induced IkappaBalpha kinase ubiquitination leading to activation of NF-kappaB in response to stimulation by the hyphal form of Candida albicans." J Biol Chem **285**(34): 25969-25977.

Bieback, K., E. Lien, I. M. Klagge, E. Avota, J. Schneider-Schaulies, W. P. Duprex, H. Wagner, C. J. Kirschning, V. Ter Meulen and S. Schneider-Schaulies (2002). "Hemagglutinin protein of wild-type measles virus activates toll-like receptor 2 signaling." J Virol **76**(17): 8729-8736.

Blonska, M. and X. Lin (2011). "NF-kappaB signaling pathways regulated by CARMA family of scaffold proteins." Cell Res **21**(1): 55-70.

Blonska, M., B. P. Pappu, R. Matsumoto, H. Li, B. Su, D. Wang and X. Lin (2007). "The CARMA1-Bcl10 signaling complex selectively regulates JNK2 kinase in the T cell receptor-signaling pathway." Immunity **26**(1): 55-66.

Boehme, K. W., M. Guerrero and T. Compton (2006). "Human cytomegalovirus envelope glycoproteins B and H are necessary for TLR2 activation in permissive cells." J Immunol **177**(10): 7094-7102.

Bouvier, N. M. and P. Palese (2008). "The biology of influenza viruses." Vaccine **26 Suppl 4**: D49-53.

Bozym, R. A., E. Delorme-Axford, K. Harris, S. Morosky, M. Ikizler, T. S. Dermody, S. N. Sarkar and C. B. Coyne (2012). "Focal adhesion kinase is a component of antiviral RIG-I-like receptor signaling." Cell Host Microbe **11**(2): 153-166.

Cantell, K., S. Hirvonen, H. L. Kauppinen and G. Myllyla (1981). "Production of interferon in human leukocytes from normal donors with the use of Sendai virus." Methods Enzymol **78**(Pt A): 29-38.

Cantell, K., S. Hirvonen and V. Koistinen (1981). "Partial purification of human leukocyte interferon on a large scale." Methods Enzymol **78**(Pt A): 499-505.

Cherrington, J. M. and E. S. Mocarski (1989). "Human cytomegalovirus ie1 transactivates the alpha promoter-enhancer via an 18-base-pair repeat element." J Virol **63**(3): 1435-1440.

Chiu, Y. H., J. B. Macmillan and Z. J. Chen (2009). "RNA polymerase III detects cytosolic DNA and induces type I interferons through the RIG-I pathway." Cell **138**(3): 576-591.

Colonna, M., A. Krug and M. Cella (2002). "Interferon-producing cells: on the front line in immune responses against pathogens." Curr Opin Immunol **14**(3): 373-379.

Compton, T., E. A. Kurt-Jones, K. W. Boehme, J. Belko, E. Latz, D. T. Golenbock and R. W. Finberg (2003). "Human cytomegalovirus activates inflammatory cytokine responses via CD14 and Toll-like receptor 2." J Virol **77**(8): 4588-4596.

Cros, J. F. and P. Palese (2003). "Trafficking of viral genomic RNA into and out of the nucleus: influenza, Thogoto and Borna disease viruses." Virus Res **95**(1-2): 3-12.

Demine, S., N. Reddy, P. Renard, M. Raes and T. Arnould (2014). "Unraveling biochemical pathways affected by mitochondrial dysfunctions using metabolomic approaches." Metabolites **4**(3): 831-878.

Detje, C. N., S. Lienenklaus, C. Chhatbar, J. Spanier, C. K. Prajeeth, C. Soldner, M. G. Tovey, D. Schluter, S. Weiss, M. Stangel and U. Kalinke (2014). "Upon intranasal VSV infection astrocytes in the olfactory bulb are important IFN-beta producers that protect from lethal encephalitis." J Virol.

Detje, C. N., T. Meyer, H. Schmidt, D. Kreuz, J. K. Rose, I. Bechmann, M. Prinz and U. Kalinke (2009). "Local type I IFN receptor signaling protects against virus spread within the central nervous system." J Immunol **182**(4): 2297-2304.

Diebold, S. S., T. Kaisho, H. Hemmi, S. Akira and C. Reis e Sousa (2004). "Innate antiviral responses by means of TLR7-mediated recognition of single-stranded RNA." Science **303**(5663): 1529-1531.

Diebold, S. S., M. Montoya, H. Unger, L. Alexopoulou, P. Roy, L. E. Haswell, A. Al-Shamkhani, R. Flavell, P. Borrow and C. Reis e Sousa (2003). "Viral infection switches non-plasmacytoid dendritic cells into high interferon producers." Nature **424**(6946): 324-328.

Fagerlund, R., K. Melen, L. Kinnunen and I. Julkunen (2002). "Arginine/lysine-rich nuclear localization signals mediate interactions between dimeric STATs and importin alpha 5." J Biol Chem **277**(33): 30072-30078.

Ferris, M. T., D. L. Aylor, D. Bottomly, A. C. Whitmore, L. D. Aicher, T. A. Bell, B. Bradel-Tretheway, J. T. Bryan, R. J. Buus, L. E. Gralinski, B. L. Haagmans, L. McMillan, D. R. Miller, E. Rosenzweig, W. Valdar, J. Wang, G. A. Churchill, D. W. Threadgill, S. K. McWeeney, M. G. Katze, F. Pardo-Manuel de Villena, R. S. Baric and M. T. Heise (2013). "Modeling host genetic regulation of influenza pathogenesis in the collaborative cross." PLoS Pathog **9**(2): e1003196.

Finkelshtein, D., A. Werman, D. Novick, S. Barak and M. Rubinstein (2013). "LDL receptor and its family members serve as the cellular receptors for vesicular stomatitis virus." Proc Natl Acad Sci U S A **110**(18): 7306-7311.

Fouchier, R. A., V. Munster, A. Wallensten, T. M. Bestebroer, S. Herfst, D. Smith, G. F. Rimmelzwaan, B. Olsen and A. D. Osterhaus (2005). "Characterization of a novel influenza A virus hemagglutinin subtype (H16) obtained from black-headed gulls." J Virol **79**(5): 2814-2822.

Fox, B. A., P. O. Sheppard and P. J. O'Hara (2009). "The role of genomic data in the discovery, annotation and evolutionary interpretation of the interferon-lambda family." PLoS One **4**(3): e4933.

Gaide, O., B. Favier, D. F. Legler, D. Bonnet, B. Brissoni, S. Valitutti, C. Bron, J. Tschopp and M. Thome (2002). "CARMA1 is a critical lipid raft-associated regulator of TCR-induced NF-kappa B activation." Nat Immunol **3**(9): 836-843.

Gaide, O., F. Martinon, O. Micheau, D. Bonnet, M. Thome and J. Tschopp (2001). "Carma1, a CARD-containing binding partner of Bcl10, induces Bcl10 phosphorylation and NF-kappaB activation." FEBS Lett **496**(2-3): 121-127.

Gao, G., X. Guo and S. P. Goff (2002). "Inhibition of retroviral RNA production by ZAP, a CCCH-type zinc finger protein." Science **297**(5587): 1703-1706.

Gao, S., A. von der Malsburg, S. Paeschke, J. Behlke, O. Haller, G. Kochs and O. Daumke (2010). "Structural basis of oligomerization in the stalk region of dynamin-like MxA." Nature **465**(7297): 502-506.

Georgel, P., Z. Jiang, S. Kunz, E. Janssen, J. Mols, K. Hoebe, S. Bahram, M. B. Oldstone and B. Beutler (2007). "Vesicular stomatitis virus glycoprotein G activates a specific antiviral Toll-like receptor 4-dependent pathway." Virology **362**(2): 304-313.

Gitlin, L., W. Barchet, S. Gilfillan, M. Cella, B. Beutler, R. A. Flavell, M. S. Diamond and M. Colonna (2006). "Essential role of mda-5 in type I IFN responses to polyriboinosinic:polyribocytidylic acid and encephalomyocarditis picornavirus." Proc Natl Acad Sci U S A **103**(22): 8459-8464.

Goff, S. P. (2004). "Retrovirus restriction factors." Mol Cell **16**(6): 849-859.

Gorjestani, S., M. Yu, B. Tang, D. Zhang, D. Wang and X. Lin (2011). "Phospholipase Cgamma2 (PLCgamma2) is key component in Dectin-2 signaling pathway, mediating anti-fungal innate immune responses." J Biol Chem **286**(51): 43651-43659.

Grabiner, B. C., M. Blonska, P.-C. Lin, Y. You, D. Wang, J. Sun, B. G. Darnay, C. Dong and X. Lin (2007). "CARMA3 deficiency abrogrates G-protein-coupled receptor-induced NF-kappaB activation." Genes Dev **21**(8).

Grabiner, B. C., M. Blonska, P. C. Lin, Y. You, D. Wang, J. Sun, B. G. Darnay, C. Dong and X. Lin (2007). "CARMA3 deficiency abrogates G protein-coupled receptor-induced NF-{kappa}B activation." Genes Dev **21**(8): 984-996.

Greenlund, A. C., M. O. Morales, B. L. Viviano, H. Yan, J. Krolewski and R. D. Schreiber (1995). "Stat recruitment by tyrosine-phosphorylated cytokine receptors: an ordered reversible affinity-driven process." Immunity **2**(6): 677-687.

Gross, O., A. Gewies, K. Finger, M. Schafer, T. Sparwasser, C. Peschel, I. Forster and J. Ruland (2006). "Card9 controls a non-TLR signalling pathway for innate anti-fungal immunity." Nature **442**(7103): 651-656.

Gyrd-Hansen, M. and P. Meier (2010). "IAPs: from caspase inhibitors to modulators of NF-kappaB, inflammation and cancer." Nat Rev Cancer **10**(8): 561-574.

Hansson, G. K. and K. Edfeldt (2005). "Toll to be paid at the gateway to the vessel wall." Arterioscler Thromb Vasc Biol **25**(6): 1085-1087.

Hayden, M. S. and S. Ghosh (2004). "Signaling to NF-kappaB." Genes Dev **18**(18): 2195-2224.

Heil, F., H. Hemmi, H. Hochrein, F. Ampenberger, C. Kirschning, S. Akira, G. Lipford, H. Wagner and S. Bauer (2004). "Species-specific recognition of single-stranded RNA via toll-like receptor 7 and 8." Science **303**(5663): 1526-1529.

Heim, M. H., I. M. Kerr, G. R. Stark and J. E. Darnell, Jr. (1995). "Contribution of STAT SH2 groups to specific interferon signaling by the Jak-STAT pathway." Science **267**(5202): 1347-1349.

Hemmi, H., T. Kaisho, O. Takeuchi, S. Sato, H. Sanjo, K. Hoshino, T. Horiuchi, H. Tomizawa, K. Takeda and S. Akira (2002). "Small anti-viral compounds activate immune cells via the TLR7 MyD88-dependent signaling pathway." Nat Immunol **3**(2): 196-200.

Henle, W. (1950). "Interference phenomena between animal viruses; a review." J Immunol **64**(3): 203-236.

Herman, M., M. Ciancanelli, Y. H. Ou, L. Lorenzo, M. Klaudel-Dreszler, E. Pauwels, V. Sancho-Shimizu, R. Perez de Diego, A. Abhyankar, E. Israelsson, Y. Guo, A. Cardon, F. Rozenberg, P. Lebon, M. Tardieu, E. Heropolitanska-Pliszka, D. Chaussabel, M. A. White, L. Abel, S. Y. Zhang and J. L. Casanova (2012). "Heterozygous TBK1 mutations impair TLR3 immunity and underlie herpes simplex encephalitis of childhood." J Exp Med **209**(9): 1567-1582.

Hoebe, K., X. Du, P. Georgel, E. Janssen, K. Tabeta, S. O. Kim, J. Goode, P. Lin, N. Mann, S. Mudd, K. Crozat, S. Sovath, J. Han and B. Beutler (2003). "Identification of Lps2 as a key transducer of MyD88-independent TIR signalling." Nature **424**(6950): 743-748.

Hoesel, B. and J. A. Schmid (2013). "The complexity of NF-kappaB signaling in inflammation and cancer." Mol Cancer **12**: 86.

Honda, K., H. Yanai, H. Negishi, M. Asagiri, M. Sato, T. Mizutani, N. Shimada, Y. Ohba, A. Takaoka, N. Yoshida and T. Taniguchi (2005). "IRF-7 is the master regulator of type-I interferon-dependent immune responses." Nature **434**(7034): 772-777.

Hong, X. X. and G. G. Carmichael (2013). "Innate immunity in pluripotent human cells: attenuated response to interferon-beta." J Biol Chem **288**(22): 16196-16205.

Hornung, V., J. Ellegast, S. Kim, K. Brzozka, A. Jung, H. Kato, H. Poeck, S. Akira, K. K. Conzelmann, M. Schlee, S. Endres and G. Hartmann (2006). "5'-Triphosphate RNA is the ligand for RIG-I." Science **314**(5801): 994-997.

Hou, F., L. Sun, H. Zheng, B. Skaug, Q. X. Jiang and Z. J. Chen (2011). "MAVS forms functional prion-like aggregates to activate and propagate antiviral innate immune response." Cell **146**(3): 448-461.

Isaacs, A. and J. Lindenmann (1957). "Virus interference. I. The interferon." Proc R Soc Lond B Biol Sci **147**(927): 258-267.

Isaacs, A., J. Lindenmann and R. C. Valentine (1957). "Virus interference. II. Some properties of interferon." Proc R Soc Lond B Biol Sci **147**(927): 268-273.

Jacobs, J. L. and C. B. Coyne (2013). "Mechanisms of MAVS regulation at the mitochondrial membrane." J Mol Biol **425**(24): 5009-5019.

Janeway, C. A., Jr. (2013). "Pillars article: approaching the asymptote? Evolution and revolution in immunology. Cold spring harb symp quant biol. 1989. 54: 1-13." J Immunol **191**(9): 4475-4487.

Jeong, M. S., E. J. Kim and S. B. Jang (2010). "Expression and RNA-binding of human zinc-finger antiviral protein." Biochem Biophys Res Commun **396**(3): 696-702.

Jiang, C. and X. Lin (2012). "Regulation of NF-kappaB by the CARD proteins." Immunol Rev **246**(1): 141-153.

Jiang, T., B. Grabiner, Y. Zhu, C. Jiang, H. Li, Y. You, J. Lang, M. C. Hung and X. Lin (2011). "CARMA3 is Crucial for EGFR-Induced Activation of NF-{kappa}B and Tumor Progression." Cancer Res **71**(6): 2183-2192.

Jiang, T., B. Grabiner, Y. Zhu, C. Jiang, H. Li, Y. You, J. Lang, M. C. Hung and X. Lin (2011). "CARMA3 is crucial for EGFR-Induced activation of NF-kappaB and tumor progression." Cancer Res **71**(6): 2183-2192.

Jiang, Z., T. W. Mak, G. Sen and X. Li (2004). "Toll-like receptor 3-mediated activation of NF-kappaB and IRF3 diverges at Toll-IL-1 receptor domain-containing adapter inducing IFN-beta." Proc Natl Acad Sci U S A **101**(10): 3533-3538.

Jin, J., H. Hu, H. S. Li, J. Yu, Y. Xiao, G. C. Brittain, Q. Zou, X. Cheng, F. A. Mallette, S. S. Watowich and S. C. Sun (2014). "Noncanonical NF-kappaB pathway controls the production of type I interferons in antiviral innate immunity." Immunity **40**(3): 342-354.

Kane, M., S. S. Yadav, J. Bitzegeio, S. B. Kutluay, T. Zang, S. J. Wilson, J. W. Schoggins, C. M. Rice, M. Yamashita, T. Hatziioannou and P. D. Bieniasz (2013). "MX2 is an interferon-induced inhibitor of HIV-1 infection." Nature **502**(7472): 563-566.

Kato, H., S. Sato, M. Yoneyama, M. Yamamoto, S. Uematsu, K. Matsui, T. Tsujimura, K. Takeda, T. Fujita, O. Takeuchi and S. Akira (2005). "Cell type-specific involvement of RIG-I in antiviral response." Immunity **23**(1): 19-28.

Kato, H., O. Takeuchi, S. Sato, M. Yoneyama, M. Yamamoto, K. Matsui, S. Uematsu, A. Jung, T. Kawai, K. J. Ishii, O. Yamaguchi, K. Otsu, T. Tsujimura, C. S. Koh, C. Reis e

Sousa, Y. Matsuura, T. Fujita and S. Akira (2006). "Differential roles of MDA5 and RIG-I helicases in the recognition of RNA viruses." Nature **441**(7089): 101-105.

Kawai, T. and S. Akira (2006). "Innate immune recognition of viral infection." Nat Immunol **7**(2): 131-137.

Kawai, T. and S. Akira (2011). "Toll-like receptors and their crosstalk with other innate receptors in infection and immunity." Immunity **34**(5): 637-650.

Kawai, T., S. Sato, K. J. Ishii, C. Coban, H. Hemmi, M. Yamamoto, K. Terai, M. Matsuda, J. Inoue, S. Uematsu, O. Takeuchi and S. Akira (2004). "Interferon-alpha induction through Toll-like receptors involves a direct interaction of IRF7 with MyD88 and TRAF6." Nat Immunol **5**(10): 1061-1068.

Kawai, T., K. Takahashi, S. Sato, C. Coban, H. Kumar, H. Kato, K. J. Ishii, O. Takeuchi and S. Akira (2005). "IPS-1, an adaptor triggering RIG-I- and Mda5-mediated type I interferon induction." Nat Immunol **6**(10): 981-988.

Klemm, S., S. Zimmermann, C. Peschel, T. W. Mak and J. Ruland (2007). "Bcl10 and Malt1 control lysophosphatidic acid-induced NF-kappaB activation and cytokine production." Proc Natl Acad Sci U S A **104**(1): 134-138.

Kok, K. H. and D. Y. Jin (2013). "Balance of power in host-virus arms races." Cell Host Microbe **14**(1): 5-6.

Kolakofsky, D., E. Kowalinski and S. Cusack (2012). "A structure-based model of RIG-I activation." RNA **18**(12): 2118-2127.

Komuro, A. and C. M. Horvath (2006). "RNA- and virus-independent inhibition of antiviral signaling by RNA helicase LGP2." J Virol **80**(24): 12332-12342.

Kotenko, S. V., G. Gallagher, V. V. Baurin, A. Lewis-Antes, M. Shen, N. K. Shah, J. A. Langer, F. Sheikh, H. Dickensheets and R. P. Donnelly (2003). "IFN-lambdas mediate antiviral protection through a distinct class II cytokine receptor complex." Nat Immunol **4**(1): 69-77.

Krug, A., G. D. Luker, W. Barchet, D. A. Leib, S. Akira and M. Colonna (2004). "Herpes simplex virus type 1 activates murine natural interferon-producing cells through toll-like receptor 9." Blood **103**(4): 1433-1437.

Lam, T. T., J. Wang, Y. Shen, B. Zhou, L. Duan, C. L. Cheung, C. Ma, S. J. Lycett, C. Y. Leung, X. Chen, L. Li, W. Hong, Y. Chai, L. Zhou, H. Liang, Z. Ou, Y. Liu, A. Farooqui, D. J. Kelvin, L. L. Poon, D. K. Smith, O. G. Pybus, G. M. Leung, Y. Shu, R. G. Webster, R. J. Webby, J. S. Peiris, A. Rambaut, H. Zhu and Y. Guan (2013). "The genesis and source of the H7N9 influenza viruses causing human infections in China." Nature **502**(7470): 241-244.

Latz, E., A. Schoenemeyer, A. Visintin, K. A. Fitzgerald, B. G. Monks, C. F. Knetter, E. Lien, N. J. Nilsen, T. Espevik and D. T. Golenbock (2004). "TLR9 signals after translocating from the ER to CpG DNA in the lysosome." Nat Immunol **5**(2): 190-198.

Lee, K. G., S. Xu, Z. H. Kang, J. Huo, M. Huang, D. Liu, O. Takeuchi, S. Akira and K. P. Lam (2012). "Bruton's tyrosine kinase phosphorylates Toll-like receptor 3 to initiate antiviral response." Proc Natl Acad Sci U S A **109**(15): 5791-5796.

Leonard, J. N., R. Ghirlando, J. Askins, J. K. Bell, D. H. Margulies, D. R. Davies and D. M. Segal (2008). "The TLR3 signaling complex forms by cooperative receptor dimerization." Proc Natl Acad Sci U S A **105**(1): 258-263.

Leoni, V., T. Gianni, S. Salvioli and G. Campadelli-Fiume (2012). "Herpes simplex virus glycoproteins gH/gL and gB bind Toll-like receptor 2, and soluble gH/gL is sufficient to activate NF-kappaB." J Virol **86**(12): 6555-6562.

Lester, S. N. and K. Li (2014). "Toll-like receptors in antiviral innate immunity." J Mol Biol **426**(6): 1246-1264.

Li, Z., L. Qu, Q. Dong, B. Huang, H. Li, Z. Tang, Y. Xu, W. Luo, L. Liu, X. Qiu and E. Wang (2012). "Overexpression of CARMA3 in non-small-cell lung cancer is linked for tumor progression." PLoS One **7**(5): e36903.

Lichty, B. D., A. T. Power, D. F. Stojdl and J. C. Bell (2004). "Vesicular stomatitis virus: re-inventing the bullet." Trends Mol Med **10**(5): 210-216.

Liu, S. L., Z. L. Zhang, Z. Q. Tian, H. S. Zhao, H. Liu, E. Z. Sun, G. F. Xiao, W. Zhang, H. Z. Wang and D. W. Pang (2012). "Effectively and efficiently dissecting the infection of influenza virus by quantum-dot-based single-particle tracking." ACS Nano **6**(1): 141-150.

Loo, Y. M., J. Fornek, N. Crochet, G. Bajwa, O. Perwitasari, L. Martinez-Sobrido, S. Akira, M. A. Gill, A. Garcia-Sastre, M. G. Katze and M. Gale, Jr. (2008). "Distinct RIG-I and MDA5 signaling by RNA viruses in innate immunity." J Virol **82**(1): 335-345.

Lozano, R., M. Naghavi, K. Foreman, S. Lim, K. Shibuya, V. Aboyans, J. Abraham, T. Adair, R. Aggarwal, S. Y. Ahn, M. Alvarado, H. R. Anderson, L. M. Anderson, K. G. Andrews, C. Atkinson, L. M. Baddour, S. Barker-Collo, D. H. Bartels, M. L. Bell, E. J. Benjamin, D. Bennett, K. Bhalla, B. Bikbov, A. Bin Abdulhak, G. Birbeck, F. Blyth, I. Bolliger, S. Boufous, C. Bucello, M. Burch, P. Burney, J. Carapetis, H. Chen, D. Chou, S. S. Chugh, L. E. Coffeng, S. D. Colan, S. Colquhoun, K. E. Colson, J. Condon, M. D. Connor,

L. T. Cooper, M. Corriere, M. Cortinovis, K. C. de Vaccaro, W. Couser, B. C. Cowie, M. H. Criqui, M. Cross, K. C. Dabhadkar, N. Dahodwala, D. De Leo, L. Degenhardt, A. Delossantos, J. Denenberg, D. C. Des Jarlais, S. D. Dharmaratne, E. R. Dorsey, T. Driscoll, H. Duber, B. Ebel, P. J. Erwin, P. Espindola, M. Ezzati, V. Feigin, A. D. Flaxman, M. H. Forouzanfar, F. G. Fowkes, R. Franklin, M. Fransen, M. K. Freeman, S. E. Gabriel, E. Gakidou, F. Gaspari, R. F. Gillum, D. Gonzalez-Medina, Y. A. Halasa, D. Haring, J. E. Harrison, R. Havmoeller, R. J. Hay, B. Hoen, P. J. Hotez, D. Hoy, K. H. Jacobsen, S. L. James, R. Jasrasaria, S. Jayaraman, N. Johns, G. Karthikeyan, N. Kassebaum, A. Keren, J. P. Khoo, L. M. Knowlton, O. Kobusingye, A. Koranteng, R. Krishnamurthi, M. Lipnick, S. E. Lipshultz, S. L. Ohno, J. Mabweijano, M. F. MacIntyre, L. Mallinger, L. March, G. B. Marks, R. Marks, A. Matsumori, R. Matzopoulos, B. M. Mayosi, J. H. McAnulty, M. M. McDermott, J. McGrath, G. A. Mensah, T. R. Merriman, C. Michaud, M. Miller, T. R. Miller, C. Mock, A. O. Mocumbi, A. A. Mokdad, A. Moran, K. Mulholland, M. N. Nair, L. Naldi, K. M. Narayan, K. Nasseri, P. Norman, M. O'Donnell, S. B. Omer, K. Ortblad, R. Osborne, D. Ozgediz, B. Pahari, J. D. Pandian, A. P. Rivero, R. P. Padilla, F. Perez-Ruiz, N. Perico, D. Phillips, K. Pierce, C. A. Pope, 3rd, E. Porrini, F. Pourmalek, M. Raju, D. Ranganathan, J. T. Rehm, D. B. Rein, G. Remuzzi, F. P. Rivara, T. Roberts, F. R. De Leon, L. C. Rosenfeld, L. Rushton, R. L. Sacco, J. A. Salomon, U. Sampson, E. Sanman, D. C. Schwebel, M. Segui-Gomez, D. S. Shepard, D. Singh, J. Singleton, K. Sliwa, E. Smith, A. Steer, J. A. Taylor, B. Thomas, I. M. Tleyjeh, J. A. Towbin, T. Truelsen, E. A. Undurraga, N. Venketasubramanian, L. Vijayakumar, T. Vos, G. R. Wagner, M. Wang, W. Wang, K. Watt, M. A. Weinstock, R. Weintraub, J. D. Wilkinson, A. D. Woolf, S. Wulf, P. H. Yeh, P. Yip,

A. Zabetian, Z. J. Zheng, A. D. Lopez, C. J. Murray, M. A. AlMazroa and Z. A. Memish (2012). "Global and regional mortality from 235 causes of death for 20 age groups in 1990 and 2010: a systematic analysis for the Global Burden of Disease Study 2010." Lancet **380**(9859): 2095-2128.

Lund, J., A. Sato, S. Akira, R. Medzhitov and A. Iwasaki (2003). "Toll-like receptor 9-mediated recognition of Herpes simplex virus-2 by plasmacytoid dendritic cells." J Exp Med **198**(3): 513-520.

Lund, J. M., L. Alexopoulou, A. Sato, M. Karow, N. C. Adams, N. W. Gale, A. Iwasaki and R. A. Flavell (2004). "Recognition of single-stranded RNA viruses by Toll-like receptor 7." Proc Natl Acad Sci U S A **101**(15): 5598-5603.

Mahanivong, C., H. M. Chen, S. W. Yee, Z. K. Pan, Z. Dong and S. Huang (2008). "Protein kinase C alpha-CARMA3 signaling axis links Ras to NF-kappa B for lysophosphatidic acid-induced urokinase plasminogen activator expression in ovarian cancer cells." Oncogene **27**(9): 1273-1280.

Matsumoto, R., D. Wang, M. Blonska, H. Li, M. Kobayashi, B. Pappu, Y. Chen, D. Wang and X. Lin (2005). "Phosphorylation of CARMA1 plays a critical role in T Cell receptor-mediated NF-kappaB activation." Immunity **23**(6): 575-585.

McAllister-Lucas, L. M., N. Inohara, P. C. Lucas, J. Ruland, A. Benito, Q. Li, S. Chen, F. F. Chen, S. Yamaoka, I. M. Verma, T. W. Mak and G. Nunez (2001). "Bimp1, a MAGUK family member linking protein kinase C activation to Bcl10-mediated NF-kappaB induction." J Biol Chem **276**(33): 30589-30597.

McAllister-Lucas, L. M., X. Jin, S. Gu, K. Siu, S. McDonnell, J. Ruland, P. C. Delekta, M. Van Beek and P. C. Lucas (2010). "The CARMA3-Bcl10-MALT1 signalosome promotes angiotensin II-dependent vascular inflammation and atherogenesis." J Biol Chem **285**(34): 25880-25884.

McAllister-Lucas, L. M., J. Ruland, K. Siu, X. Jin, S. Gu, D. S. Kim, P. Kuffa, D. Kohrt, T. W. Mak, G. Nunez and P. C. Lucas (2007). "CARMA3/Bcl10/MALT1-dependent NF-kappaB activation mediates angiotensin II-responsive inflammatory signaling in nonimmune cells." Proc Natl Acad Sci U S A **104**(1): 139-144.

McBride, K. M., G. Banninger, C. McDonald and N. C. Reich (2002). "Regulated nuclear import of the STAT1 transcription factor by direct binding of importin-alpha." EMBO J **21**(7): 1754-1763.

McCartney, S. A., L. B. Thackray, L. Gitlin, S. Gilfillan, H. W. Virgin and M. Colonna (2008). "MDA-5 recognition of a murine norovirus." PLoS Pathog **4**(7): e1000108.

McLaren, J. E. and D. P. Ramji (2009). "Interferon gamma: a master regulator of atherosclerosis." Cytokine Growth Factor Rev **20**(2): 125-135.

Medina, R. A. and A. Garcia-Sastre (2011). "Influenza A viruses: new research developments." Nat Rev Microbiol **9**(8): 590-603.

Melen, K., L. Kinnunen and I. Julkunen (2001). "Arginine/lysine-rich structural element is involved in interferon-induced nuclear import of STATs." J Biol Chem **276**(19): 16447-16455.

Merika, M., A. J. Williams, G. Chen, T. Collins and D. Thanos (1998). "Recruitment of CBP/p300 by the IFN beta enhanceosome is required for synergistic activation of transcription." Mol Cell **1**(2): 277-287.

Meylan, E., K. Burns, K. Hofmann, V. Blancheteau, F. Martinon, M. Kelliher and J. Tschopp (2004). "RIP1 is an essential mediator of Toll-like receptor 3-induced NF-kappa B activation." Nat Immunol **5**(5): 503-507.

Meylan, E., J. Curran, K. Hofmann, D. Moradpour, M. Binder, R. Bartenschlager and J. Tschopp (2005). "Cardif is an adaptor protein in the RIG-I antiviral pathway and is targeted by hepatitis C virus." Nature **437**(7062): 1167-1172.

Miao, Z., T. Zhao, Z. Wang, Y. Xu, Y. Song, J. Wu and H. Xu (2012). "CARMA3 is overexpressed in colon cancer and regulates NF-kappaB activity and cyclin D1 expression." Biochem Biophys Res Commun **425**(4): 781-787.

Munir, M. and M. Berg (2013). "The multiple faces of proteinkinase R in antiviral defense." Virulence **4**(1): 85-89.

Nabel, G. and D. Baltimore (1987). "An inducible transcription factor activates expression of human immunodeficiency virus in T cells." Nature **326**(6114): 711-713.

Nasr, N., S. Maddocks, S. G. Turville, A. N. Harman, N. Woolger, K. J. Helbig, J. Wilkinson, C. R. Bye, T. K. Wright, D. Rambukwelle, H. Donaghy, M. R. Beard and A. L. Cunningham (2012). "HIV-1 infection of human macrophages directly induces viperin which inhibits viral production." Blood **120**(4): 778-788.

Natoli, G. (2010). "NF-kappaB: no longer an island, but a piece of a continent." EMBO Rep **11**(4): 246-248.

Nobusawa, E., T. Aoyama, H. Kato, Y. Suzuki, Y. Tateno and K. Nakajima (1991). "Comparison of complete amino acid sequences and receptor-binding properties among 13 serotypes of hemagglutinins of influenza A viruses." Virology **182**(2): 475-485.

Oeckinghaus, A. and S. Ghosh (2009). "The NF-kappaB family of transcription factors and its regulation." Cold Spring Harb Perspect Biol **1**(4): a000034.

Okumura, A., P. M. Pitha, A. Yoshimura and R. N. Harty (2010). "Interaction between Ebola virus glycoprotein and host toll-like receptor 4 leads to induction of proinflammatory cytokines and SOCS1." J Virol **84**(1): 27-33.

Pahl, H. L. (1999). "Activators and target genes of Rel/NF-kappaB transcription factors." Oncogene **18**(49): 6853-6866.

Pan, D. and X. Lin (2013). "Epithelial growth factor receptor-activated nuclear factor kappaB signaling and its role in epithelial growth factor receptor-associated tumors." Cancer J **19**(6): 461-467.

Patterson, K. D. and G. F. Pyle (1991). "The geography and mortality of the 1918 influenza pandemic." Bull Hist Med **65**(1): 4-21.

Perez-Caballero, D., T. Zang, A. Ebrahimi, M. W. McNatt, D. A. Gregory, M. C. Johnson and P. D. Bieniasz (2009). "Tetherin inhibits HIV-1 release by directly tethering virions to cells." Cell **139**(3): 499-511.

Perez, J. T., A. Varble, R. Sachidanandam, I. Zlatev, M. Manoharan, A. Garcia-Sastre and B. R. tenOever (2010). "Influenza A virus-generated small RNAs regulate the switch from transcription to replication." Proc Natl Acad Sci U S A **107**(25): 11525-11530.

Perkins, N. D. (2007). "Integrating cell-signalling pathways with NF-kappaB and IKK function." Nat Rev Mol Cell Biol **8**(1): 49-62.

Pinto, L. H. and R. A. Lamb (2006). "The M2 proton channels of influenza A and B viruses." J Biol Chem **281**(14): 8997-9000.

Plumet, S., F. Herschke, J. M. Bourhis, H. Valentin, S. Longhi and D. Gerlier (2007). "Cytosolic 5'-triphosphate ended viral leader transcript of measles virus as activator of the RIG I-mediated interferon response." Plos One **2**(3): e279.

Poeck, H., M. Bscheider, O. Gross, K. Finger, S. Roth, M. Rebsamen, N. Hannesschlager, M. Schlee, S. Rothenfusser, W. Barchet, H. Kato, S. Akira, S. Inoue, S. Endres, C. Peschel, G. Hartmann, V. Hornung and J. Ruland (2010). "Recognition of RNA virus by RIG-I results in activation of CARD9 and inflammasome signaling for interleukin 1 beta production." Nat Immunol **11**(1): 63-69.

Poltorak, A., X. He, I. Smirnova, M. Y. Liu, C. Van Huffel, X. Du, D. Birdwell, E. Alejos, M. Silva, C. Galanos, M. Freudenberg, P. Ricciardi-Castagnoli, B. Layton and B. Beutler (1998). "Defective LPS signaling in C3H/HeJ and C57BL/10ScCr mice: mutations in Tlr4 gene." Science **282**(5396): 2085-2088.

Prokunina-Olsson, L., B. Muchmore, W. Tang, R. M. Pfeiffer, H. Park, H. Dickensheets, D. Hergott, P. Porter-Gill, A. Mumy, I. Kohaar, S. Chen, N. Brand, M. Tarway, L. Liu, F. Sheikh, J. Astemborski, H. L. Bonkovsky, B. R. Edlin, C. D. Howell, T. R. Morgan, D. L. Thomas, B. Rehermann, R. P. Donnelly and T. R. O'Brien (2013). "A variant upstream of IFNL3 (IL28B) creating a new interferon gene IFNL4 is associated with impaired clearance of hepatitis C virus." Nat Genet **45**(2): 164-171.

Qiao, Q., C. Yang, C. Zheng, L. Fontan, L. David, X. Yu, C. Bracken, M. Rosen, A. Melnick, E. H. Egelman and H. Wu (2013). "Structural architecture of the CARMA1/Bcl10/MALT1 signalosome: nucleation-induced filamentous assembly." Mol Cell **51**(6): 766-779.

Rehman, A. O. and C. Y. Wang (2009). "CXCL12/SDF-1 alpha activates NF-kappaB and promotes oral cancer invasion through the Carma3/Bcl10/Malt1 complex." Int J Oral Sci **1**(3): 105-118.

Rong, B. L., T. A. Libermann, K. Kogawa, S. Ghosh, L. X. Cao, D. Pavan-Langston and E. C. Dunkel (1992). "HSV-1-inducible proteins bind to NF-kappa B-like sites in the HSV-1 genome." Virology **189**(2): 750-756.

Roth-Cross, J. K., S. J. Bender and S. R. Weiss (2008). "Murine coronavirus mouse hepatitis virus is recognized by MDA5 and induces type I interferon in brain macrophages/microglia." J Virol **82**(20): 9829-9838.

Russell, R. J., S. J. Gamblin, L. F. Haire, D. J. Stevens, B. Xiao, Y. Ha and J. J. Skehel (2004). "H1 and H7 influenza haemagglutinin structures extend a structural classification of haemagglutinin subtypes." Virology **325**(2): 287-296.

Saito, T., R. Hirai, Y. M. Loo, D. Owen, C. L. Johnson, S. C. Sinha, S. Akira, T. Fujita and M. Gale, Jr. (2007). "Regulation of innate antiviral defenses through a shared repressor domain in RIG-I and LGP2." Proc Natl Acad Sci U S A **104**(2): 582-587.

Samanta, M., D. Iwakiri, T. Kanda, T. Imaizumi and K. Takada (2006). "EB virus-encoded RNAs are recognized by RIG-I and activate signaling to induce type I IFN." EMBO J **25**(18): 4207-4214.

Santoro, M. G., A. Rossi and C. Amici (2003). "NF-kappaB and virus infection: who controls whom." EMBO J **22**(11): 2552-2560.

Sassone-Corsi, P., A. Wildeman and P. Chambon (1985). "A trans-acting factor is responsible for the simian virus 40 enhancer activity in vitro." Nature **313**(6002): 458-463.

Sato, M., H. Suemori, N. Hata, M. Asagiri, K. Ogasawara, K. Nakao, T. Nakaya, M. Katsuki, S. Noguchi, N. Tanaka and T. Taniguchi (2000). "Distinct and essential roles of transcription factors IRF-3 and IRF-7 in response to viruses for IFN-alpha/beta gene induction." Immunity **13**(4): 539-548.

Sato, S., M. Sugiyama, M. Yamamoto, Y. Watanabe, T. Kawai, K. Takeda and S. Akira (2003). "Toll/IL-1 receptor domain-containing adaptor inducing IFN-beta (TRIF) associates with TNF receptor-associated factor 6 and TANK-binding kinase 1, and activates two distinct transcription factors, NF-kappa B and IFN-regulatory factor-3, in the Toll-like receptor signaling." J Immunol **171**(8): 4304-4310.

Satoh, T., H. Kato, Y. Kumagai, M. Yoneyama, S. Sato, K. Matsushita, T. Tsujimura, T. Fujita, S. Akira and O. Takeuchi (2010). "LGP2 is a positive regulator of RIG-I- and MDA5-mediated antiviral responses." Proc Natl Acad Sci U S A **107**(4): 1512-1517.

Schindler, C., K. Shuai, V. R. Prezioso and J. E. Darnell, Jr. (1992). "Interferon-dependent tyrosine phosphorylation of a latent cytoplasmic transcription factor." Science **257**(5071): 809-813.

Schneider, W. M., M. D. Chevillotte and C. M. Rice (2014). "Interferon-stimulated genes: a complex web of host defenses." Annu Rev Immunol **32**: 513-545.

Sekimoto, T., N. Imamoto, K. Nakajima, T. Hirano and Y. Yoneda (1997). "Extracellular signal-dependent nuclear import of Stat1 is mediated by nuclear pore-targeting complex formation with NPI-1, but not Rch1." EMBO J **16**(23): 7067-7077.

Seth, R. B., L. Sun, C. K. Ea and Z. J. Chen (2005). "Identification and characterization of MAVS, a mitochondrial antiviral signaling protein that activates NF-kappaB and IRF 3." Cell **122**(5): 669-682.

Sheppard, P., W. Kindsvogel, W. Xu, K. Henderson, S. Schlutsmeyer, T. E. Whitmore, R. Kuestner, U. Garrigues, C. Birks, J. Roraback, C. Ostrander, D. Dong, J. Shin, S. Presnell, B. Fox, B. Haldeman, E. Cooper, D. Taft, T. Gilbert, F. J. Grant, M. Tackett, W. Krivan, G. McKnight, C. Clegg, D. Foster and K. M. Klucher (2003). "IL-28, IL-29 and their class II cytokine receptor IL-28R." Nat Immunol **4**(1): 63-68.

Shuai, K., C. Schindler, V. R. Prezioso and J. E. Darnell, Jr. (1992). "Activation of transcription by IFN-gamma: tyrosine phosphorylation of a 91-kD DNA binding protein." Science **258**(5089): 1808-1812.

Sommer, K., B. Guo, J. L. Pomerantz, A. D. Bandaranayake, M. E. Moreno-Garcia, Y. L. Ovechkina and D. J. Rawlings (2005). "Phosphorylation of the CARMA1 linker controls NF-kappaB activation." Immunity **23**(6): 561-574.

Spiropoulou, C. F., P. Ranjan, M. B. Pearce, T. K. Sealy, C. G. Albarino, S. Gangappa, T. Fujita, P. E. Rollin, S. T. Nichol, T. G. Ksiazek and S. Sambhara (2009). "RIG-I activation inhibits ebolavirus replication." Virology **392**(1): 11-15.

Stark, G. R. and J. E. Darnell, Jr. (2012). "The JAK-STAT pathway at twenty." Immunity **36**(4): 503-514.

Steinhauer, D. A. (1999). "Role of hemagglutinin cleavage for the pathogenicity of influenza virus." Virology **258**(1): 1-20.

Sumpter, R., Jr., Y. M. Loo, E. Foy, K. Li, M. Yoneyama, T. Fujita, S. M. Lemon and M. Gale, Jr. (2005). "Regulating intracellular antiviral defense and permissiveness to hepatitis C virus RNA replication through a cellular RNA helicase, RIG-I." J Virol **79**(5): 2689-2699.

Sun, J. and X. Lin (2008). "Beta-arrestin 2 is required for lysophosphatidic acid-induced NF-kappaB activation." Proc Natl Acad Sci U S A **105**(44): 17085-17090.

Sun, Q., L. Sun, H. H. Liu, X. Chen, R. B. Seth, J. Forman and Z. J. Chen (2006). "The specific and essential role of MAVS in antiviral innate immune responses." Immunity **24**(5): 633-642.

Tabeta, K., P. Georgel, E. Janssen, X. Du, K. Hoebe, K. Crozat, S. Mudd, L. Shamel, S. Sovath, J. Goode, L. Alexopoulou, R. A. Flavell and B. Beutler (2004). "Toll-like receptors 9 and 3 as essential components of innate immune defense against mouse cytomegalovirus infection." Proc Natl Acad Sci U S A **101**(10): 3516-3521.

Tang, E. D. and C. Y. Wang (2009). "MAVS self-association mediates antiviral innate immune signaling." J Virol **83**(8): 3420-3428.

Thanos, D. and T. Maniatis (1995). "Virus induction of human IFN beta gene expression requires the assembly of an enhanceosome." Cell **83**(7): 1091-1100.

Tong, S., Y. Li, P. Rivailler, C. Conrardy, D. A. Castillo, L. M. Chen, S. Recuenco, J. A. Ellison, C. T. Davis, I. A. York, A. S. Turmelle, D. Moran, S. Rogers, M. Shi, Y. Tao, M. R. Weil, K. Tang, L. A. Rowe, S. Sammons, X. Xu, M. Frace, K. A. Lindblade, N. J. Cox, L. J.

Anderson, C. E. Rupprecht and R. O. Donis (2012). "A distinct lineage of influenza A virus from bats." Proc Natl Acad Sci U S A **109**(11): 4269-4274.

van Boxel-Dezaire, A. H., M. R. Rani and G. R. Stark (2006). "Complex modulation of cell type-specific signaling in response to type I interferons." Immunity **25**(3): 361-372.

Wagner, R., M. Matrosovich and H. D. Klenk (2002). "Functional balance between haemagglutinin and neuraminidase in influenza virus infections." Rev Med Virol **12**(3): 159-166.

Walter, M. R., W. T. Windsor, T. L. Nagabhushan, D. J. Lundell, C. A. Lunn, P. J. Zauodny and S. K. Narula (1995). "Crystal structure of a complex between interferon-gamma and its soluble high-affinity receptor." Nature **376**(6537): 230-235.

Wang, D., Y. You, S. M. Case, L. M. McAllister-Lucas, L. Wang, P. S. DiStefano, G. Nunez, J. Bertin and X. Lin (2002). "A requirement for CARMA1 in TCR-induced NF-kappa B activation." Nat Immunol **3**(9): 830-835.

Wang, D., Y. You, P. C. Lin, L. Xue, S. W. Morris, H. Zeng, R. Wen and X. Lin (2007). "Bcl10 plays a critical role in NF-kappaB activation induced by G protein-coupled receptors." Proc Natl Acad Sci U S A **104**(1): 145-150.

Wang, J., S. H. Basagoudanavar, X. Wang, E. Hopewell, R. Albrecht, A. Garcia-Sastre, S. Balachandran and A. A. Beg (2010). "NF-kappa B RelA subunit is crucial for early IFN-beta expression and resistance to RNA virus replication." J Immunol **185**(3): 1720-1729.

Wang, L., Y. Guo, W. J. Huang, X. Ke, J. L. Poyet, G. A. Manji, S. Merriam, M. A. Glucksmann, P. S. DiStefano, E. S. Alnemri and J. Bertin (2001). "Card10 is a novel caspase

recruitment domain/membrane-associated guanylate kinase family member that interacts with BCL10 and activates NF-kappa B." J Biol Chem **276**(24): 21405-21409.

Wang, X., E. R. Hinson and P. Cresswell (2007). "The interferon-inducible protein viperin inhibits influenza virus release by perturbing lipid rafts." Cell Host Microbe **2**(2): 96-105.

Wang, X., S. Hussain, E. J. Wang, X. Wang, M. O. Li, A. Garcia-Sastre and A. A. Beg (2007). "Lack of essential role of NF-kappa B p50, RelA, and cRel subunits in virus-induced type 1 IFN expression." J Immunol **178**(11): 6770-6776.

Wang, Y., X. Wang, J. Li, Y. Zhou and W. Ho (2013). "RIG-I activation inhibits HIV replication in macrophages." J Leukoc Biol **94**(2): 337-341.

Wise, H. M., A. Foeglein, J. Sun, R. M. Dalton, S. Patel, W. Howard, E. C. Anderson, W. S. Barclay and P. Digard (2009). "A complicated message: Identification of a novel PB1-related protein translated from influenza A virus segment 2 mRNA." J Virol **83**(16): 8021-8031.

Xiao, W., D. R. Hodge, L. Wang, X. Yang, X. Zhang and W. L. Farrar (2004). "NF-kappaB activates IL-6 expression through cooperation with c-Jun and IL6-AP1 site, but is independent of its IL6-NFkappaB regulatory site in autocrine human multiple myeloma cells." Cancer Biol Ther **3**(10): 1007-1017.

Xu, L. G., Y. Y. Wang, K. J. Han, L. Y. Li, Z. Zhai and H. B. Shu (2005). "VISA is an adapter protein required for virus-triggered IFN-beta signaling." Mol Cell **19**(6): 727-740.

Yamashita, M., S. Chattopadhyay, V. Fensterl, P. Saikia, J. L. Wetzel and G. C. Sen (2012). "Epidermal growth factor receptor is essential for Toll-like receptor 3 signaling." Sci Signal **5**(233): ra50.

Yen, H. L. and R. G. Webster (2009). "Pandemic influenza as a current threat." Curr Top Microbiol Immunol **333**: 3-24.

Zaidi, M. R. and G. Merlino (2011). "The two faces of interferon-gamma in cancer." Clin Cancer Res **17**(19): 6118-6124.

Zeng, W., L. Sun, X. Jiang, X. Chen, F. Hou, A. Adhikari, M. Xu and Z. J. Chen (2010). "Reconstitution of the RIG-I pathway reveals a signaling role of unanchored polyubiquitin chains in innate immunity." Cell **141**(2): 315-330.

Zhu, Y., G. Chen, F. Lv, X. Wang, X. Ji, Y. Xu, J. Sun, L. Wu, Y. T. Zheng and G. Gao (2011). "Zinc-finger antiviral protein inhibits HIV-1 infection by selectively targeting multiply spliced viral mRNAs for degradation." Proc Natl Acad Sci U S A **108**(38): 15834-15839.

Zhicheng Zhou was born in Jiayu country, Hubei province, China on January 28, 1982, the Son of Xiaoming Zhou and Wenmin Lu. After completing his work at Wuhan No.1 Middle School, China, in 2000, he entered The Shanghai Ocean University, China. He received the degree of Bachelor of Science with a major in Biology in July, 2004.In September of 2004, he entered The Sun Yat-sen University for further study. He received the degree of Master of Science with a major in Marine Biology in December, 2006. For the next a year and a half, he worked as full-time research investigator in Sun Yat-sen University. In September of 2008, he entered The University of Texas Health Science Center at Houston Graduate School of Biomedical Sciences.

Permanent address:

Baibuting North Huayuan Rd

Jiang'an, Wuhan,

Hubei, China

Apt# 14-3.